Biomarkers and Correlates of Aging

Doctoral thesis

to obtain a doctorate (PhD)

from the Faculty of Medicine

of the University of Bonn

Dan Liu

Sichuan, China

2021

Written with authorization of

the Faculty of Medicine of the University of Bonn

First reviewer: Prof. Dr. Dr. Monique M.B. Breteler

Second reviewer: Prof. Dr. Cornelia M van Duijn

Day of oral examination: 27 September 2021

For the German Centre for Neurodegenerative Diseases (DZNE e.V.), Population Health Sciences

Director: Prof. Dr. Dr. Monique M.B. Breteler

Table of Contents

List of abbreviations

ABI	Ankle-Brachial Index
BMI	Body mass index
BSA	Body surface area
CE	Cholesteryl ester
CER	Ceramide
CHD	Coronary heart disease
CI	Cardiac index
Cis	Confidence intervals
CO	Cardiac output
CpG	Cytosine-phosphate-guanine
CRP	C-reactive protein
CVs	Coefficients of variation
CVDs	Cardiovascular diseases
DAG	Diacylglycerol
DBP	Diastolic blood pressure
DCER	Dihydroceramide
DNAm	DNA methylation
eGFR	Estimated glomerular filtration rate
EWAS	Epigenome-wide association study
FDR	False discovery rate

GWAS	Genome-wide association analyses
HbA1c	Glycated haemoglobin
HCER	Hexosylceramide
HDL	High-density lipoprotein
ICG	Impedance cardiography
KEGG	Kyoto Encyclopedia of Genes and Genomes
LCER	Lactosylceramide
LDL	Low-density lipoprotein
LPC	Lysophosphatidylcholine
LPE	Lysophosphatidylethanolamine
LTL	Leukocyte telomere length
MAG	Monoacylglycerol
MAP	Mean arterial pressure
MR	Mendelian randomization
MRM	Multiple reaction monitoring
MUFA	Monounsaturated fatty acids
PhenoAge	Phenotypic Age
PC	Phosphocholine
PCs	Principal components
PE	Phosphoethanolamine
PE(O)	Phosphatidylethanolamine ether
PE(P)	Phosphatidylethanolamine plasmalogen

PI	Phosphatidylinositol
PP	Pulse pressure
PRS	Polygenic risk score
PUFA	Polyunsaturated fatty acids
PWV	Pulse wave velocity
qPCR	Quantitative polymerase chain reaction
RSH	Reactive skin hyperemia
SBF	Skin blood flow
SBP	Systolic blood pressure
SD	Standard deviation
SFA	Saturated fatty acids
SI	Stroke index
SM	Sphingomyelin
SNPs	Single-nucleotide polymorphisms
SV	Stroke volume
SVR	Systemic vascular resistance
SVRI	Systemic vascular resistance index
TAC	Total arterial compliance
TACI	Total arterial compliance index
TAGs	Triacylglycerols
TERT	Telomerase catalytic component
WC	Waist circumference

1. Introduction

1.1 Biomarkers of aging

The rapid aging of the global population has resulted in an increase in the personal and societal burden of age-associated diseases and disability, warranting urgent development of novel strategies for stimulating healthy aging (WHO 2015). Chronological age is a major risk factor for functional impairment, chronic diseases as well as mortality. However, individuals with the same chronological age often exhibit heterogeneous trajectories of age-related functional decline as well as marked differences in their risk of morbidity and mortality (Levine 2013; Lowsky et al. 2014). It is thought that different rates of biological aging could underlie inter-individual differences in the occurrence of age-related health outcomes. Therefore, interventions tailored towards slowing the biological process of aging might be more effective in maximizing health span (Fontana et al. 2014). Thus, a better estimation of biological aging and the elucidation of correlates of biological aging are critical for stimulating healthy aging. Recently, various measures of biological aging have been proposed, including, but not limited to, epigenetic biomarkers of aging and telomere length.

1.1.1 Epigenetic biomarkers of aging

DNA methylation is a major form of epigenetic modulation that is critically involved in the regulation of gene expression. With increasing chronological age, the methylation status of numerous DNA cytosine-phosphate-guanine (CpG) sites differentially changes across the genome, reflecting the effects of cumulative exposure to major risk factors involved in the pathogenesis of age-related conditions (Bell et al. 2012; Fraga and Esteller 2007; Jones et al. 2015). Consequently, DNA methylation patterns have been used to estimate biological age, also known DNA methylation (DNAm) age or epigenetic clock.

First-generation DNAm-based biomarkers of aging, including Horvath's and Hannum's clocks, were developed using chronological age as a surrogate for biological age (Hannum et al. 2013; Horvath 2013). However, chronological age is a suboptimal proxy for biological age. It is crucial to not only include CpGs that display changes with chronological time, but also those that account for substantial inter-individual variation in

physiological and molecular characteristics among individuals of the same chronological age. Thus, second-generation DNAm age estimators, also known as lifespan estimators, including DNAm Phenotypic Age (PhenoAge) and DNAm GrimAge were optimized to capture multi-system physiological dysfunctions and health span (Levine et al. 2018; Lu et al. 2019). PhenoAge, trained on mortality-related clinical biomarkers, and GrimAge, developed using plasma proteins that are associated with age-related conditions, more closely reflect the high interindividual variability in the underlying biological aging processes than the first-generation estimators. Moreover, transcriptional analysis revealed that genes linked to Horvath/Hannum's clocks are only related to development and differentiation pathways (Horvath and Raj 2018). By contrast, genes associated with lifespan estimators are involved in crucial aging pathways, including increased activation of pro-inflammatory and interferon pathways, cytokine-mediated signaling pathway, mitochondrial signatures, and fatty acid transmembrane transport (Levine et al. 2018; Lu et al. 2019). Studies have shown that the discrepancy (accelerated or decelerated) between an individual's estimated biological age and chronological age, referred as DNAm age acceleration estimators (including AgeAccel.Horvath, AgeAccel.Hannum, AgeAccelPheno and AgeAccelGrim), is a strong predictor of mortality and associated with age-related phenotypes, especially cardiovascular diseases and vascular aging (Breitling et al. 2016; Chen et al. 2016; Fransquet et al. 2019; Horvath and Raj 2018; Marioni et al. 2015a; Marioni et al. 2015b; Roetker et al. 2018). Recent studies further showed that AgeAccelGrim outperforms other epigenetic age acceleration estimators in the prediction of age-related diseases and all-cause mortality (McCrory et al. 2021; Protsenko et al. 2021).

1.1.2 Telomere length

Telomeres are repetitive DNA-protein structures, comprising thousands of tandem repeats of the TTAGGG sequence, which are located at the ends of chromosomes. They serve to maintain genomic stability and determine cellular lifespan (O'Sullivan and Karlseder 2010). During each cell division, telomere length progressively shortens because of the inability of DNA polymerase to fully replicate the 3' end of the DNA strand. When these sequences reach a critical length, the cellular DNA damage machinery is activated, which, in turn, triggers cellular senescence (Blackburn et al. 2015). Telomere

length is usually measured as leukocyte telomere length (LTL), which is relatively easy to obtain from blood samples and is highly correlated with telomere length in other tissues (Demanelis et al. 2020). LTL has been proposed as a biomarker of biological aging as it reflects the amount of cellular turnover within an individual. There is considerable variation in LTL across individuals, including those of the same chronological age. Accumulating evidence has suggested that telomere-triggered cellular senescence, a hallmark of biological aging, is highly associated with age-related diseases. Especially, telomere shortening could contribute to cardiovascular aging and thereby increase the risk of developing cardiovascular diseases (CVDs) (Fyhrquist et al. 2013).

1.2 Correlates of aging

1.2.1 Cardiovascular correlates of epigenetic aging

CVDs are the leading causes of morbidity and mortality worldwide (CollaboratorsGBDCoD 2017; North and Sinclair 2012). Chronological age is by far the single most important predictor of CVD occurrence (North and Sinclair 2012). However, substantial inter-individual variation in cardiovascular aging and associated morbidity remains in individuals with the same chronological age, pointing towards markedly different rates of biological aging (Ben-Shlomo et al. 2014; Hamczyk et al. 2020; Medina-Lezama et al. 2018; Patel et al. 2015; Yusuf et al. 2020). Nevertheless, the extent to which different cardiovascular risk factors contribute to biological aging is still unclear. Elucidation of the relation between inter-individual differences in cardiovascular risk factors and the rate of biological aging is crucial for developing more potent preventive and therapeutic strategies for CVDs based on antiaging approaches.

Several studies have shown that classical cardiovascular risk factors causally affect DNA methylation status. Large scale (epi)genomic analyses have shown that body mass index drives differential methylation status in blood, adipose tissue, and liver, as well as changes in methylation over time (Horvath et al. 2014; Mendelson et al. 2017; Sun et al. 2019; Wahl et al. 2017). Inter-individual variation in blood lipids, as well as hyperglycemia, could induce differential methylation changes in blood cells, human endothelial cells and skeletal muscle (Aref-Eshghi et al. 2020; Dekkers et al. 2016; Mudry et al. 2017). In addition, data from in-vitro studies suggest that blood flow induced methylation modifications are related

to endothelial and vascular functions, which may lead to atherosclerosis and CVDs (Dunn et al. 2014; Jiang et al. 2014). The latter is also supported by a recent population-based epigenetic study, which has shown a bidirectional association between blood pressure and DNA methylation (Richard et al. 2017). However, the association of quantitative markers of cardiovascular aging, including age-related changes in arterial stiffness, endothelial function and hemodynamics, with DNA methylation remains largely unknown.

Importantly, it is still unknown whether and how inter-individual differences in cardiovascular risk factor profiles, as well as age-associated changes in cardiovascular functional parameters (arterial stiffness, endothelial function, systemic hemodynamics), are associated with DNAm age acceleration estimators at the population-level. In particular, studies that assess the relation between cardiovascular risk factors and lifespan acceleration estimators are lacking (Huang et al. 2019; Nannini et al. 2019; Quach et al. 2017). Moreover, no studies investigated the association of quantitative and highly sensitive markers of cardiovascular aging with both generations DNAm age acceleration estimators and compared the utility of the first and second-generation DNAm age acceleration estimators in capturing similarities and differences in multi-domain cardiovascular dysfunction.

1.2.2 Lipidomic correlates of epigenetic aging

Lipid metabolism has been suggested to play an important role in biological aging. Key pathways that have been implicated in the aging process, including the insulin-like growth factor-Akt-mTOR pathway, the nuclear factor kB (NF-kB) pathway and the AMP-activated protein kinase (AMPK) pathway, are also crucial regulators of lipid metabolism (Burkewitz et al. 2014; Jesko et al. 2019; Rozing et al. 2009). Lipid metabolites are essential components of biological membranes and signaling molecules, and the lipidome represents an individual's biological state that is influenced by both genetic and epigenetic factors (Hahn et al. 2017). Importantly, various circulating lipid species have been linked to age-related phenotypes. Higher levels of plasma ceramides carrying different fatty acids were associated with various prediabetes markers (Lemaitre et al. 2018). A number of lipidomic features have been linked to obesity (Yin et al. 2020), and Alzheimer’s disease (Proitsi et al. 2017). Further evidence for the crucial role of lipid metabolism in aging stems

from studies of nonagenarians and centenarians and their offspring, which found favorable lipid profiles in healthy agers (Gonzalez-Covarrubias et al. 2013; Montoliu et al. 2014; Vaarhorst et al. 2011). Notably, in the Leiden Longevity Study, it was found that offspring of nonagenarians had higher levels of phosphocholine (PC) and sphingomyelin (SM) species and lower levels of phosphoethanolamine (PE) (38:6) and long-chain triacylglycerols (TAGs), independent of total triglyceride levels (Gonzalez-Covarrubias et al. 2013; Vaarhorst et al. 2011). Similarly, in another longevity cohort it was found that healthy agers had lower concentrations of lysophospatidylcholines and higher levels of SM species compared to their unhealthy contemporaries (Collino et al. 2013).

There is ample evidence that levels of blood lipids, including HDL cholesterol, LDL cholesterol, TAGs, total cholesterol, and lipoprotein subfractions, are associated with DNA methylation status (Braun et al. 2017; Dekkers et al. 2016; Frazier-Wood et al. 2014; Gomez-Alonso et al. 2021; Hedman et al. 2017; Irvin et al. 2014; Nuotio et al. 2020; Pfeiffer et al. 2015; Xie et al. 2019). A recent large-scale epigenome-wide association study (EWAS) (N=16,265) found that numerous CpGs were associated with HDL, LDL, and TG in either trans-ethnic or ethnic-specific meta-analyses (Jhun et al. 2021). EWAS combined with Mendelian randomization analyses indicated that inter-individual variations in lipid levels are likely to be causally related to changes in DNA methylation (Dekkers et al. 2016; Jhun et al. 2021). Furthermore, many of the lipid-related CpGs have also been linked to age-related phenotypes, including metabolic syndrome, type 2 diabetes, and coronary artery disease (Gomez-Alonso et al. 2021; Hedman et al. 2017; Xie et al. 2019). Taken together, current evidence suggests that lipid changes may exert at least part of their (pathological) effects through epigenomic remodeling.

Despite the intriguing connection between lipid metabolism and aging as detailed above, it is still unknown whether and how inter-individual differences in lipid profiles could contribute to different rates of biological aging in the general population. The heterogeneous chemical structure of lipids poses challenges for their accurate quantification, and until now only a few lipid species have been investigated in relation to aging and age-related health outcomes. Yet the vast diversity of lipid functions is reflected in the wide variation in the structure and composition of lipid molecules, which ultimately

determine their specific effects. Recently, high-throughput, in-depth molecular characterization of many lipid species has become available through Metabolon's novel complex lipid assay platform. This lipidomics platform provides absolute quantitation of 14 lipid classes across phospholipids, sphingolipids, and neutral lipids, as well as the complete fatty acid composition of each lipid class, including absolute concentrations of their constituent molecular species. These recent technological developments make it possible to investigate the contribution of complex lipids to biological aging – as estimated by epigenetic age acceleration – at a population level.

1.2.3 Leukocyte telomere length and vascular phenotypes

Accumulating evidence has suggested that telomere shortening may be part of the mechanistic pathway leading to endothelial and hemodynamic dysfunction (Fyhrquist et al. 2013). Indeed, progressive telomere shortening reduced human vascular smooth muscle cell life span triggering endothelial dysfunction, which was reversed by inhibition of telomere shortening (Maeda et al. 2019; Minamino et al. 2001; Minamino et al. 2002). Increased rates of cell turnover in the arterial system reportedly accelerate telomere loss, which in turn leads to higher levels of hemodynamic stress and endothelial senescence (Chang and Harley 1995; Chen et al. 2021). Treatment that reduced telomere length could also accelerate endothelial dysfunction (Yepuri et al. 2016).

In contrast to many *in vitro* studies, only a few epidemiological and clinical studies have investigated the role of telomere length in relation to endothelial function, hemodynamics and other vascular phenotypes, with inconsistent results (De Meyer et al. 2009; Fitzpatrick et al. 2007; Gonzalez-Guardia et al. 2014; Masi et al. 2014; McDonnell et al. 2017; Nguyen et al. 2019). Shorter LTL was associated with thicker carotid intima-media thickness in older participants (Fitzpatrick et al. 2007), but neither cross-sectional nor longitudinal LTL were associated with cardiac measurements (Masi et al. 2014) or pulse wave velocity (Nguyen et al. 2019). In contrast, in the Anglo-Cardiff Collaborative Trial LTL was associated with PWV, but only in people older than 50 years of age (McDonnell et al. 2017). Altogether, detailed findings about the association between LTL and quantitative and sensitive preclinical markers of vascular function are lacking, especially in the general population across the adult lifespan.

Prior studies have reported cross-sectional associations between LTL and some vascular phenotypes, yet these findings may have been subject to residual confounding or due to reverse causation (De Meyer et al. 2009; Fernandez-Alvira et al. 2016; Fitzpatrick et al. 2007; Masi et al. 2014; Nguyen et al. 2019). LTL has a strong inherited genetic component in humans, with an estimated heritability ranging from 44 % to 86 % (Broer et al. 2013; Njajou et al. 2007). Recently, a large genome-wide meta-analysis found 52 independent variants associated with LTL, accounting for ~2.93 % of the variance in LTL (Li et al. 2020). Of note, these variants were located in gene regions involved in telomere regulation, maintenance, as well as cellular aging and senescence. Therefore, taking advantage of these new genetic findings, weighted polygenic risk scores (PRS) of LTL can be created to assess the association between genetic predisposition to longer LTL and vascular phenotypes.

1.3 Overall aim and study specific aim

The overall aim of this thesis was to investigate biomarkers and correlates of biological aging across the adult lifespan in a population-based setting. More specifically, I aimed to address the following:

Study I: Cardiovascular correlates of epigenetic aging across the adult lifespan: a population-based study

In study I, I aimed to examine the relation of cardiovascular risk factors and cardiovascular aging markers with four different estimators of accelerated biological aging across the adult lifespan in a population-based study.

Study II: The lipidomic correlates of epigenetic aging across the adult lifespan: a population-based study

In study II, I aimed to delineate the contribution of complex lipids to biological aging – as estimated through epigenetic age acceleration – in a large population-based cohort.

Study III: Associations of measured and genetically predicted leukocyte telomere length with vascular phenotypes: a population-based study

In study III, I aimed to elucidate the role of telomere-triggered cell senescence, a hallmark of biological aging, in the pathogenesis of endothelial and hemodynamic dysfunction. Here we systematically assessed the relations of both measured and genetically predicted LTL and four different vascular functional domains, including endothelial function, hemodynamics, arterial stiffness, and blood pressure.

2. Material and methods

2.1 Study population

2.1.1 The Rhineland Study

All analyses were embedded within the Rhineland Study. The Rhineland Study is an ongoing single-center, population-based prospective cohort study that aims to invite up to 20,000 participants among people aged 30 years and above in Bonn, Germany. All individuals living in two pre-defined recruitment areas are invited to participate in the study. The only exclusion criterion is an insufficient command of the German language to provide informed consent. Participants living in the two recruitment areas are predominantly German of Caucasian descent. One of the Rhineland Study's primary objectives is to identify determinants and markers of healthy aging, applying a deep-phenotyping approach. At baseline, participants complete an 8-hour in-depth multi-domain phenotypic assessment of anthropometry, physical activity and fitness, cardiovascular health, brain imaging, cognitive testing, neurologic functioning, ophthalmologic health, and other sensory systems, and various types of biomaterials (blood, urine, stool, and hair) are collected.

Approval to undertake the study is obtained from the ethics committee of the University of Bonn, Medical Faculty. We obtain written informed consent from all participants in accordance with the Declaration of Helsinki.

2.1.2 Study specific analysis samples

The recruitment of the participants in the Rhineland Study started in March 2016 and is still ongoing. Each study was conducted based on the number of participants available at that time. We only measured LTL in the first 1828 samples.

Study I

For this study, we used baseline data of the first 3332 participants of the Rhineland Study with methylation data. We excluded samples that did not meet the methylation data quality control criteria (n = 4). The final analysis sample comprised 3328 participants.

Study II

For this study, we used baseline data of the first 4471 participants of the Rhineland Study in whom complex lipids data were available. We excluded participants without methylation data (n=290). The final analysis sample consisted of 4181 participants.

Study III

In a subset of participants both measured LTL and vascular phenotypes were available (n = 1828). Baseline data of the first 4180 participants of the Rhineland Study with both genetic data and vascular phenotype data were used to assess the association between genetically predicted LTL and vascular phenotypes.

2.2 Blood samples collection

Blood samples were mainly collected between 7:00 to 9:45 in the morning from an antecubital or dorsal hand vein after overnight fasting. They were used in the measurement of DNA methylation, clinical biochemistry, complex lipids, genetics and LTL, as detailed below.

2.3 DNA Methylation

2.3.1 DNA methylation assessment

Genomic DNA was extracted from buffy coat fractions of anti-coagulated blood samples using Chemagic DNA buffy coat kit (PerkinElmer, Germany), and was subsequently bisulfite converted using the DNA methylation kit according to the manufacturer's instructions. DNA methylation levels were measured using Illumina's Human MethylationEPIC BeadChip. The methylation level for each probe was derived as a beta value representing the fractional level of DNA methylation at that probe. Sample-level and probe-level quality control were performed using the 'minfi' package (Fortin et al. 2017) in R (version 3.5.0). Probes with a missing rate >1 % (at a detection p-value >0.01) were excluded. Samples with sex mismatch or a missing rate at >1 % across all probes were also excluded following previously published recommendation guidelines for analyzing methylation data (Wu and Kuan 2018).

2.3.2 Estimation of DNAm age acceleration

Four measures of DNAm age were calculated. DNAmAge.Horvath and DNAmAge.Hannum were calculated according to the algorithms described by Horvath and Hannum et al., using 353 and 71 CpG sites, respectively (Hannum et al. 2013; Horvath 2013). DNAm PhenoAge and DNAm GrimAge were calculated based on the algorithms developed by Levine et al. and Lu et al., using 513 and 1030 CpG sites, respectively (Levine et al. 2018; Lu et al. 2019). DNAm age acceleration estimator is defined as the residual (in years) that results from regressing DNAm age on chronological age. The corresponding age-adjusted measures of DNAm age acceleration estimator are denoted as AgeAccel.Horvath, AgeAccel.Hannum, AgeAccelPheno and AgeAccelGrim.

2.4 Cardiovascular phenotypes measurement

2.4.1 Measurement of classical cardiovascular risk factors

Low-density lipoprotein (LDL) cholesterol, high-density lipoprotein (HDL) cholesterol, triglycerides, total cholesterol, C-reactive protein (CRP), insulin, glucose, glycated haemoglobin (HbA1c) concentrations in venous blood samples were measured using standard methods at the local clinical chemistry laboratory of the University Hospital of Bonn. Insulin resistance was calculated as: insulin (mIU/L) × glucose (mmol/L)/22.5. Estimated glomerular filtration rate (eGFR) was estimated using the CKD-EPI equation (Inker et al. 2012). Percentage of body fat was measured by direct segmental multi-frequency bioelectrical impedance analysis (InBody770). Body mass index (BMI) was calculated as weight in kilograms dived by height in meters squared. Waist circumference (WC) was measured according to the WHO recommendation, localizing the middle anatomical point between the lowest rib and the iliac crest with an anthropometric tape (SECA 201). Systolic blood pressure (SBP) and diastolic blood pressure (DBP) were measured three times (separated by ten minutes intervals), using an oscillometric blood pressure device (Omron 705 IT). The measurements were performed while people were sitting in a resting chair in a quiet environment, and the average of the second and third measurements was used for further calculation. Mean arterial pressure (MAP) was calculated as (SBP + 2 × DBP)/3. The Framingham 10-year cardiovascular risk score was calculated for individuals from 30 to 79 years old without coronary heart disease, stroke, or peripheral arterial diseases, using the published gender-specific algorithms (D'Agostino et al. 2008).

2.4.2 Measurement of hemodynamic and arterial stiffness

All examinations were performed in temperature-controlled rooms after acclimatization of the participants in the study center and 5 minutes of rest in the supine position. Aorta-femoral pulse wave velocity (PWV [m/s]) was assessed with an integrated oscillometric method, defining the propagation time of pulse wave as the delay between opening of the aortic valve determined with impedance cardiography (ICG) waves and the arrival of the pulse wave to mid-femoral cuff. PWV was calculated as the distance measured between supra-sternal notch and mid-femoral cuff divided by propagation time. Ankle-Brachial Index (ABI), calculated as the ratio of the ipsilateral ankle and brachial SBP, was measured on both sides with the oscillometric method. In cases where the ABI on both sides was lower than 1.40, the lower value was used for analysis, whereas in other cases the higher value was used as recommended previously (Aboyans et al. 2012).

Hemodynamic variables were measured beat-to-beat for approximately 8 minutes with an impedance cardiography device (CardioScreen 2000, Medis, Germany). All hemodynamic variables were computed by Cardiovascular Lab Software (Medis, Germany), based on stroke volume (SV [mL]), simultaneously registered electrocardiography signals and blood pressure measured with 2-minute intervals. Average values of each variable were used for the analysis. Briefly, cardiac output (CO [L/min]) was computed as SV multiplied heart rate [beat per minute]. Total arterial compliance (TAC [mL/mmHg]) was calculated as SV divided by brachial pulse pressure (PP). PP was assessed as the difference between SBP and DBP. Systemic vascular resistance (SVR [dynes/sec/cm^5]) was approximated as MAP divided by CO and multiplied by 80. These parameters were also divided by body surface area (BSA, m^2) to obtain stroke index (SI), cardiac index (CI), total arterial compliance index (TACI) and SVR was multiplied with BSA to compute systemic vascular resistance index (SVRI).

2.4.3 Measurement of endothelial function

Endothelial function was assessed as reactive skin hyperemia (RSH) with a laser Doppler flowmetry device (Moors, UK) using a local thermal heating protocol. Skin blood flow (SBF) on the ventral surface of the forearm was measured for a total of 26 minutes. After 2 minutes of baseline SBF measurement, the area was heated up to 40 degrees Celsius

with an integrated heating probe and kept constant until the end of the examination. The baseline SBF is followed by a nadir and after approximately 20 minutes it reaches a plateau that is linked to nitric oxide production capacity of the endothelial cells (Choi et al. 2014). RSH was calculated as the percentage increase in SBF from baseline to the last 2 minutes of plateau level ([(Plateau SBF - Baseline SBF) / Baseline SBF] x 100).

2.5 Complex Lipids panel and the quality control

The absolute concentration (*μM*) of 14 lipid classes, including cholesteryl ester (CE), triacylglycerol (TAG), diacylglycerol (DAG), monoacylglycerol (MAG), phosphatidylcholine (PC), phosphatidylethanolamine (PE) (including phosphatidylethanolamine ether (PE(O)) and phosphatidylethanolamine plasmalogen (PE(P))), phosphatidylinositol (PI), lysophosphatidylcholine (LPC), lysophosphatidylethanolamine (LPE), sphingomyelin (SM), ceramide (CER), hexosylceramide (HCER), lactosylceramide (LCER), dihydroceramide (DCER), as well as the molecular species which were defined by the number of carbons and the number of double bonds in all the side chains [e.g. CE (16:1), DAG(14:0/18:1), and PC(16:0/22:6)] of each of the 14 covered lipid classes, were measured in serum samples (100 *μL*) using the True Mass Complex Lipid Panel (Metabolon, Research Triangle Park, NC, USA). Additional to the individual molecular species, one-fatty-acid-tail composition which consisted of one specific fatty acid of that class (e.g. DAG [FA14:1], PC[FA18:2]) was also measured.

Lipids were extracted from the bio-fluid in the presence of deuterated internal standards using an automated BUME extraction according to the method of Lofgren et al (van Dijk et al. 2012). The extracts were dried under nitrogen and reconstituted in ammonium acetate dichloromethane: methanol (50:50). The extracts were transferred to vials for infusion-mass spectroscopy analysis, performed on a Shimadzu LC with nano PEEK tubing and the Sciex SelexIon-5500 QTRAP. The samples were analyzed via both positive and negative mode electrospray. The 5500 QTRAP was operated in multiple reaction monitoring (MRM) mode with a total of more than 1100 MRMs. Individual lipid molecular species were quantified by taking the ratio of the signal intensity of each target compound to that of its assigned internal standard, then multiplying by the concentration of internal standard added to the sample. Lipid class concentrations were calculated from the sum

of all molecular species within a class, and one-fatty-acid compositions were determined by calculating the proportion of each class comprised of individual fatty acid. The differences between each run day were normalised out by subtracting the background and normalising against its run day median for each dataset and then post-multiplied by the overall median of all datasets. The coefficients of variation (CVs) of lipid concentrations were all below 10 %. The median CV of species at 1 μM concentration in serum samples was approximately 5 %.

The number of molecular species and the one-fatty-acid-tail compositions of each lipid class measured are presented in **Table 1**. In total, 1050 molecular species and 278 one-fatty-acid-tail composition covering these 14 classes were measured in the complex lipids panel. Individual lipid species that contained more than 90 % missing values across all the participants were not included for statistical analysis (86 molecular species and 11 one-fatty-acid-tail compositions), leaving a total of 964 molecular species and 267 one-fatty-acid-tail compositions for the analyses (**Table 1**). Lipids with zero double bond are defined as saturated fatty acids (SFA), lipids with one double bond are defined as monounsaturated fatty acids (MUFA), and lipids with more than one double bond are defined as polyunsaturated fatty acids (PUFA).

Table 1. Lipid class and molecular species measured in complex lipids panel and were included in the analysis

Group	Abbreviation	Lipid class	Molecular species		One-fatty-acid-tail composition	
			No. of measured (n= 1050)	No. of included in the analysis (n = 964)	No. of measured (n = 278)	No. of included in the analysis (n = 267)
Neutral lipids	CE	Cholesteryl ester	27	27	26	26
	MAG	Monoacylglycerol	27	27	26	26
	TAG	Triacylglycerol	519	519	21	21
	DAG	Diacylglycerol	59	59	19	19
Phospholipids	PC	Phosphatidylcholine	121	106	23	23
	PE	Phosphatidylethanolamine	80	42	21	16
	PE(O)	phosphatidylethanolamine ether	26	17	-	-
	PE(P)	phosphatidylethanolamine plasmalogen	53	36	-	-

	PI	Phosphatidylinositol	29	28	13	13
	LPC	Lysophosphatidylcholine	22	19	21	18
	LPE	Lysophosphatidylethanolamine	21	18	20	17
Sphingolipids	SM	Sphingomyelin	13	13	12	12
	CER	Ceramide	13	13	12	12
	HCER	Hexosylceramide	13	13	12	12
	LCER	Lactosylceramide	13	13	12	12
	DCER	Dihydroceramide	14	14	12	12
	TOTAL FA	Total fatty acid composition	-	-	28	28

2.6 Measurement of leukocyte telomere length

LTL was measured using the quantitative polymerase chain reaction (qPCR) method adapted from the published original method (Cawthon 2009). Genomic DNA was extracted from buffy coat fractions of anti-coagulated blood samples using Chemagic DNA buffy coat kit (PerkinElmer, Germany) and stored at -80°C before use. The relative mean LTL (T/S ratio) was measured as the relative quantity of the telomeric TTAGGG repeat (T) and the single copy of a housekeeping gene, albumin (S). Each reaction contained 25ng of DNA, 400 nM of the telomere length primers (tel-forward: ACA CTA AGG TTT GGG TTT GGG TTT GGG TTT GGG TTA GTGT; tel-reverse: TGT TAG GTA TCC CTA TCC CTA TCC CTA TCC CTA TCC CTA ACA) and 200 nM of the albumin primers (alb-forward: CGG CGG CGG GCG GCG CGG GCT GGG CGG AAA TGC TGC ACA GAA TCC TTG; alb-reverse: GCC CGG CCC GCC GCG CCC GTC CCG CCG GAA AAG CAT GGT CGC CTG TT) and 1x SYBR green PCR Mastermix (iTaq Universal SYBR Green Supermix). The reactions were performed in triplicates for each sample using 7900HT machine (Applied biosystems). The intra-assay coefficient of variability was 4 % and the inter-assay coefficient of variability was 6 %. LTL (kb pairs) was calculated using the following equation: 3274 + 2413 * T/S ratio/ 1000 according to the literature (Rehkopf et al. 2016).

2.7 Weighted polygenic scores for longer leukocyte telomere length

DNA extracted from buffy coat samples were genotyped using Infinium Omni2.5Exome-8 BeadChip containing 2,612,357 SNPs and processed using GenomeStudio (version 2.0.5). Quality control of genotypes was performed using PLINK (version 1.9). Single-

nucleotide polymorphisms (SNP) exclusion criteria were Hardy-Weinberg disequilibrium ($p<1*10^{-6}$), minor allele frequency (<0.01) and poor genotyping rate (<99%) (Marees et al. 2018). Participants with potentially problematic samples were excluded, comprising 34 cases with poor call rate (<95%), 47 cases with abnormal heterozygosity, 143 cases with cryptic relatedness and 7 cases with gender mismatch. Since variation in population structure can cause systematic differences in allele frequencies, we used EIGENSTRAT (version 16000), which uses principal components (PCs) to detect and correct for variation in population structure (Price et al. 2006). Based on the EIGENSTRAT estimation, we exclude 101 cases of non-Caucasian descent and keeping only the participants with the Caucasian descent for the analysis. We used 1000 Genomes phase 3 reference panel for the imputation of missing genotypes using impute2 (version 2). To include only SNPs with high imputation quality, we filtered the SNPs based on an info score metric > 0.3 (Verma et al. 2014).

A previous genome-wide association study including 78,592 individuals of European descent identified 52 variants independently associated with LTL at a false discovery rate (FDR) <0.05, accounting for ~2.93% of the variance in LTL (Li et al. 2020). Among these, 20 sentinel variants reached genome-wide significance ($5*10^{-8}$); 47 out of 52 SNPs were available in our genetic array. Of the missing ones, rs754017156, rs7510583, rs112347796 were not present in our imputed dataset. In addition, rs201375979 was excluded because it is an indel variant, and rs7510583 was excluded because it is tri-allelic. Individual SNPs were coded for effect allele dosage associated with longer LTL, ranging from zero (no effect alleles) to two (two effect alleles). Two weighted polygenic risk scores (PRSs) for telomere length were calculated: one using 47 variants that were significant at FDR < 0.05 (PRS_{FDR} of LTL) and one using 20 variants that reached genome-wide significance (PRS_{GWAS} of LTL), with a higher PRS scores representing longer LTL. The published regression coefficient (beta) estimates representing the per-allele effect on normalized LTL were assigned as weights for each SNP. These two PRSs were further standardized to have a mean of 0 and a standard deviation of 1 and were used in the analyses as proxies for genetically predicted LTL.

We defined delta LTL (**Δ**LTL) as the difference between measured and genetically predicted LTL for each participant, and estimated it as the residual remaining after regressing measured LTL on PRS of LTL, batch information of measured LTL and the first 10 genetic PCs.

2.8 Demographic and health variables

We included age, sex and education level as demographic factors. Education level was grouped as less than high school, high school, or higher. Smoking status was defined as current smoker or non-current smoker. Participants were considered to have diabetes if they had a self-reported physician diagnosis of diabetes, glycated hemoglobin (%) levels of 6.5 % or more, or used insulin or other anti-diabetic drugs. Hypertension was defined as a self-reported physician diagnosis of hypertension, use of antihypertensive drugs, or an average systolic blood pressure $\geq$ 140 mmHg and/or diastolic blood pressure $\geq$ 90 mmHg. Stroke and myocardial infarction were defined as self-reported physician diagnosis.

2.9 Statistical analyses

2.9.1 Study I

Data were summarized as mean ± standard deviation (SD) or counts with proportions, for continuous and categorical variables, respectively. Differences between women and men were compared using linear regression for continuous variables, and logistic regression for categorical variables adjusting for age. Pearson correlation coefficients were used to assess correlations among cardiovascular risk factors, markers of cardiovascular aging, and DNAm age acceleration estimators. Multiple linear regression analyses were applied to assess the association between each cardiovascular factor (independent variable) and each different DNAm age acceleration estimator (dependent variable). All cardiovascular variables were standardized before further analyses to better compare the effect sizes across different physiological domains. For all the analyses, complete data were used. There is no missing for age, sex, batch information of methylation data. The missingness rate for each main independent variable was less than 5 %, therefore we did not impute missing values. In total, 3016 participants had all the complete data. Model 1 was adjusted for batch information of the methylation data. In model 2, we additionally adjusted for sex.

Model 3 was further adjusted for smoking status (current or not). Hierarchical clustering was applied to group cardiovascular risk factors, as well as blood pressure, arterial stiffness, endothelial function and hemodynamic variables into homogenous clusters according to their degree of interrelatedness (R package 'ClustOfVar'). Average Z-scores were calculated across each cluster, and were included in the multivariable regression model to assess the independent relation between each cluster and DNAm age acceleration estimator, adjusting for sex, batch information of the methylation data and smoking status. To explore sex differences between cardiovascular factors and DNAm age acceleration estimator, we assessed the interaction between sex and each cardiovascular factor and performed sex-stratified analyses if the interaction term was statistically significant. To test whether our results would be affected by cardiovascular co-morbidity, we also performed a sensitivity analysis by excluding participants with diabetes, stroke or myocardial infarction. Potential nonlinear relationships were examined by plotting each cardiovascular factor against DNAm age acceleration estimator. If there was a potentially nonlinear relationship based on visual inspection, quadratic terms for cardiovascular factor were added to the regression models. All statistical analyses were performed using R version 3.5.2. All standardized effect estimates are reported with their 95 % confidence intervals (CIs). Statistical significance level was set at $P < 0.05$.

2.9.2 Study II

Data were summarized as mean $\pm$ standard deviation (SD) or counts with proportions, for continuous and categorical variables, respectively. Differences between women and men were compared using linear regression for continuous variables, and logistic regression for categorical variables adjusting for age. Age and sex-adjusted partial-correlations were used to assess the correlations among standard clinical lipid measures (i.e. LDL, HDL, total cholesterol, TAG, LDL/HDL ratio), BMI and the 14 main lipid classes (i.e. CE, MAG, DAG, TAG, PC, PE, PI, LPC, LPE, SM, CER, DCER). All lipid variables were z-transformed to have a mean of 0 and standard deviation of 1 before further analyses to enable a better comparison of the effect sizes across different lipid classes. Given the low missingness rate, for all analyses we used complete data without imputation of missing values.

Association analysis

Multiple linear regression analyses were applied to assess the association between each lipid class, molecular species, one-fatty-acid-tail composition (independent variable), and each different DNAm age acceleration estimator (dependent variable). The base model was adjusted for sex, batch information of lipids as well as methylation data, smoking status (current or not). As HDL and LDL transport lipids in the circulation and have important clinical utility, we further adjusted for HDL and LDL separately and jointly. To assess whether the association of lipid species and DNAm age acceleration estimators was independent of BMI, we also adjusted for BMI based on the base model. The false discovery rate (FDR) method was used to account for multiple comparisons, considering FDR < 0.05 as statistically significant.

The overall patterns between all lipid classes/species and DNAm age acceleration estimators were shown as forest plots. Patterns across all species of specific lipid class were also shown as forest plots. To assess whether the effect (strength and direction) of the associations depended on the total number of carbon and double bonds in the lipids, the effect estimates of the lipid species were plotted as circles with their position in the 2-dimensional lipid class graphs determined by the total acyl chain carbon numbers (*x*-axis) and double bonds (*y*-axis). To assess whether the effect (strength and direction) of the associations depended on the number of carbons in one specific fatty acid tail, heat maps were shown for the effect estimates of the lipid species at FDR <0.05 level. To examine whether the associations differed by degree of saturation in each lipid molecular species, beta estimates across lipid classes were shown as forest plots.

Sex interaction and sex-stratified analysis

To examine sex differences between lipid class and lipid molecular species and DNAm age acceleration estimators, we assessed the interaction effects between sex and each lipid species on AgeAccel. In case statistically significant sex-lipid interactions were identified, additional sex-stratified analyses were performed.

Pathway analysis

Epigenome-wide association analyses were performed for each AgeAccel-associated lipid species, adjusted for age, sex, smoking status, batch information of lipids as well as

methylation data, first 10 genetic PCs and cell counts which includes CD8T, CD4T, natural killer cells, B cells, monocytes, and granulocytes. The associated CpGs were used as a proxy for each lipid to perform the Kyoto Encyclopedia of Genes and Genomes (KEGG) pathway analysis using g:Profiler (https://biit.cs.ut.ee/gprofiler/).

2.9.3 Study III

Data were summarized as mean ± standard deviation (SD) or counts with proportions, for continuous and categorical variables, respectively. Multiple linear regression analyses were applied to assess the association between measured LTL and each vascular phenotype. All vascular phenotypes were standardized using z-scores before further analyses to enable a better comparison of the effect sizes across different physiological domains. The missingness rate for each main independent variable was less than 5 %, therefore we did not impute missing values and used complete data for the analyses. Model 1 was adjusted for age, sex, batch information of LTL. In model 2, we additionally adjusted for smoking status and BMI. As a previous study found that controlling for leukocyte compositions attenuated the association between LTL and cardiovascular risk factors by between 10 % to 20 % (Rehkopf et al. 2016), model 3 was further adjusted for cell type proportions estimated from the same DNA samples, including CD8T, CD4T, natural killer cells, B cells, monocytes, and granulocytes (Houseman et al. 2012).

For assessing the association of measured and genetically determined LTL, LTL was standardized using z-scores. First, we assessed and confirmed whether the previously reported genetic variants of LTL were associated with measured LTL in our cohort using multiple linear regression. The model was adjusted for age, sex, and the first 10 PCs, following the approach described in a previous GWAS (Li et al. 2020). Second, multiple linear regression analyses were applied to examine the association between PRS of LTL and measured LTL, adjusted for age, sex, and the first 10 PCs. Third, the association between PRS of LTL and each vascular phenotype was assessed using multiple linear regression. Base model was adjusted for age, sex, and the first 10 genetic PCs. In model 2, we additionally adjusted for smoking status. Model 3 was further adjusted for BMI. Finally, the association between **Δ**LTL and each vascular phenotype was assessed while adjusting for age, sex, PRS of LTL, BMI and smoking.

To assess whether age, sex, and smoking modified the associations between LTL and vascular phenotypes, we assessed the interaction between age, sex, smoking status and each vascular phenotype. In case of significant interaction effects, additional stratified analyses were performed.

All statistical analyses were performed using R version 3.5.2. All standardized effect estimates are reported with their 95 % confidence intervals (CIs). The statistical significance level was set at $P < 0.05$.

3. Results

3.1 Results study I: Cardiovascular Correlates of Epigenetic Aging across the Adult Lifespan: A population-based Study

The characteristics of the study population are presented in **Table 2**. A total of 3,328 participants had DNA methylation data and were included in the analyses.

Table 2. Characteristics of the study population

	Overall (n=3328)	**Women (n=1864)**	**Men (n=1464)**	***Adjusted p* value***
Demographic characteristics				
Age, year				0.352
Mean (SD)	55.3 (14.3)	55.1 (14.0)	55.5 (14.7)	
Median [Min, Max]	54.0 [30.0, 95.0]	54.0 [30.0, 95.0]	55.0 [30.0, 91.0]	
Education, n (%)				<0.001
Low	67 (2.0 %)	52 (2.8 %)	15 (1.0 %)	
Middle	1484 (44.6 %)	919 (49.3 %)	565 (38.6 %)	
High	1745 (52.4 %)	873 (46.8 %)	872 (59.6 %)	
BMI, kg/m^2, mean (SD)	25.8 (4.4)	25.3 (4.7)	26.5 (3.9)	<0.001
SBP, mmHg, mean (SD)	127 (16.1)	124 (16.8)	131 (14.1)	<0.001
DBP, mmHg, mean (SD)	75.9 (9.3)	74.3 (9.0)	78.0 (9.4)	<0.001
Current smoking, n (%)	424 (12.7 %)	218 (11.7 %)	206 (14.1 %)	0.036
Hypertension, n (%)	1296 (39.0 %)	642 (34.4 %)	654 (44.7 %)	<0.001
Diabetes, n (%)	173 (5.2 %)	68 (3.7 %)	105 (7.2 %)	<0.001
Stroke, n (%)	102 (3.1 %)	47 (2.5 %)	55 (3.8 %)	0.065
Myocardial infarction, n (%)	61 (1.8 %)	15 (0.8 %)	46 (3.1 %)	<0.001
DNAm age acceleration estimators, year, mean (SD)				
AgeAccel.Horvath	0 (5.1)	-0.6 (5.0)	0.7 (5.1)	<0.001
AgeAccel.Hannum	0 (5.7)	-0.9 (5.7)	1.1 (5.5)	<0.001
AgeAccelPheno	0 (6.8)	-0.5 (6.9)	0.6 (6.5)	<0.001
AgeAccelGrim	0 (3.8)	-1.1 (3.4)	1.4 (3.7)	<0.001
Cardiovascular risk factors, arterial stiffness, endothelial function and hemodynamics, mean (SD)				
LDL, mg/dL	126 (35.9)	125 (36.9)	127 (34.7)	0.066
HDL, mg/dL	62.8 (18.0)	70.2 (17.3)	53.5 (14.0)	<0.001
LDL/HDL ratio, %	2.2 (0.9)	1.9 (0.8)	2.6 (1.0)	<0.001

Triglyceride, mg/dL	113 (71.0)	98.5 (52.9)	131 (85.4)	<0.001
Total cholesterol, mg/dL	200 (40.0)	204 (40.4)	195 (38.9)	<0.001
Cystatin C, mg/L	0.9 (0.2)	0.9 (0.2)	1.0 (0.2)	<0.001
Estimated glomerular filtration rate, ml/min/1.73m^2	91.4 (19.3)	91.4 (18.3)	91.3 (20.5)	0.340
C-reactive protein, mg/L	1.9 (3.5)	1.9 (3.5)	1.9 (3.4)	0.650
Percentage of body fat, %	28.4 (9.1)	32.2 (8.6)	23.7 (7.3)	<0.001
Waist circumference, cm	88.2 (13.4)	82.8 (12.1)	95.1 (11.7)	<0.001
Insulin, mIU/L	10.8 (8.1)	9.7 (6.7)	12.1 (9.4)	<0.001
Insulin resistance	2.6 (2.5)	2.2 (1.8)	3.0 (3.0)	<0.001
Glucose, mg/dL	93.0 (17.2)	90.3 (15.8)	96.4 (18.3)	<0.001
HbA1c, mmol/mol	37.0 (6.2)	36.7 (5.6)	37.3 (6.9)	0.010
Mean arterial pressure, mmHg	93.1 (10.6)	90.9 (10.6)	95.8 (9.9)	<0.001
Pulse pressure, mmHg	51.8 (10.6)	50.5 (11.1)	53.3 (9.7)	<0.001
Cardiovascular risk score[#]	0.4 (0.4)	0.1 (0.1)	0.8 (0.2)	<0.001
Total arterial compliance index, mL/mmHg/m^2	1.0 (0.3)	1.1 (0.3)	0.9 (0.2)	<0.001
Pulse wave velocity, m/s	6.8 (1.4)	6.6 (1.4)	7.0 (1.5)	<0.001
Ankle-Brachial index	1.1 (0.1)	1.1 (0.1)	1.2 (0.1)	0.002
Log reactive skin hyperemia, log (%)	5.8 (1.0)	5.8 (1.0)	5.8 (1.0)	0.287
Cardiac index, L/min/m^2	3.2 (0.5)	3.3 (0.5)	3.0 (0.5)	<0.001
Systemic vascular resistance index, dynes· sec/cm^5/m^2	2130 (471)	1980 (405)	2300 (483)	<0.001
Stroke index, mL/m^2	51.8 (8.5)	53.3 (8.5)	50.0 (8.2)	<0.001

Abbreviations: BMI, body mass index; SBP, systolic blood pressure; DBP, diastolic blood pressure; HDL, high-density lipoproteins; LDL, low-density lipoproteins; HbA1c, glycated hemoglobin. SD, standard deviation. The missingness for each variable is less than 5 %. [#]Cardiovascular risk score was calculated among participants < 80 years old without cardiovascular diseases (n=3016). * Comparison between women and men, adjusted for age.

Estimations of DNAm age acceleration

Table 2 displays the descriptive characteristics of AgeAccel.Horvath, AgeAccel.Hannum, AgeAccelPheno, AgeAccelGrim. Compared to women, DNAm age acceleration estimator was significantly higher in men for all the four measures. The correlation structure of DNAm age acceleration estimators is shown in **Figure 1**.

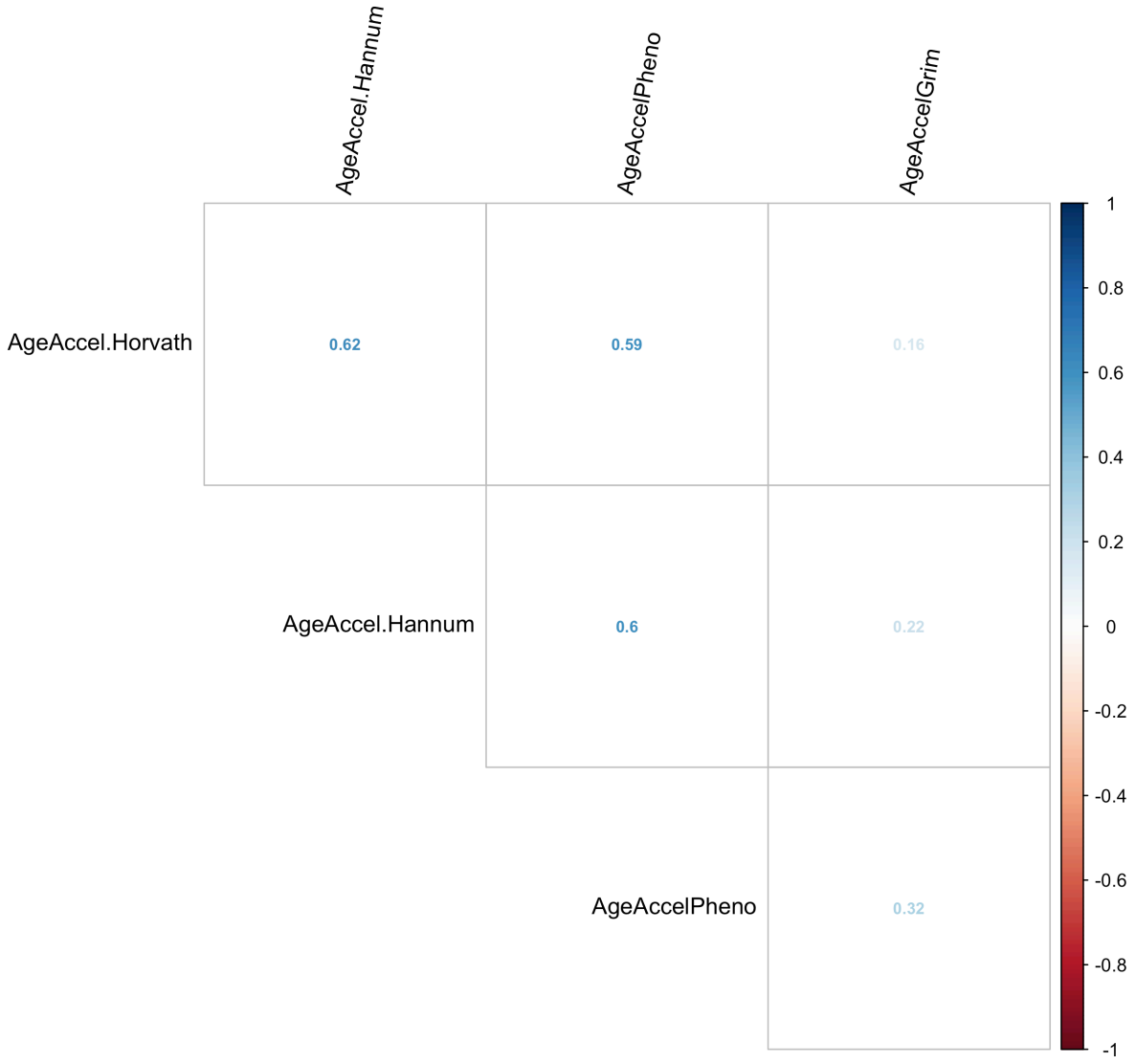

Figure 1. Correlation structure of DNAm age acceleration estimators

Relation between classical cardiovascular risk factors and DNAm age acceleration estimators

Most classical cardiovascular risk factor categories (including lipoproteins, kidney function, inflammation, adiposity and measures of glucose homeostasis) were only weakly correlated with each other (**Figure 2**), suggesting that different risk factor categories represent different physiological domains. **Figure 3** shows the effects of each classical cardiovascular risk factor on DNAm age acceleration estimators within the five categories, i.e. lipoproteins, kidney function, inflammation, adiposity, glucose homeostasis, as well as

an overall cardiovascular risk score. Eleven out of 16 cardiovascular risk factors were significantly associated with all four DNAm age acceleration estimators in model 1. Most of these associations remained significant after adjustment for sex, batch information and smoking status (**Figure 3**). Most DNAm age acceleration estimators decreased by more than 0.30 years per SD increase in kidney function (eGFR) and increased by approximately 0.20 – 0.90 years per SD increase in measures of inflammation (CRP), adiposity (% body fat, BMI, and waist circumference), and glucose homeostasis (insulin, insulin resistance and blood glucose). Moreover, per SD increase in cardiovascular risk score, DNAm age acceleration estimator increased by between 0.80 – 1.40 years, depending on the aging acceleration estimators (**Figure 3**). However, within the lipoprotein category, HDL and triglyceride levels were only associated AgeAccelPheno and AgeAccelGrim. Moreover, except for the CVD risk score, effect sizes were larger for AgeAccelPheno and AgeAccelGrim compared to the AgeAccel.Horvath and AgeAccel.Hannum for all cardiovascular risk factors. These findings indicate that variations in cardiovascular risk factors across multiple physiological domains underlie variations in accelerated biological aging beyond chronological age, and that, compared to the first-generation aging acceleration estimators, lifespan acceleration estimators are more sensitive in capturing age-related changes across different physiological systems.

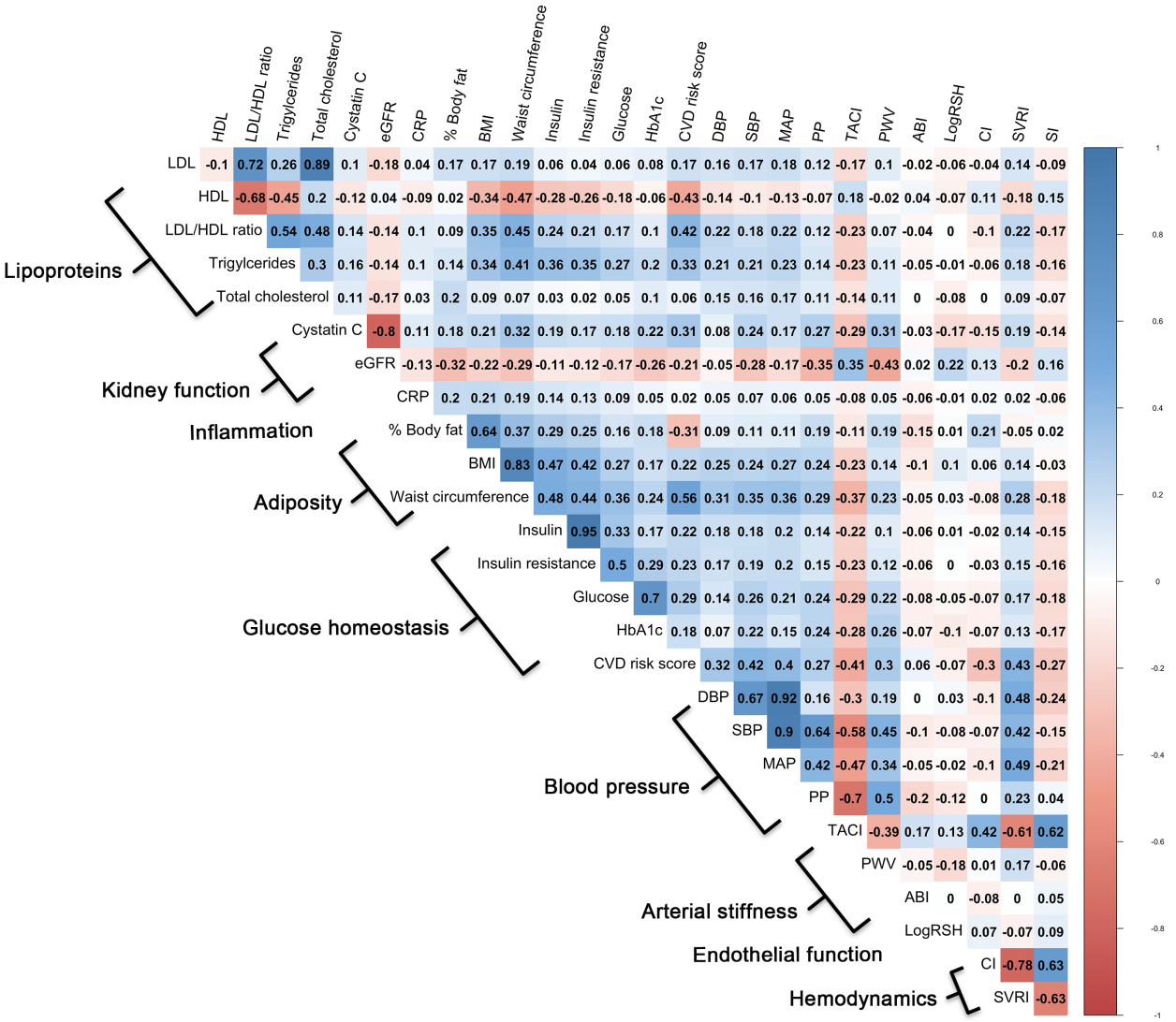

Figure 2. Correlation structure of cardiovascular variables

Abbreviations: LDL, low-density lipoproteins; HDL, high-density lipoproteins; eGFR, estimated glomerular filtration rate; CRP, C-reactive protein; BMI, body mass index; HbA1c, glycated hemoglobin; DBP, diastolic blood pressure; SBP, systolic blood pressure; MAP, mean arterial pressure; PP, pulse pressure; TACI, total arterial compliance index; PWV, pulse wave velocity; ABI, ankle-brachial index; RSH, reactive skin hyperemia; CI, cardiac index; SVRI, systemic vascular resistance index; SI, stroke index

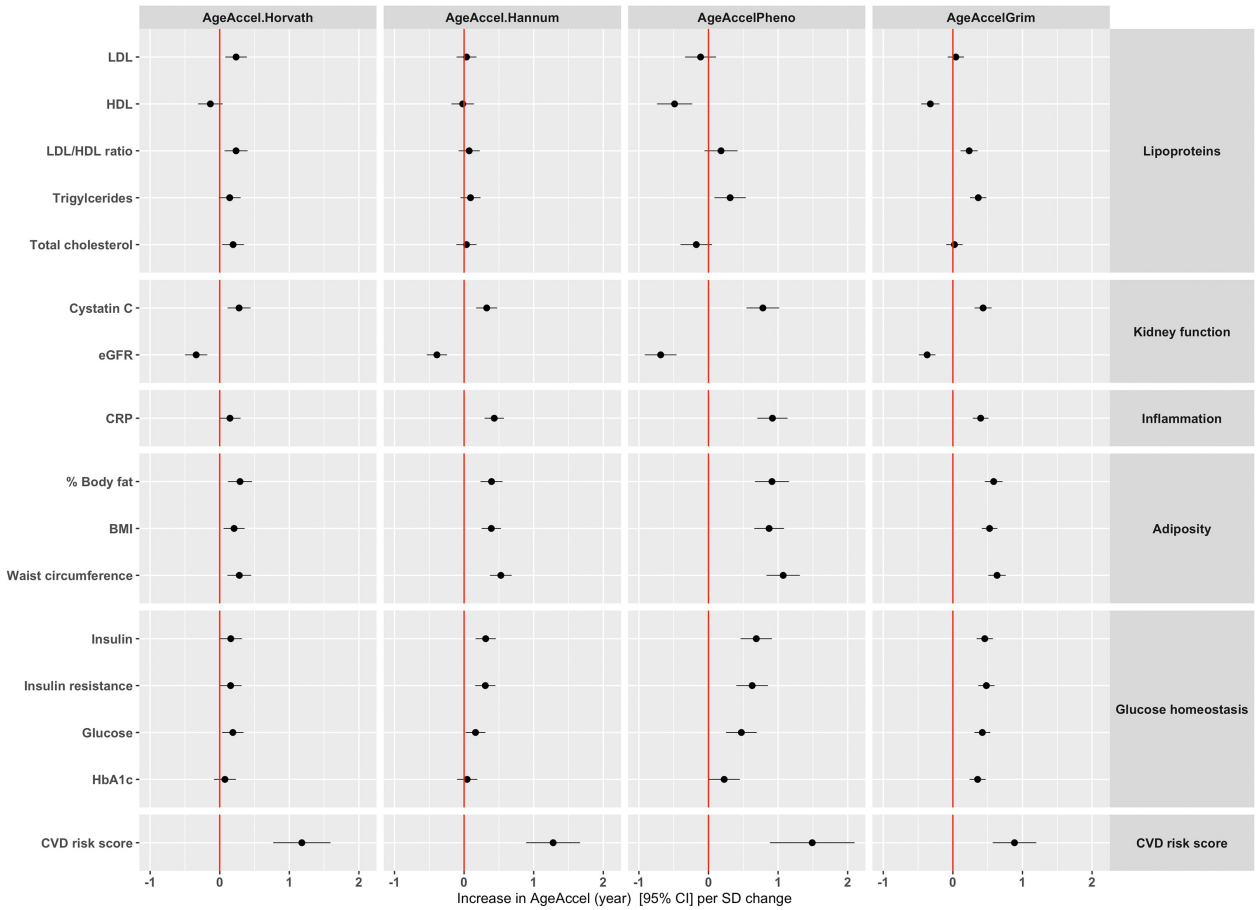

Figure 3. Relation between classical cardiovascular risk factors and DNAm age acceleration estimators
Abbreviations: LDL, low-density lipoproteins; HDL, high-density lipoproteins; eGFR, estimated glomerular filtration rate; CRP, C-reactive protein; BMI, body mass index; HbA1c, glycated hemoglobin; SD, standard deviation.
Model: DNAm age acceleration estimator ~ each independent variable + batch information + sex + smoking status.

Relation between blood pressure, arterial stiffness, endothelial function, hemodynamics and DNAm age acceleration estimators

Measures of blood pressure, arterial stiffness, endothelial function and hemodynamics were only weakly correlated with most of the classical cardiovascular risk factors and across the categories, with expected higher correlation within each category (**Figure 2**). Measures of blood pressure (including DBP, SBP, MAP), arterial stiffness (including TACI and PWV) and hemodynamic function (SI) were consistently associated with different DNAm age acceleration estimators (**Figure 4**). Most DNAm age acceleration estimators increased by more than 0.20 years per SD increase of DBP, SBP, MAP, and PWV, while

they decreased by around 0.20 years for each SD increase of TACI and SI. Endothelial function was only significantly associated with AgeAccelGrim [-0.13 (-0.25, -0.01)].

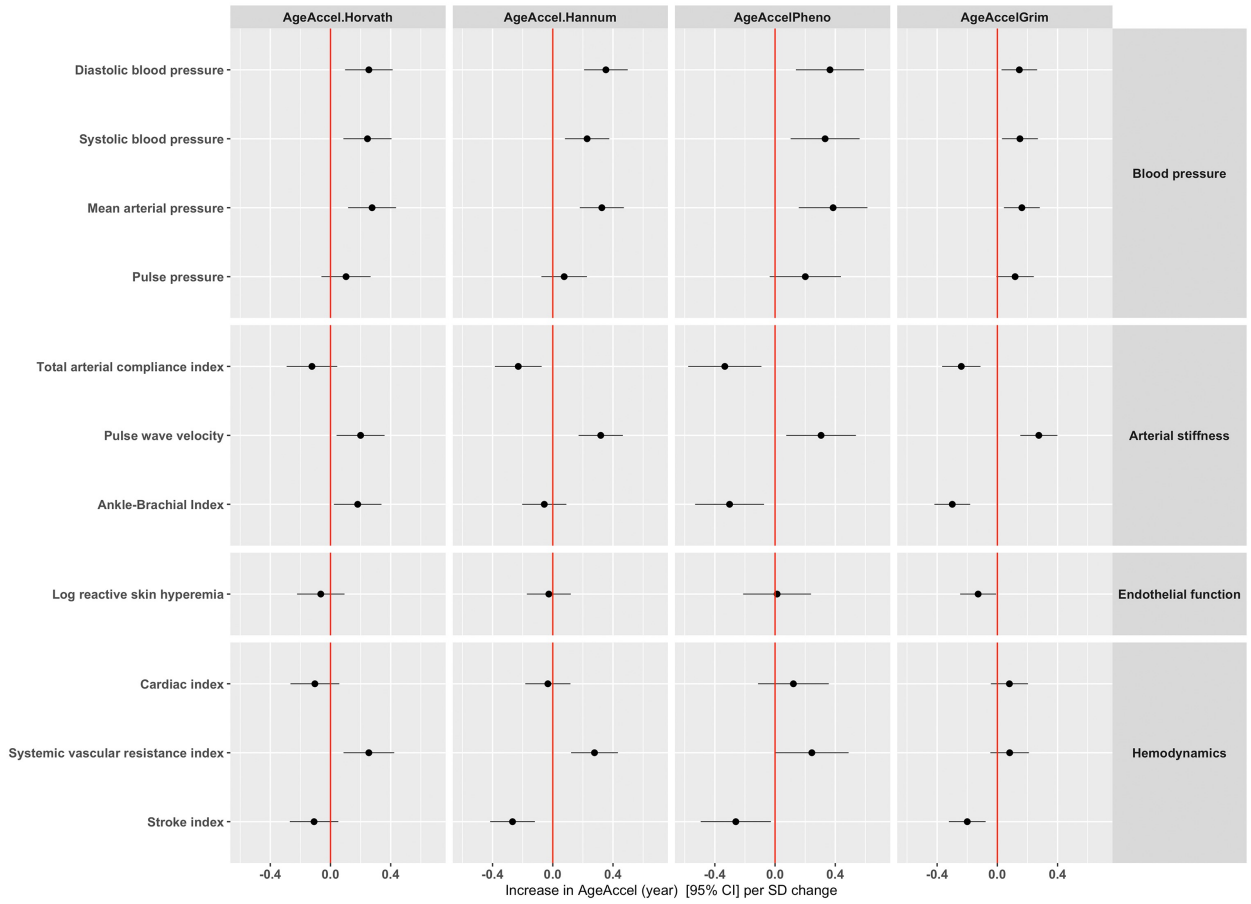

Figure 4. Relation between quantitative markers of cardiovascular aging and DNAm age acceleration estimators
Model: DNAm age acceleration estimator ~ each independent variable + batch information + sex + smoking status.

The independent effects of cardiovascular risk factor clusters on DNAm age acceleration estimators

Conforming to their known physiological interrelations, hierarchical clustering of the classical cardiovascular risk factors yielded five categories **(Figure 5A)**, comprising of lipoproteins (LDL, total cholesterol, triglyceride, HDL, LDL/HDL ratio), kidney function (cystatin C and eGFR), inflammation (CRP), adiposity (% Body fat, BMI, waist circumference), and glucose homeostasis (insulin, insulin resistance, glucose, HbA1c). Decreased kidney function, increased inflammation and adiposity profiles were

independently associated with higher AgeAccel.Hannum, AgeAccelPheno and AgeAccelGrim after adjusting for sex, batch information, and smoking status. Lower levels of lipoproteins or higher levels of glucose homeostasis was also independently associated with higher AgeAccelPheno and AgeAccelGrim. Higher levels of lipoproteins, and decreased kidney function were independently associated with higher AgeAccel.Horvath **(Figure 6).**

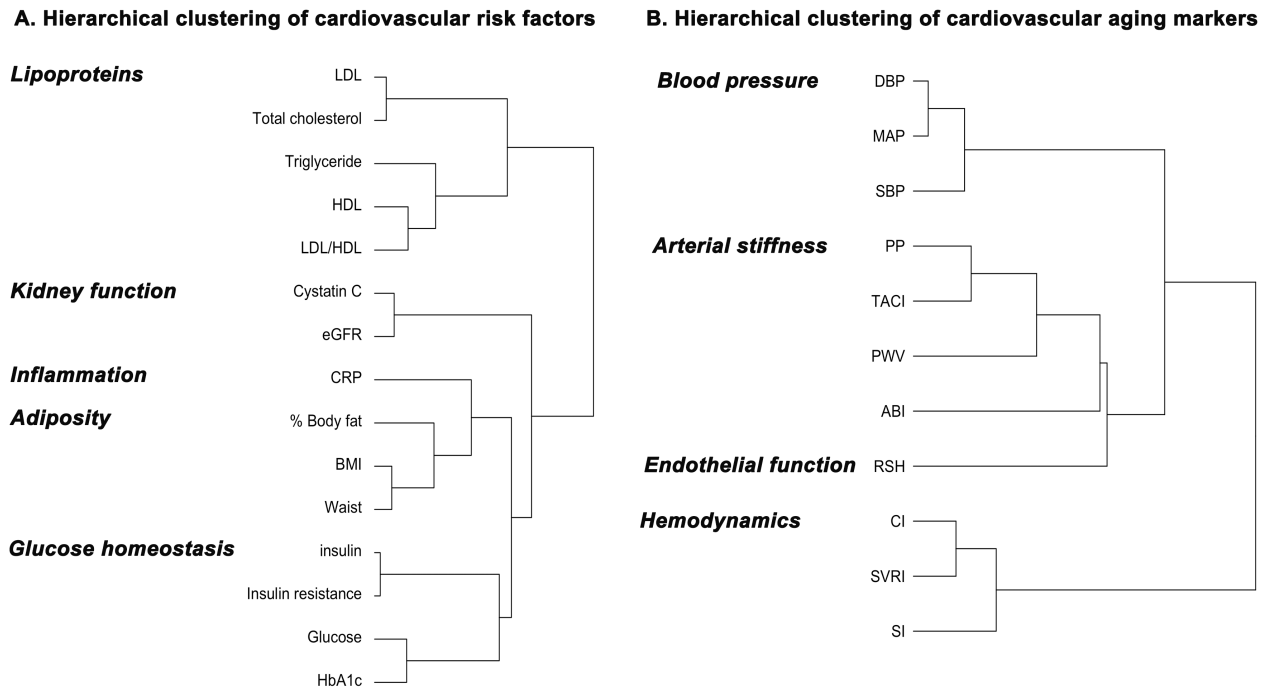

Figure 5. Hierarchical clustering of cardiovascular correlates
Abbreviations: LDL, low-density lipoproteins; HDL, high-density lipoproteins; eGFR, estimated glomerular filtration rate; CRP, C-reactive protein; BMI, body mass index; HbA1c, glycated hemoglobin; DBP, diastolic blood pressure; MAP, mean arterial pressure; SBP, systolic blood pressure; PP, pulse pressure; TACI, total arterial compliance index; PWV, pulse wave velocity; ABI, ankle-brachial index; RSH, reactive skin hyperemia; CI, cardiac index; SVRI, systemic vascular resistance index; SI, stroke index.

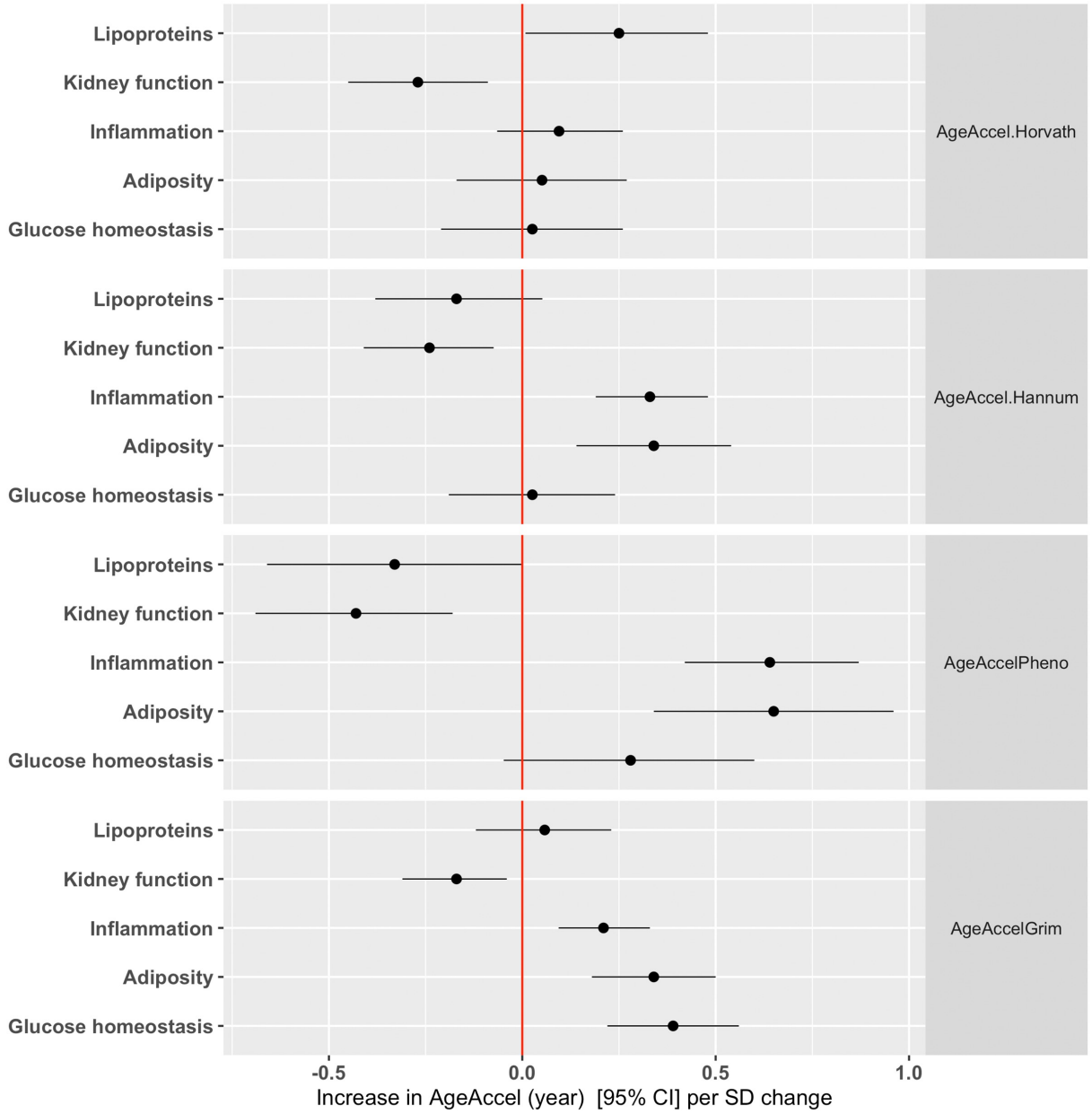

Figure 6. Independent effects of cardiovascular risk factor clusters on DNAm age acceleration estimators

Model: DNAm age acceleration estimator ~ Lipoproteins + Kidney function + Inflammation + Adiposity + Glucose homeostasis + Sex + Batch information + Smoking status.

The independent effects of quantitative markers of cardiovascular aging clusters on DNAm age acceleration estimators

Conforming to their known physiological interrelations, hierarchical clustering of quantitative markers of cardiovascular aging yielded four categories, comprising of blood pressure (DBP, MAP, SBP), arterial stiffness (PP, TACI, PWV, ABI), endothelial function (RSH), and hemodynamics (CI, SVRI, SI) **(Figure 5B**). An unfavourable blood pressure

profile was independently associated with AgeAccel.Horvath and AgeAccel.Hannum, whereas arterial stiffness was independently associated with AgeAccelPheno and AgeAccelGrim **(Figure 7)**.

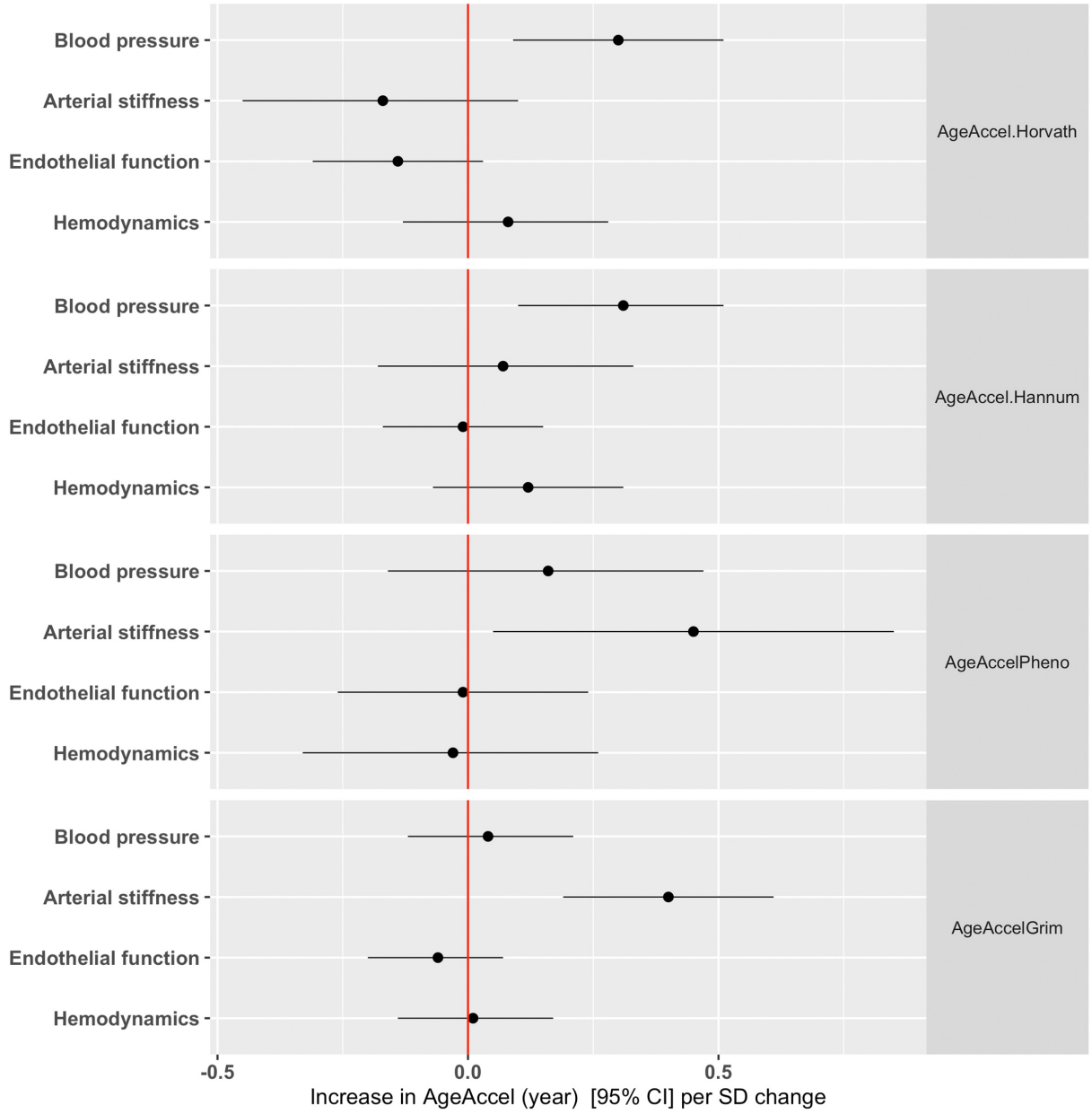

Figure 7. Independent effects of blood pressure, arterial stiffness, endothelial function and hemodynamics clusters on DNAm age acceleration estimators
Model: DNAm age acceleration estimator ~ Blood pressure + Arterial stiffness + Endothelial function + Hemodynamics + Sex + Batch information + Smoking status

Sex-stratified analyses

All four DNAm age acceleration estimators were consistently higher in men compared to women (**Table 2**). Several sex-specific effects of classical cardiovascular risk factors on AgeAccelGrim were observed (**Figure 8**). **Table 3** shows the effects of unfavorable profiles of cystatin C, eGFR, CRP, % body fat, glucose, and HbA1c on AgeAccelGrim were more than 0.20 year/SD larger in men than in women. Sex differences were more apparent when assessing the effects of arterial stiffness, endothelial function and hemodynamics on DNAm age acceleration estimators (**Figure 8**). Compared to women, men with an unfavorable arterial stiffness (e.g. higher PWV) and hemodynamic profile (e.g. higher SVRI, lower SI) had around 0.30 year/SD higher increases in AgeAccel.Hannum, AgeAccelPheno, AgeAccelGrim (**Table 3**).

Sensitivity analyses

The estimated effects of all cardiovascular risk factors and cardiovascular aging markers on DNAm age acceleration estimators remained virtually identical after exclusion of participants with diabetes or who had had a stroke or myocardial infarction (n = 305). We also examined potentially nonlinear relationships between cardiovascular risk factors and cardiovascular aging markers and DNAm age acceleration estimators. None of the associations obviously deviated from linearity.

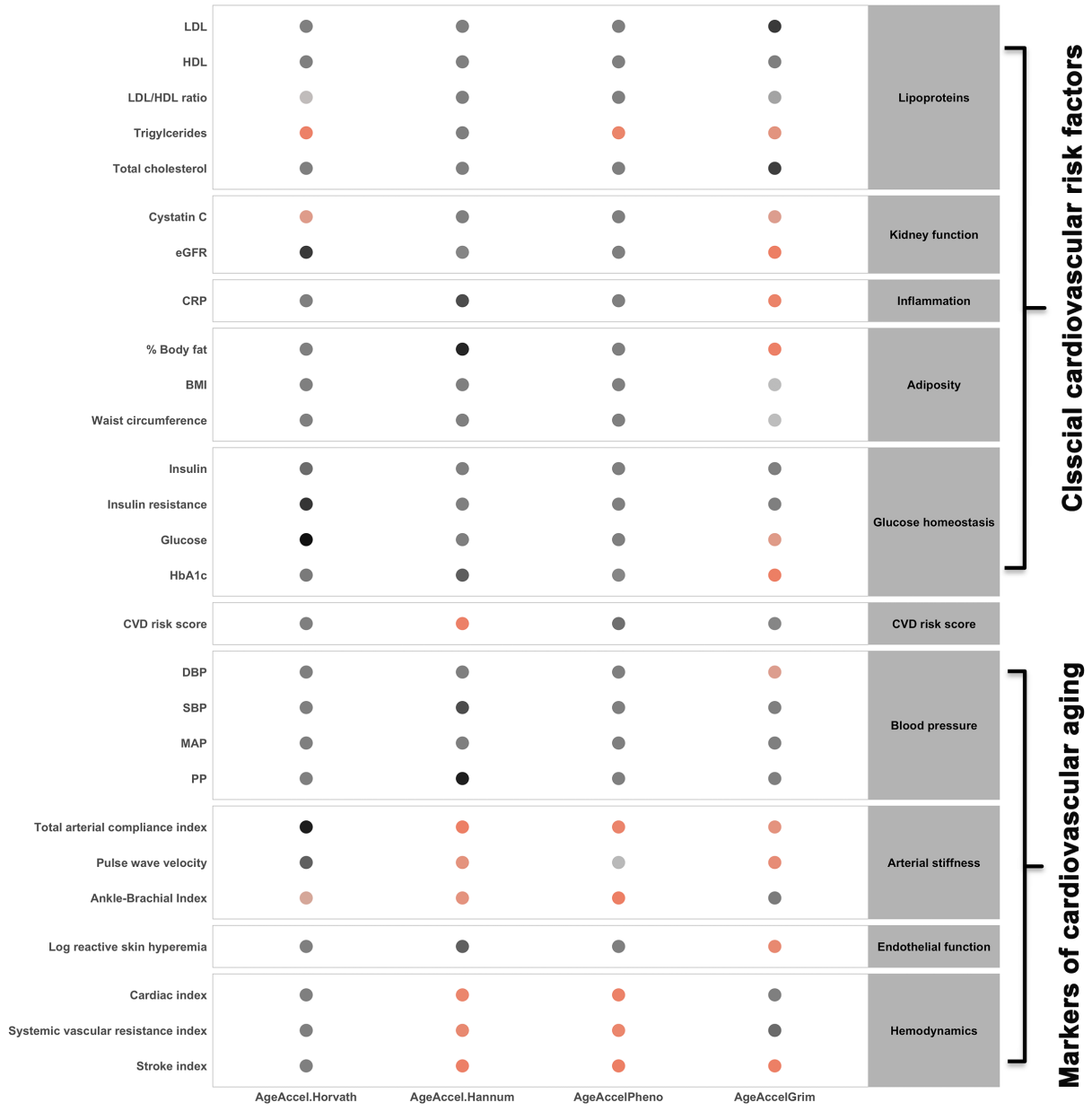

Figure 8. Assessment of interaction effects between sex and cardiovascular variables on DNAm age acceleration estimators

Abbreviations: LDL, low-density lipoproteins; HDL, high-density lipoproteins; eGFR, estimated glomerular filtration rate; CRP, C-reactive protein; BMI, body mass index; HbA1c, glycated hemoglobin; DBP, diastolic blood pressure; MAP, mean arterial pressure; SBP, systolic blood pressure; PP, pulse pressure.

Table 3. Sex-stratified analyses of the relation between cardiovascular variables and DNAm age acceleration estimators

Determinant (Standardized)	Increase in AgeAccel.Horvath (year)		Increase in AgeAccel.Hannum (year)		Increase in AgeAccelPheno (year)		Increase in AgeAccelGrim (year)	
	Men	Women	Men	Women	Men	Women	Men	Women
	Estimate (95 % CI)	Estimate (95 % CI)	Estimate (95 % CI)	Estimate (95 % CI)	Estimate (95 % CI)	Estimate (95 % CI)	Estimate (95 % CI)	Estimate (95 % CI)
Cardiovascular risk factors								
LDL	0.21 (-0.06, 0.49)	0.25 (0.05, 0.46)	-0.04 (-0.29, 0.21)	0.04 (-0.16, 0.24)	-0.24 (-0.61, 0.13)	-0.06 (-0.38, 0.26)	-0.09 (-0.3, 0.13)	0.13 (-0.02, 0.29)
HDL	-0.20 (-0.55, 0.14)	-0.10 (-0.33, 0.13)	-0.16 (-0.47, 0.14)	-0.02 (-0.24, 0.2)	-0.58 (-1.03, -0.12)	-0.48 (-0.84, -0.13)	-0.45 (-0.71, -0.18)	-0.24 (-0.40, -0.07)
HDL/LDL ratio	0.16 (-0.11, 0.42)	0.34 (0.09, 0.59)	0.05 (-0.19, 0.28)	0.09 (-0.14, 0.33)	0.07 (-0.28, 0.42)	0.29 (-0.09, 0.68)	0.15 (-0.06, 0.35)	0.31 (0.12, 0.49)
Triglycerides	-0.02 (-0.24, 0.21)	***0.43*** ***(0.15, 0.71)***	0.08 (-0.11, 0.28)	0.22 (-0.05, 0.49)	0.10 (-0.19, 0.39)	***0.78*** ***(0.35, 1.22)***	0.28 (0.11, 0.45)	***0.54*** ***(0.34, 0.75)***
Total cholesterol	0.13 (-0.14, 0.41)	0.24 (0.03, 0.46)	-0.07 (-0.31, 0.18)	0.05 (-0.15, 0.26)	-0.33 (-0.69, 0.04)	-0.08 (-0.41, 0.25)	-0.10 (-0.31, 0.11)	0.13 (-0.02, 0.29)
Cystatin C	0.21 (-0.05, 0.47)	0.38 (0.13, 0.62)	0.41 (0.18, 0.64)	0.32 (0.09, 0.56)	0.84 (0.50, 1.17)	0.80 (0.42, 1.18)	***0.59*** ***(0.40, 0.79)***	0.30 (0.12, 0.48)
eGFR	-0.30 (-0.56, -0.05)	-0.38 (-0.61, -0.14)	-0.51 (-0.73, -0.28)	-0.35 (-0.58, -0.13)	-0.86 (-1.19, -0.52)	-0.59 (-0.95, -0.23)	***-0.57*** ***(-0.76, -0.37)***	-0.21 (-0.39, -0.04)
CRP	0.13 (-0.13, 0.4)	0.16 (-0.04, 0.37)	***0.57*** ***(0.34, 0.8)***	0.38 (0.19, 0.58)	0.83 (0.49, 1.18)	0.92 (0.6, 1.23)	***0.55*** ***(0.35, 0.75)***	0.24 (0.09, 0.40)
% Body fat	0.25 (-0.07, 0.58)	0.34 (0.11, 0.57)	0.51 (0.23, 0.8)	0.35 (0.13, 0.56)	0.93 (0.5, 1.36)	0.92 (0.58, 1.26)	***0.80*** ***(0.55, 1.05)***	0.45 (0.28, 0.61)
BMI	0.03 (-0.26, 0.32)	0.32 (0.12, 0.52)	0.37 (0.12, 0.63)	0.39 (0.2, 0.58)	0.77 (0.39, 1.15)	0.90 (0.6, 1.2)	***0.55*** ***(0.33, 0.77)***	0.45 (0.31, 0.60)
Waist circumference	0.13 (-0.17, 0.43)	0.39 (0.15, 0.63)	0.54 (0.28, 0.81)	0.53 (0.3, 0.75)	0.94 (0.55, 1.34)	1.10 (0.74, 1.45)	0.69 (0.46, 0.92)	0.55 (0.38, 0.72)
Insulin	0.05 (-0.18, 0.28)	0.29 (0.02, 0.55)	0.32 (0.12, 0.53)	0.31 (0.06, 0.56)	0.48 (0.18, 0.78)	0.85 (0.44, 1.25)	0.43 (0.25, 0.6)	0.41 (0.22, 0.60)
Insulin resistance	0.09 (-0.13, 0.3)	0.28 (-0.01, 0.58)	0.32 (0.13, 0.51)	0.33 (0.05, 0.61)	0.43 (0.15, 0.71)	0.87 (0.42, 1.32)	0.42 (0.26, 0.59)	0.51 (0.30, 0.72)
Glucose	0.19 (-0.05, 0.44)	0.22 (-0.01, 0.45)	0.15 (-0.07, 0.37)	0.25 (0.03, 0.47)	0.55 (0.23, 0.88)	0.41 (0.06, 0.76)	***0.60*** ***(0.41, 0.79)***	0.29 (0.12, 0.45)
HbA1c	0 (-0.25, 0.25)	0.16 (-0.08, 0.4)	***0.22*** ***(0, 0.44)***	-0.05 (-0.28, 0.18)	0.42 (0.09, 0.74)	0.10 (-0.27, 0.47)	***0.58*** ***(0.39, 0.77)***	0.20 (0.02, 0.38)
Cardiovascular Disease risk score*								
CVD risk score	0.93 (0.42, 1.44)	0.34 (-0.56, 1.24)	***1.15*** ***(0.7, 1.59)***	0.20 (-0.65, 1.06)	1.53 (0.86, 2.2)	0.72 (-0.67, 2.1)	0.92 (0.54, 1.31)	0.54 (-0.12, 1.2)
Blood pressure, arterial stiffness, endothelial function and hemodynamics								
DBP	0.28 (0.01, 0.54)	0.24 (0.02, 0.47)	0.32 (0.08, 0.55)	0.34 (0.12, 0.55)	0.37 (0.03, 0.72)	0.33 (-0.01, 0.68)	0.02 (-0.18, 0.22)	0.26 (0.1, 0.43)
SBP	0.25 (-0.05, 0.56)	0.19 (-0.02, 0.4)	0.29 (0.01, 0.56)	0.2 (0, 0.4)	0.38 (-0.02, 0.79)	0.24 (-0.08, 0.56)	0.22 (-0.02, 0.46)	0.19 (0.04, 0.34)

MAP	0.30 (0.02, 0.58)	0.23 (0.02, 0.45)	0.34 (0.09, 0.59)	0.29 (0.09, 0.5)	0.42 (0.05, 0.8)	0.31 (-0.02, 0.65)	0.11 (-0.11, 0.33)	0.25 (0.09, 0.41)
TACI	-0.26 (-0.59, 0.07)	-0.01 (-0.23, 0.21)	***-0.53 (-0.82, -0.24)***	-0.08 (-0.29, 0.13)	-0.60 (-1.04, -0.17)	-0.07 (-0.41, 0.28)	***-0.47 (-0.72, -0.22)***	-0.18 (-0.35, -0.01)
PWV	***0.38 (0.11, 0.64)***	0.08 (-0.15, 0.31)	***0.51 (0.28, 0.74)***	0.15 (-0.08, 0.37)	***0.49 (0.14, 0.84)***	0.13 (-0.24, 0.5)	***0.43 (0.23, 0.63)***	0.19 (0, 0.38)
ABI	***0.31 (0.05, 0.57)***	0.05 (-0.19, 0.29)	0.05 (-0.18, 0.28)	-0.32 (-0.56, -0.09)	0.03 (-0.32, 0.37)	***-0.77 (-1.15, -0.39)***	***-0.25 (-0.44, -0.05)***	-0.42 (-0.6, -0.24)
Log RSH	-0.22 (-0.49, 0.04)	-0.04 (-0.26, 0.19)	-0.16 (-0.4, 0.08)	0.07 (-0.14, 0.28)	-0.31 (-0.66, 0.04)	0.15 (-0.19, 0.49)	***-0.29 (-0.50, -0.08)***	0.02 (-0.14, 0.19)
CI	-0.23 (-0.53, 0.07)	0.03 (-0.19, 0.24)	-0.09 (-0.35, 0.18)	0.15 (-0.06, 0.36)	-0.26 (-0.66, 0.13)	***0.43 (0.09, 0.77)***	0.08 (-0.15, 0.31)	0.13 (-0.03, 0.30)
SVRI	0.34 (0.07, 0.60)	0.10 (-0.16, 0.36)	***0.31 (0.08, 0.54)***	0.04 (-0.21, 0.29)	***0.48 (0.13, 0.83)***	-0.19 (-0.60, 0.22)	0.14 (-0.06, 0.35)	-0.01 (-0.21, 0.19)
SI	-0.24 (-0.52, 0.04)	0.00 (-0.23, 0.22)	***-0.48 (-0.72, -0.23)***	-0.08 (-0.30, 0.14)	***-0.78 (-1.15, -0.41)***	0.20 (-0.15, 0.56)	***-0.42 (-0.63, -0.20)***	-0.06 (-0.23, 0.11)

Abbreviations: LDL, low-density lipoproteins; HDL, high-density lipoproteins; eGFR, estimated glomerular filtration rate; CRP, C-reactive protein; BMI, body mass index; HbA1c, glycated hemoglobin; DBP, diastolic blood pressure; SBP, systolic blood pressure; MAP, mean arterial pressure; TACI, total arterial compliance index; PWV, pulse wave velocity; ABI, Ankle-brachial index; RSH, reactive skin hyperemia; CI, cardiac index; SVRI, Systemic vascular resistance index; SI, stroke index.
*The analyses were among participants < 80 years old without cardiovascular diseases (n=3016).
The missingness for each determinant is less than 5 %.
Boldface indicates statistical significance.

3.2 Results study II: The Lipidomic Correlates of Epigenetic Aging across the Adult Lifespan: A Population-based Study

Estimations of DNAm age acceleration

The characteristics of the study population are presented in **Table 4**. AgeAccelPheno and AgeAccelGrim were significantly higher in men than in women.

Table 4. Characteristics of the study population

	Overall (N=4181)	Women (N=2354)	Men (N=1827)	*Adjusted p* value*
Age, year				
Mean (SD)	55.1 (14.0)	54.9 (13.7)	55.3 (14.4)	<0.001
Median [Min, Max]	55.0 [30.0, 95.0]	54.0 [30.0, 95.0]	55.0 [30.0, 91.0]	
Current smoking, n (%)	529 (12.7 %)	279 (11.9 %)	250 (13.7 %)	0.068
BMI, kg/m^2, mean (SD)	25.9 (4.5)	25.4 (4.8)	26.5 (3.9)	<0.001
SBP, mmHg, mean (SD)	126 (15.9)	123 (16.4)	131 (14.1)	<0.001
DBP, mmHg, mean (SD)	75.5 (9.4)	73.8 (9.1)	77.5 (9.3)	<0.001
Hypertension, n (%)	1569 (37.5 %)	783(33.2 %)	786 (43.1 %)	<0.001
Diabetes, n (%)	218 (5.2 %)	85 (3.6 %)	133 (7.3 %)	<0.001
HDL, mg/dL	62.6 (17.9)	69.9 (17.3)	53.2 (13.9)	<0.001
LDL, mg/dL	126 (35.6)	126 (36.4)	127 (34.6)	0.137
Cholesterol, mg/dL	199 (39.3)	203 (39.6)	194 (38.4)	<0.001
Triglyceride, mg/dL	112 (70.4)	97.9 (51.7)	130 (85.6)	<0.001
DNAm age acceleration estimators, year, mean (SD)				
AgeAccelPheno	0.2 (6.6)	-0.3 (6.7)	0.8 (6.4)	<0.001
AgeAccelGrim	0.0 (6.8)	-1.0 (6.6)	1.3 (6.8)	<0.001
Complex lipid class, *μM*, mean (SD)				
Neutral lipids				
Cholesteryl ester (CE)	2870 (645)	2900 (654)	2820 (632)	<0.001
Monoacylglycerol (MAG)	2.2 (5.34)	2.1 (3.99)	2.4 (6.69)	0.070
Diacylglycerol (DAG)	25.9 (16.2)	22.8 (12.1)	29.9 (19.6)	<0.001
Triacylglycerol (TAG)	1060 (667)	924 (511)	1230 (794)	<0.001
Phospholipids				
Phosphatidylcholine (PC)	2010 (408)	2080 (401)	1920 (399)	<0.001
Phosphatidylethanolamine (PE)	157 (42.8)	161 (41.6)	152 (43.7)	<0.001
Phosphatidylinositol (PI)	38.1 (10.2)	39.2 (10.2)	36.8 (10.1)	<0.001

Lysophosphatidylcholine (LPC)	163 (38.4)	156 (36.6)	171 (38.9)	<0.001
Lysophosphatidylethanolamine (LPE)	6.2 (2.1)	6.1 (2.1)	6.3 (2.2)	0.001
Sphingolipids				
Sphingomyelin (SM)	486 (89.3)	505 (90.0)	460 (81.9)	<0.001
Ceramide (CER)	5.1 (1.4)	5.0 (1.4)	5.2 (1.4)	<0.001
Dihydroceramide (DCER)	1.3 (0.4)	1.3 (0.4)	1.3 (0.5)	<0.001
Hexosylceramide (HCER)	4.3 (1.2)	4.4 (1.2)	4.3 (1.1)	0.077
Lactosylceramide (LCER)	3.4 (0.8)	3.5 (0.8)	3.3 (0.7)	<0.001

Abbreviations: BMI, body mass index; SBP, systolic blood pressure; DBP, diastolic blood pressure; HDL, high-density lipoproteins; LDL, low-density lipoproteins; SD, standard deviation. The missingness for each variable is less than 5 %.
* Comparison between women and men, adjusted for age.

Associations of lipid class and molecular species with DNAm age acceleration estimators

Age-, sex-, and batch-adjusted partial-correlations showed that all lipid classes except for MAG, LPE, LPC were moderately to highly correlated. The strongest correlations for LDL and cholesterol were with CE, PC, PI and sphingolipids, whereases HDL was only weakly correlated with almost all main lipid classes, except for DAG and TAG. As expected, clinically measured total triglycerides were highly correlated with DAG and TAG, and moderately correlated with PC, PE, PI, CER and DCER. BMI was only weakly correlated with DAG, TAG, LPC, LPE, HCER, and LCER (**Figure 9**).

Out of 964 lipid species, 196 and 525 were associated with AgeAccelPheno and AgeAccelGrim at FDR < 0.05, respectively (**Figure 10).** For MAG, TAG, DAG, PE, CER and DCER classes, each SD concentration increase in each molecular species was associated with around 0.25 – 0.75 year increase in AgeAccelPheno and AgeAccelGrim. For LPC, HCER and LCER classes, each SD concentration increase in each molecular species was associated with around 0.25 – 1.00 year decrease in AgeAccelPheno and AgeAccelGrim. Concentration changes of molecular species in CE, PC, PI, and LPE classes were both negatively and positively associated with AgeAccelPheno and AgeAccelGrim. However, there were more molecular species associated with AgeAccelGrim, and the effect sizes were larger compared to AgeAccelPheno (**Figure 10**).

After adjustment for HDL and/or LDL levels, the associations of many molecular species belonging to the neutral lipids and phospholipids classes − especially TAG, DAG, PC, PE – with AgeAccelPheno and AgeAccelGrim became non-significant. Conversely, adjustment for HDL and/or LDL levels did not materially affect the results for sphingolipids. These findings are in line with the known function of lipoproteins as key regulators of mainly neutral lipids and phospholipids metabolism, which however, have a smaller influence on sphingolipids metabolism (Borodzicz et al. 2015). The results remained almost identical after adjustment for BMI (**Figure 10**).

As LPC species were mainly negatively associated with both AgeAccelPheno and AgeAccelGrim, but the pattern across all the species remains unknown. **Figure 11** shows more details of all the LPC species. In general, the effect sizes increased with shorter chain lengths for SFA (except for LPC 16:0). There is no clear pattern for double bonds. LPE species showed a very similar pattern of association with AgeAccelPheno and AgeAccelGrim (**Figure 11**).

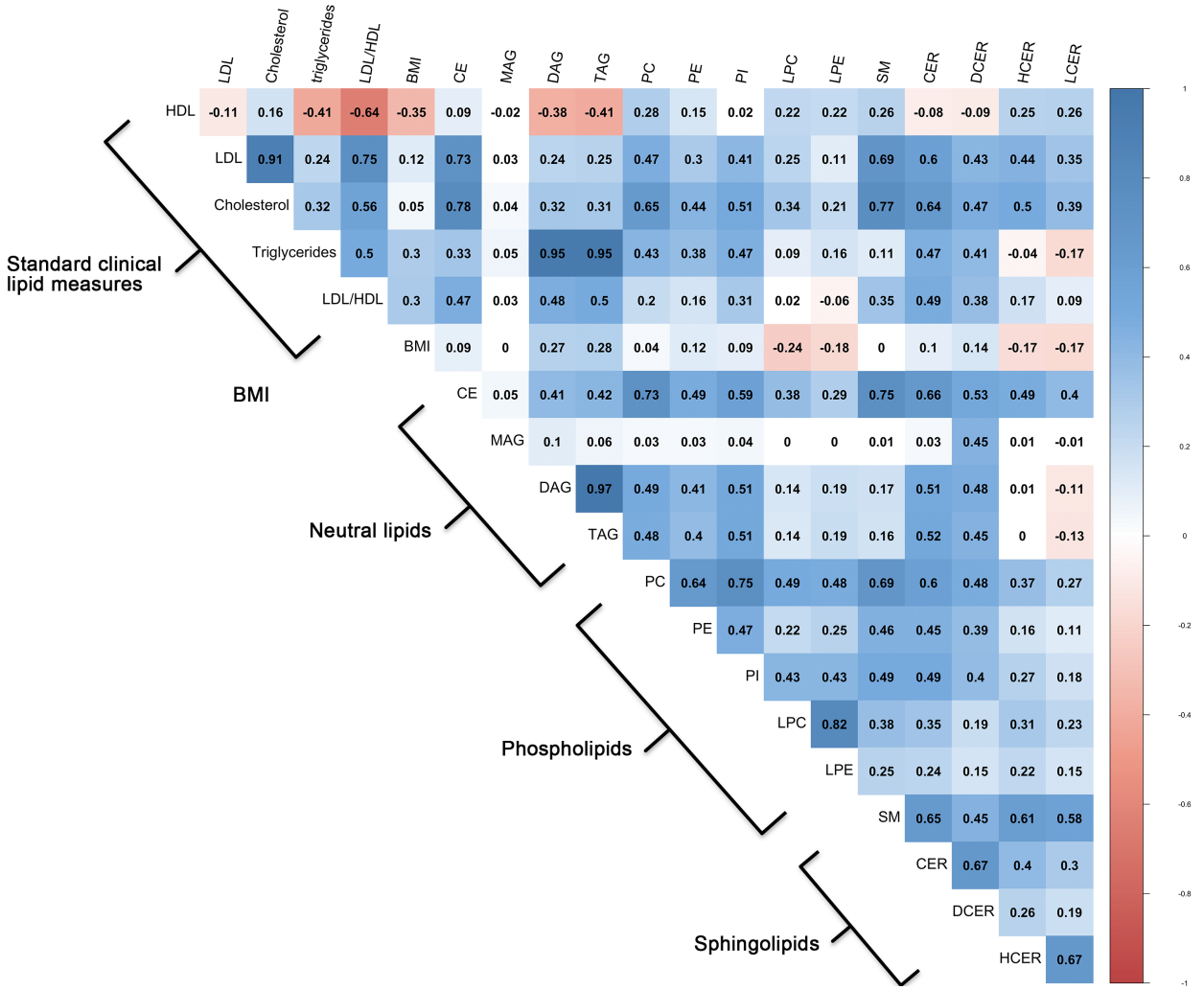

Figure 9. Age, sex, batch-adjusted partial-correlation matrix of standard clinical lipid measures, BMI, and main lipid classes

Abbreviations: high-density-lipoprotein (HDL), low-density-lipoprotein (LDL), BMI, body mass index, cholesteryl ester (CE), triacylglycerol (TAG), diacylglycerol (DAG), monoacylglycerol (MAG), phosphatidylcholine (PC), phosphatidylethanolamine (PE), phosphatidylinositol (PI), lysophosphatidylcholine (LPC), lysophosphatidylethanolamine (LPE), sphingomyelin (SM), ceramide (CER), hexosylceramide (HCER), lactosylceramide (LCER), dihydroceramide (DCER).

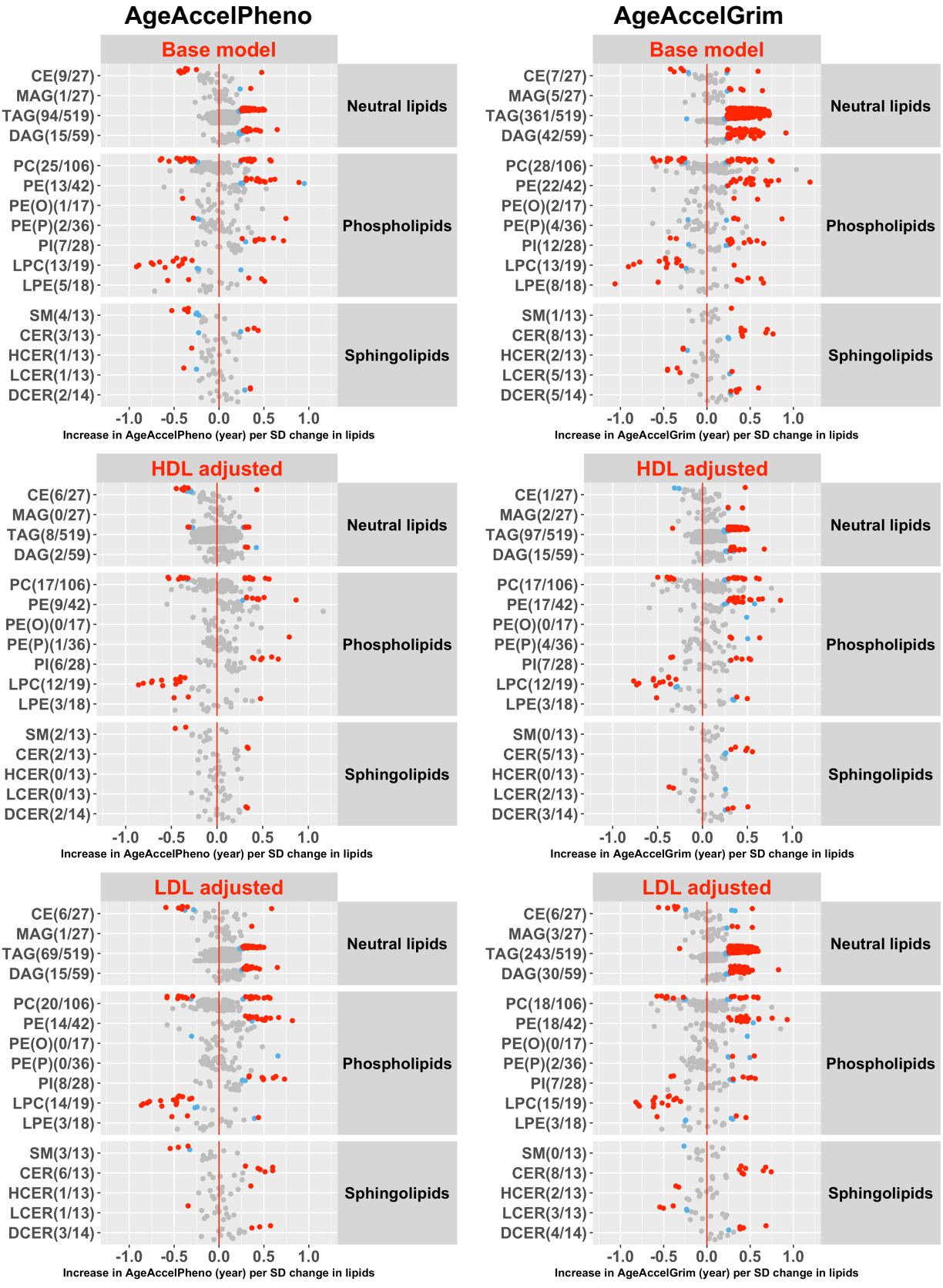
AgeAccelPheno
AgeAccelGrim
Base model
HDL adjusted
LDL adjusted
Neutral lipids
Phospholipids
Sphingolipids
CE(9/27)
MAG(1/27)
TAG(94/519)
DAG(15/59)
PC(25/106)
PE(13/42)
PE(O)(1/17)
PE(P)(2/36)
PI(7/28)
LPC(13/19)
LPE(5/18)
SM(4/13)
CER(3/13)
HCER(1/13)
LCER(1/13)
DCER(2/14)
CE(7/27)
MAG(5/27)
TAG(361/519)
DAG(42/59)
PC(28/106)
PE(22/42)
PE(O)(2/17)
PE(P)(4/36)
PI(12/28)
LPC(13/19)
LPE(8/18)
SM(1/13)
CER(8/13)
HCER(2/13)
LCER(5/13)
DCER(5/14)
CE(6/27)
MAG(0/27)
TAG(8/519)
DAG(2/59)
PC(17/106)
PE(9/42)
PE(O)(0/17)
PE(P)(1/36)
PI(6/28)
LPC(12/19)
LPE(3/18)
SM(2/13)
CER(2/13)
HCER(0/13)
LCER(0/13)
DCER(2/14)
CE(1/27)
MAG(2/27)
TAG(97/519)
DAG(15/59)
PC(17/106)
PE(17/42)
PE(O)(0/17)
PE(P)(4/36)
PI(7/28)
LPC(12/19)
LPE(3/18)
SM(0/13)
CER(5/13)
HCER(0/13)
LCER(2/13)
DCER(3/14)
CE(6/27)
MAG(1/27)
TAG(69/519)
DAG(15/59)
PC(20/106)
PE(14/42)
PE(O)(0/17)
PE(P)(0/36)
PI(8/28)
LPC(14/19)
LPE(3/18)
SM(3/13)
CER(6/13)
HCER(1/13)
LCER(1/13)
DCER(3/14)
CE(6/27)
MAG(3/27)
TAG(243/519)
DAG(30/59)
PC(18/106)
PE(18/42)
PE(O)(0/17)
PE(P)(2/36)
PI(7/28)
LPC(15/19)
LPE(3/18)
SM(0/13)
CER(8/13)
HCER(2/13)
LCER(3/13)
DCER(4/14)
-1.0 -0.5 0.0 0.5 1.0
Increase in AgeAccelPheno (year) per SD change in lipids
Increase in AgeAccelGrim (year) per SD change in lipids
p value
FDR > 0.1
0.05 <= FDR <= 0.1
FDR < 0.05

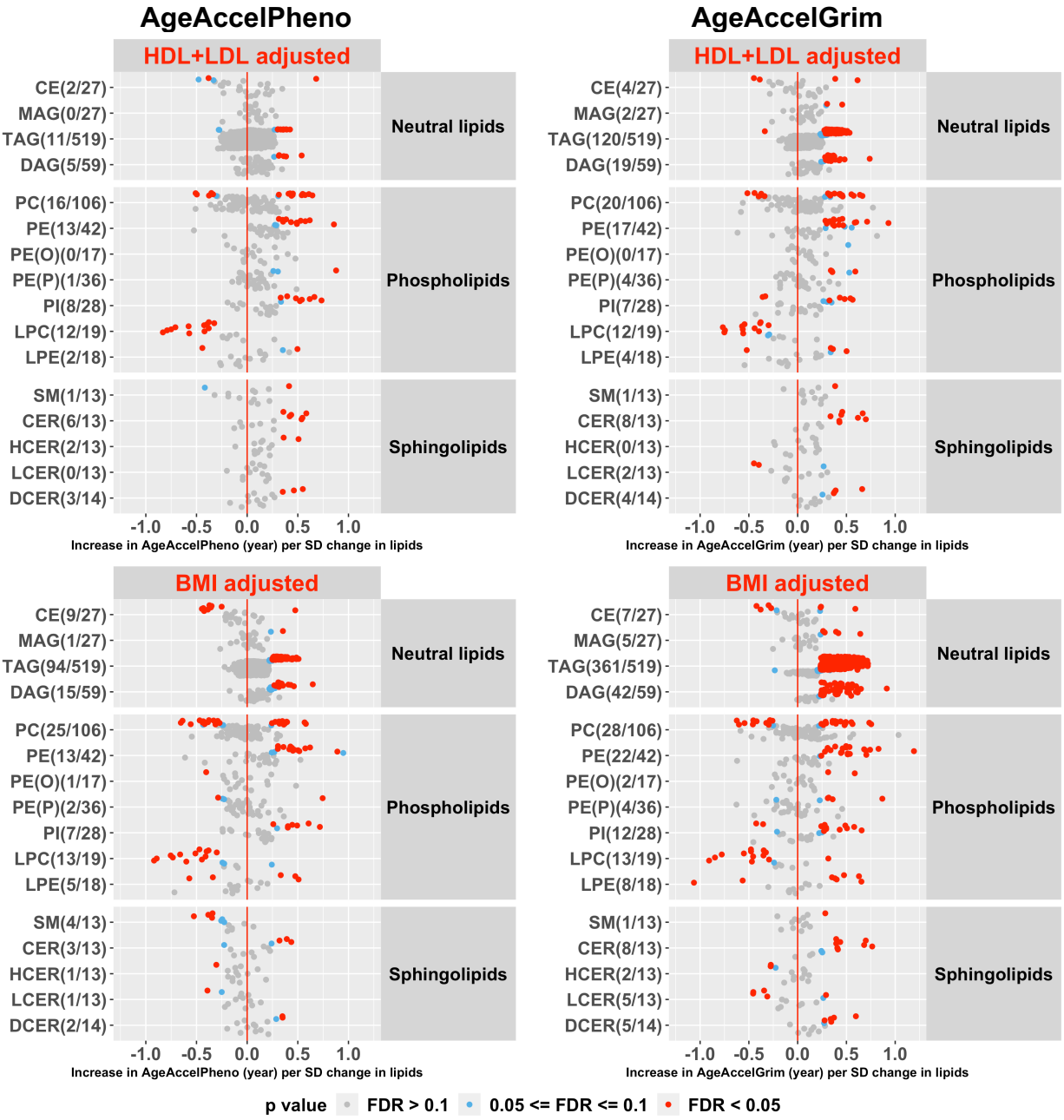

Figure 10. Associations of lipid species with AgeAccelPheno and AgeAccelGrim
Each dot represents one molecular species; dot color indicates the significance level. Base model: AgeAccel ~ lipid + sex + batch information + smoking status. Abbreviations: cholesteryl ester (CE), monoacylglycerol (MAG), triacylglycerol (TAG), diacylglycerol (DAG), phosphatidylcholine (PC), phosphatidylethanolamine (PE), phosphatidylethanolamine ether (PE(O)), phosphatidylethanolamine plasmalogen (PE(P)),phosphatidylinositol (PI), lysophosphatidylcholine (LPC), lysophosphatidylethanolamine (LPE), sphingomyelin (SM), ceramide (CER), hexosylceramide (HCER), lactosylceramide (LCER), dihydroceramide (DCER), high-density-lipoprotein (HDL), low-density-lipoprotein (LDL), body mass index (BMI), false discovery rate (FDR).

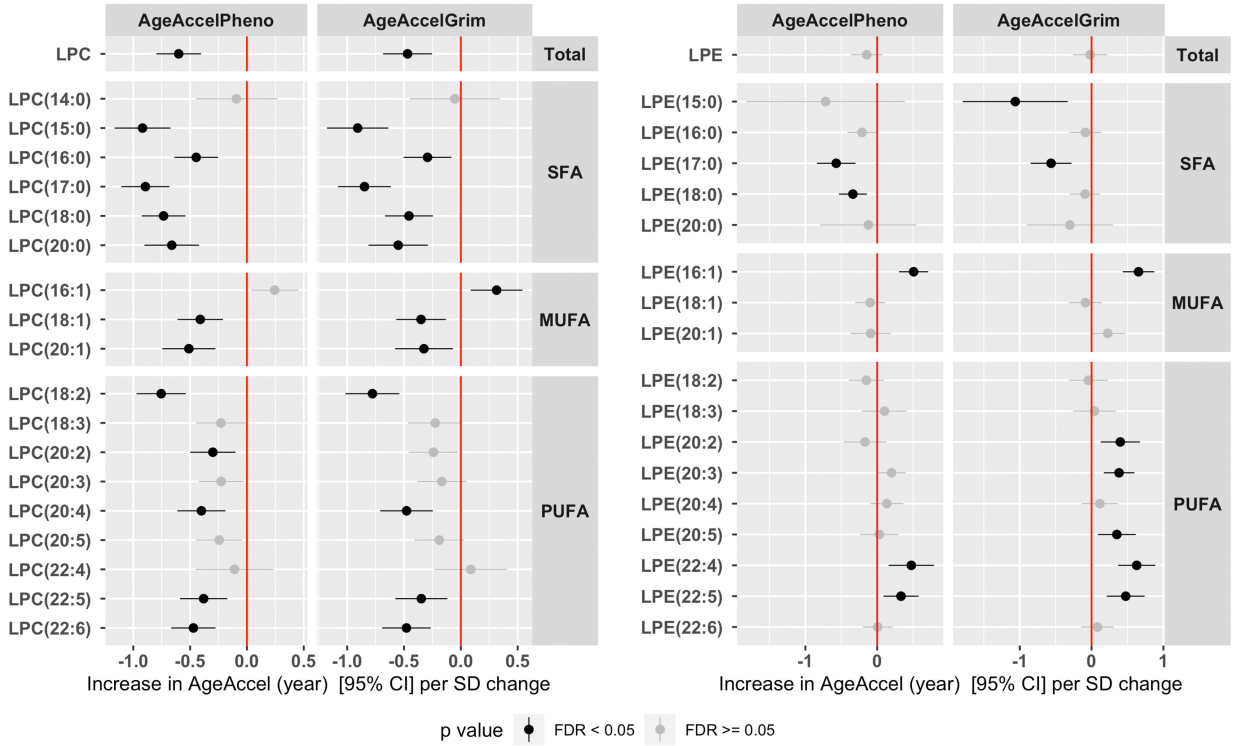

Figure 11. LPC, LPE species associated with DNAm age acceleration estimators
Abbreviations: lysophosphatidylcholine (LPC), lysophosphatidylethanolamine (LPE), saturated fatty acid (SFA), monounsaturated fatty acid (MUFA), polyunsaturated fatty acid (PUFA).

Associations of the total number of carbons and double bonds and DNAm age acceleration estimators

Within the neutral lipid category, TAG molecular species with even numbers of carbons were positively associated with AgeAccelPheno and AgeAccelGrim, whereas fewer significant associations were observed with species containing an odd numbered chain length. Regarding phospholipids, molecular species belonging to PC, PE(O), PE(P), and PI classes with more double bonds (i.e. polyunsaturated fatty acids) and more carbons tended to be negatively associated with AgeAccelPheno and AgeAccelGrim, while species with fewer double bonds and fewer carbons tended to be positively associated with AgeAccelPheno and AgeAccelGrim. Predominantly LPC and LPE molecular species with fewer carbons were associated with lower AgeAccelPheno and AgeAccelGrim (**Figures 12** and **13**). There was no clear pattern for the association of sphingolipids species with AgeAccelPheno and AgeAccelGrim (**Figure 14**).

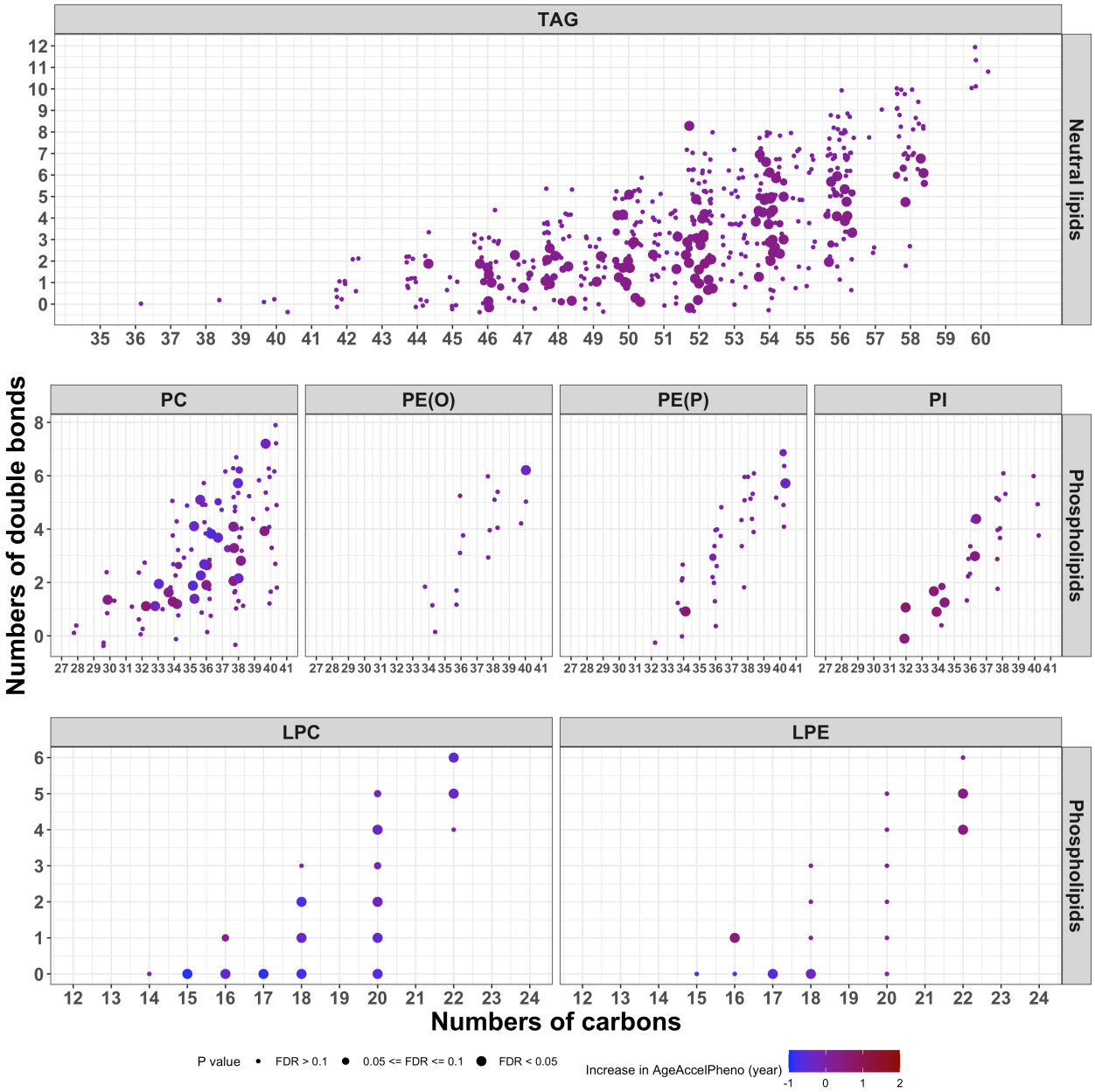

Figure 12. Associations between total numbers of carbons and double bonds in lipid species and AgeAccelPheno

Individual lipid species are depicted by filled circles and arranged by lipid class according to the total number of carbon atoms (x-axes) and double bonds (y-axes). Color indicates the magnitude and direction (positive or negative) of effect size, and circle size corresponds to the significance level. Lipids with the same number of carbon atoms and double bonds are pulled apart vertically to increase their visibility. Abbreviations: triacylglycerol (TAG), phosphatidylcholine (PC), phosphatidylethanolamine ether (PE(O)), phosphatidylethanolamine plasmalogen (PE(P)), phosphatidylinositol (PI), lysophosphatidylcholine (LPC), lysophosphatidylethanolamine (LPE), false discovery rate (FDR).

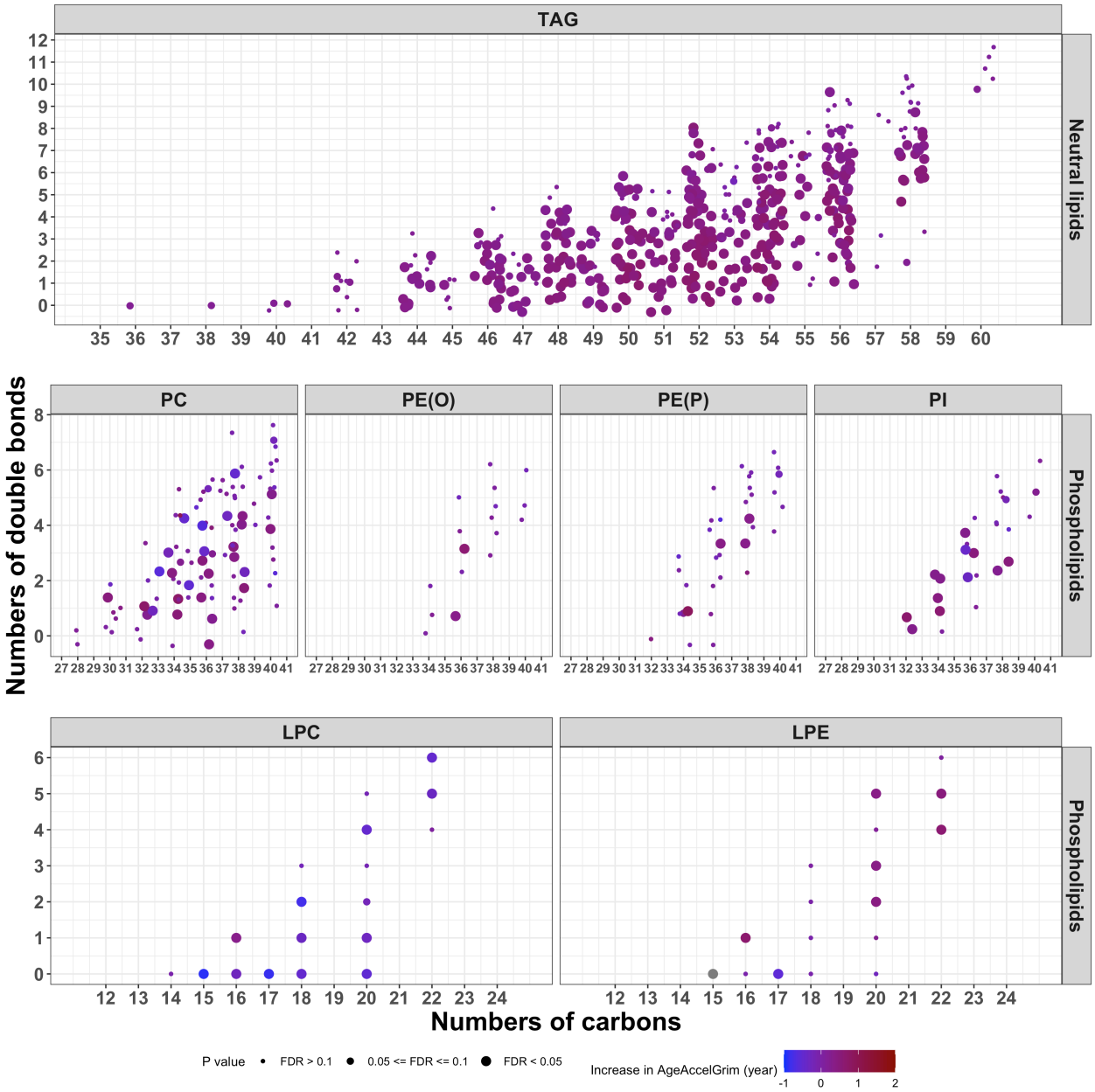

Figure 13. Associations between total numbers of carbons and double bonds in lipid species and AgeAccelGrim

Individual lipid species are depicted by filled circles and arranged by lipid class according to the number of total carbon atoms (x-axes) and number of double bonds (y-axes). Color indicates the magnitude of effect size, and circle size corresponds to the significance level. Lipids with the same number of carbon atoms and double bonds are pulled apart vertically to increase their visibility. Abbreviations: cholesteryl ester (CE), triacylglycerol (TAG), phosphatidylcholine (PC), phosphatidylethanolamine ether (PE(O)), phosphatidyl-ethanolamine plasmalogen (PE(P)), phosphatidylinositol (PI), lysophosphatidylcholine (LPC), lysophosphatidylethanolamine (LPE), false discovery rate (FDR).

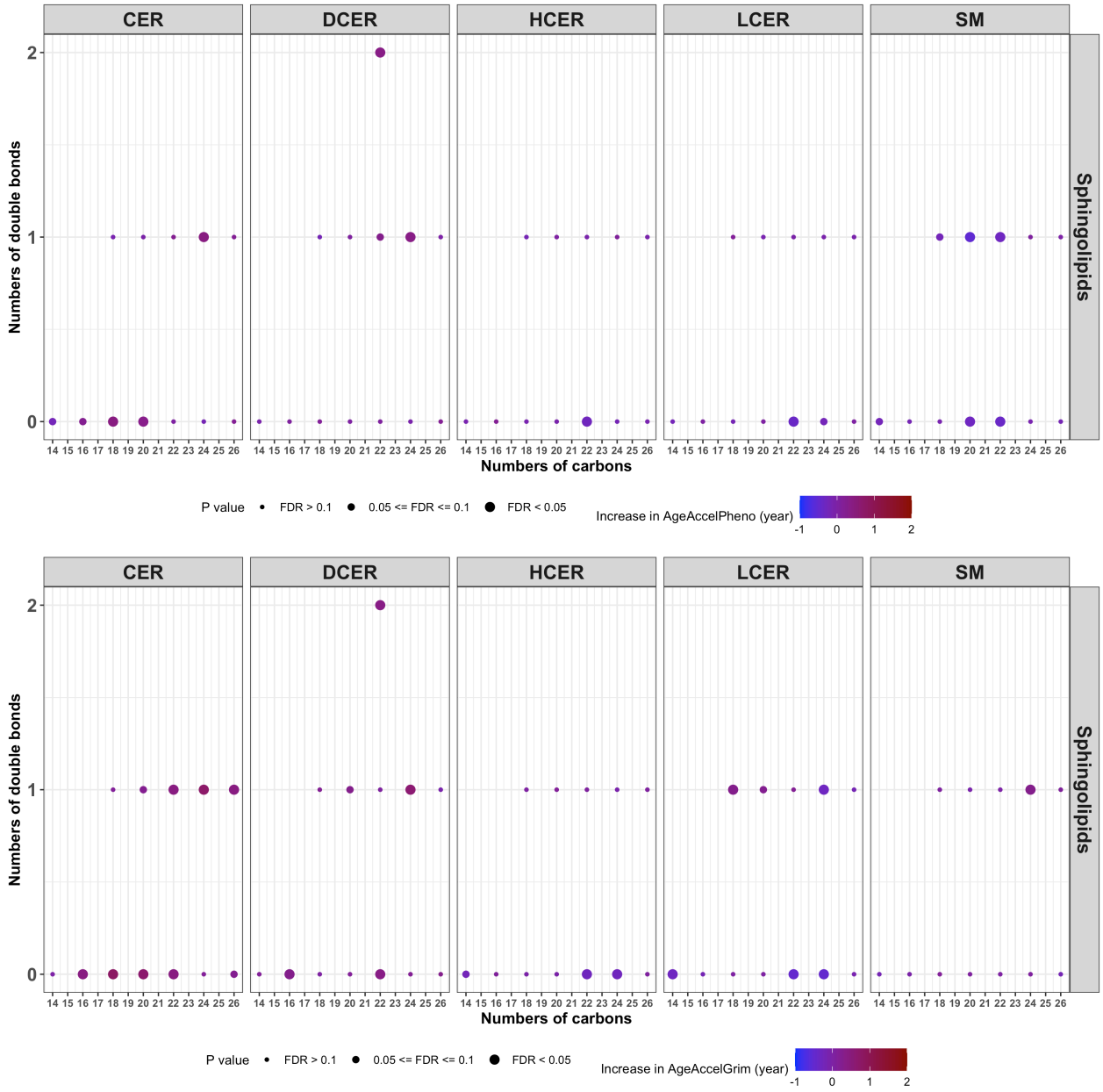

Figure 14. Associations of total numbers of carbons and double bonds in sphingolipids with AgeAccelPheno and AgeAccelGrim

Individual lipid species are depicted by filled circles and arranged by lipid class according to the number of total carbon atoms (x-axes) and number of double bonds (y-axes). Color indicates the magnitude of effect size, and circle size corresponds to the significance level. Lipids with the same number of carbon atoms and double bonds are pulled apart vertically to increase their visibility. Abbreviations: ceramide (CER), dihydroceramide (DCER), hexosylceramide (HCER), lactosylceramide (LCER), sphingomyelin (SM), false discovery rate (FDR).

Associations of number of carbons in one specific fatty acid tail across lipid classes with DNAm age acceleration estimators

Each lipid carries specific fatty acid tail with varying numbers of acyl chain carbons, which define their specific biological effects. In this analysis, 267 lipids with one specific fatty acid tail covering 14 lipid classes were included. In general, across lipid classes, the direction and strength of the effect on DNAm age acceleration estimators were determined by the chain length of this specific fatty acid tail (**Figure 15**). Lipid molecular species with an even number (i.e. 14, 16, 18, 20, 22, 24, and 26) of carbons in the fatty acid tail were positively associated with DNAm age acceleration estimators across lipid classes (except for lysophospholipids, HCER, and LCER), while lipid species with an odd number (i.e. 15 and 17) of carbons in the fatty acid tail were negatively associated with DNAm age acceleration estimators. In addition, shorter fatty acid tails were related to larger effect sizes (**Figure 15**). Importantly, the direction of the effects also depended on the lipid class (**Figure 10).**

Associations of saturation of fatty acid tails with DNAm age acceleration estimators

Differences in the content and fraction of mono- and polyunsaturated lipids determine membrane peroxidation, which has been linked to longevity (Gonzalez-Covarrubias et al. 2013). For saturated and monounsaturated lipids, the effect on DNAm age acceleration estimators became stronger with shorter (even numbered) chain lengths of the fatty acid tail. In contrast, for polyunsaturated lipids with the same chain length, fewer double bonds were related to a stronger effect on DNAm age acceleration estimators (**Figure 16**).

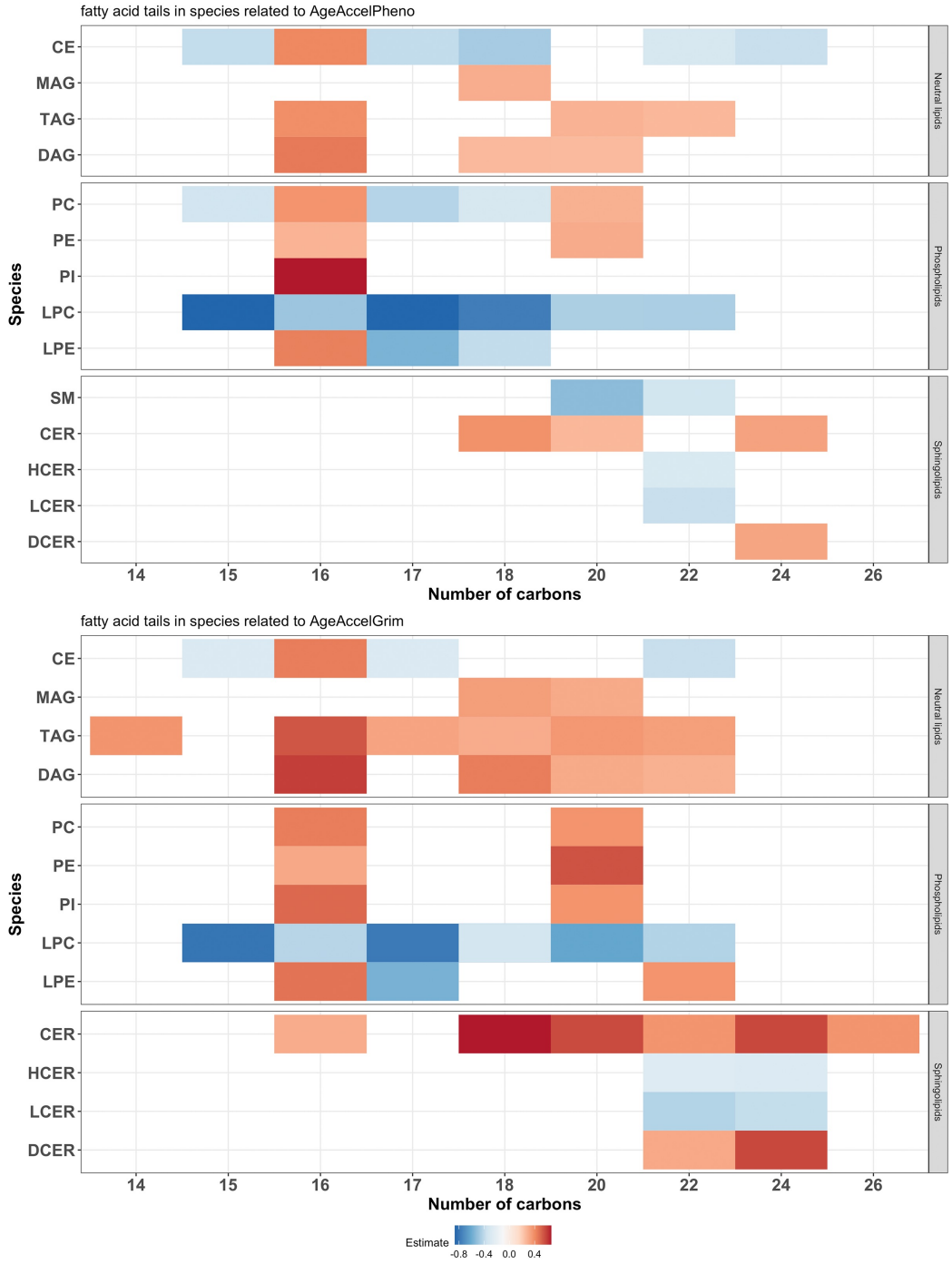

Figure 15. Relationship between numbers of carbons in one fatty acid tail and DNAm age acceleration estimators

Color indicates the magnitude of effect size. To better visualize the results, only the effect sizes of lipid species at FDR < 0.05 level were shown. Abbreviations: cholesteryl ester (CE), triacylglycerol (TAG), diacylglycerol (DAG), monoacylglycerol (MAG), phosphatidylcholine (PC), phosphatidylethanolamine (PE), phosphatidylinositol (PI), lysophosphatidylcholine (LPC), lysophosphatidylethanolamine (LPE), sphingomyelin (SM), ceramide (CER), hexosylceramide (HCER), lactosylceramide (LCER), dihydroceramide (DCER).

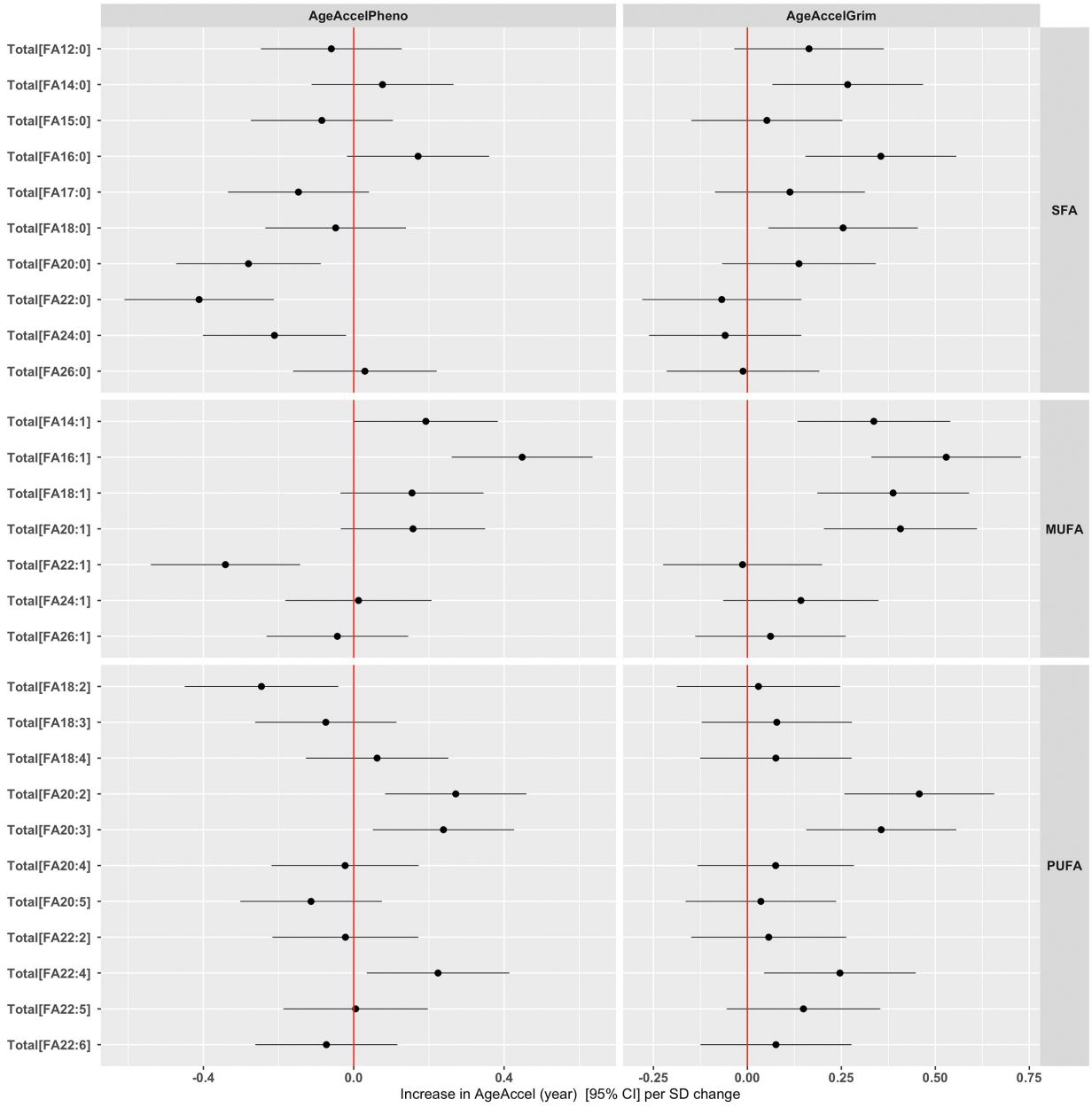

Figure 16. Relationship between fatty acid tails and DNAm age acceleration estimators
Abbreviations: saturated fatty acid (SFA), monounsaturated fatty acids (MUFA), polyunsaturated fatty acid (PUFA).

Sex-interaction and sex-stratified analyses

We found a few lipid species, mostly within the neutral lipids, that were differently associated with DNAm age acceleration estimators between men and women (**Figure 17**). Sex-stratified analyses on these lipid species showed that each SD increase of the

concentration of these MAG, DAG or TAG species, AgeAccelPheno increased with 0.5-years in women, but not in men. Each SD increase of the concentration of PE(P-16:0/16:0), MAG (18:1), MAG (18:2), and 8 DAG species, AgeAccelGrim increased with around 0.5-years in women, whereases per SD increase of the concentration of PI (18:0/16:1) and PI (16:0/16:1), AgeAccelGrim increased with around 0.5-years in men. Concentrations of TAG (42:2-FA18:2), TAG (42:2-FA12:0) and TAG (40:0-FA14:0) were only negatively associated with AgeAccelGrim in women (**Figure 18 and Figure 19**).

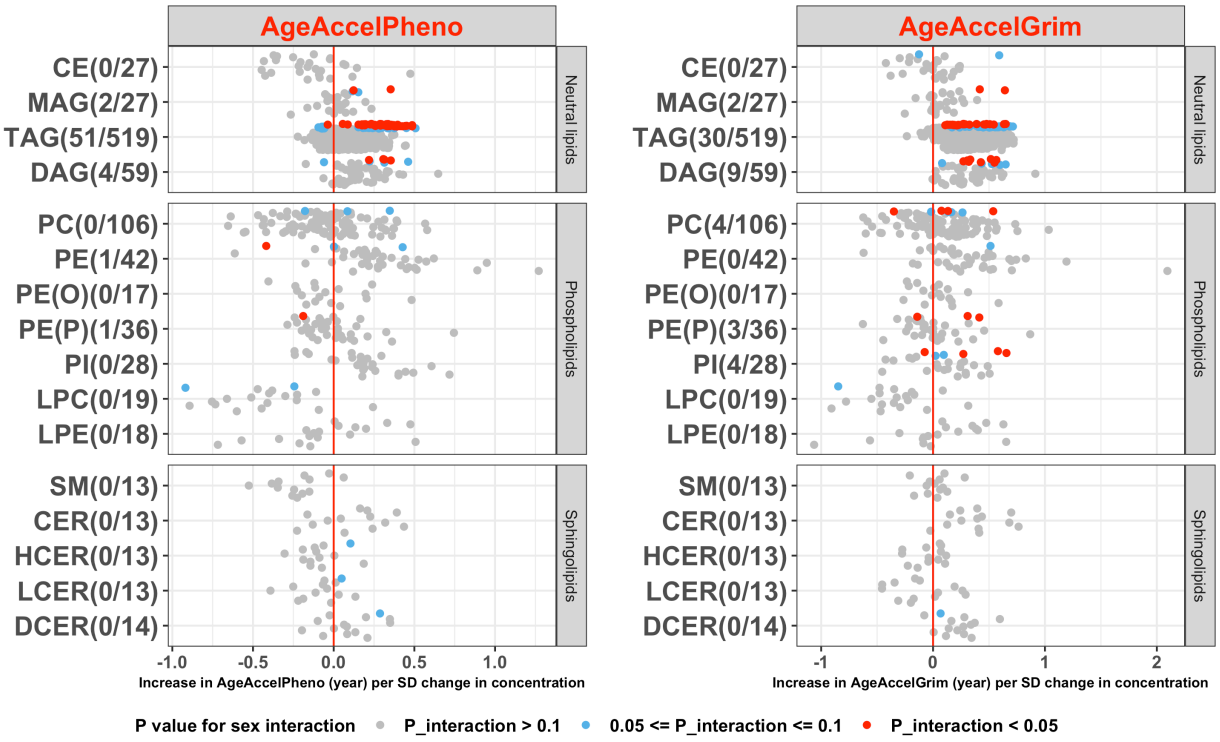

Figure 17. Interaction effects between sex and lipid species on DNAm age acceleration estimators
Numbers between brackets behind each class indicate number of significant sex-interaction lipid species/total number of lipid species in that class. Abbreviations: cholesteryl ester (CE), triacylglycerol (TAG), diacylglycerol (DAG), monoacylglycerol (MAG), phosphatidylcholine (PC), phosphatidylethanolamine (PE), phosphatidylinositol (PI), lysophosphatidylcholine (LPC), lysophosphatidylethanolamine (LPE), sphingomyelin (SM), ceramide (CER), hexosylceramide (HCER), lactosylceramide (LCER), dihydro-ceramide (DCER).

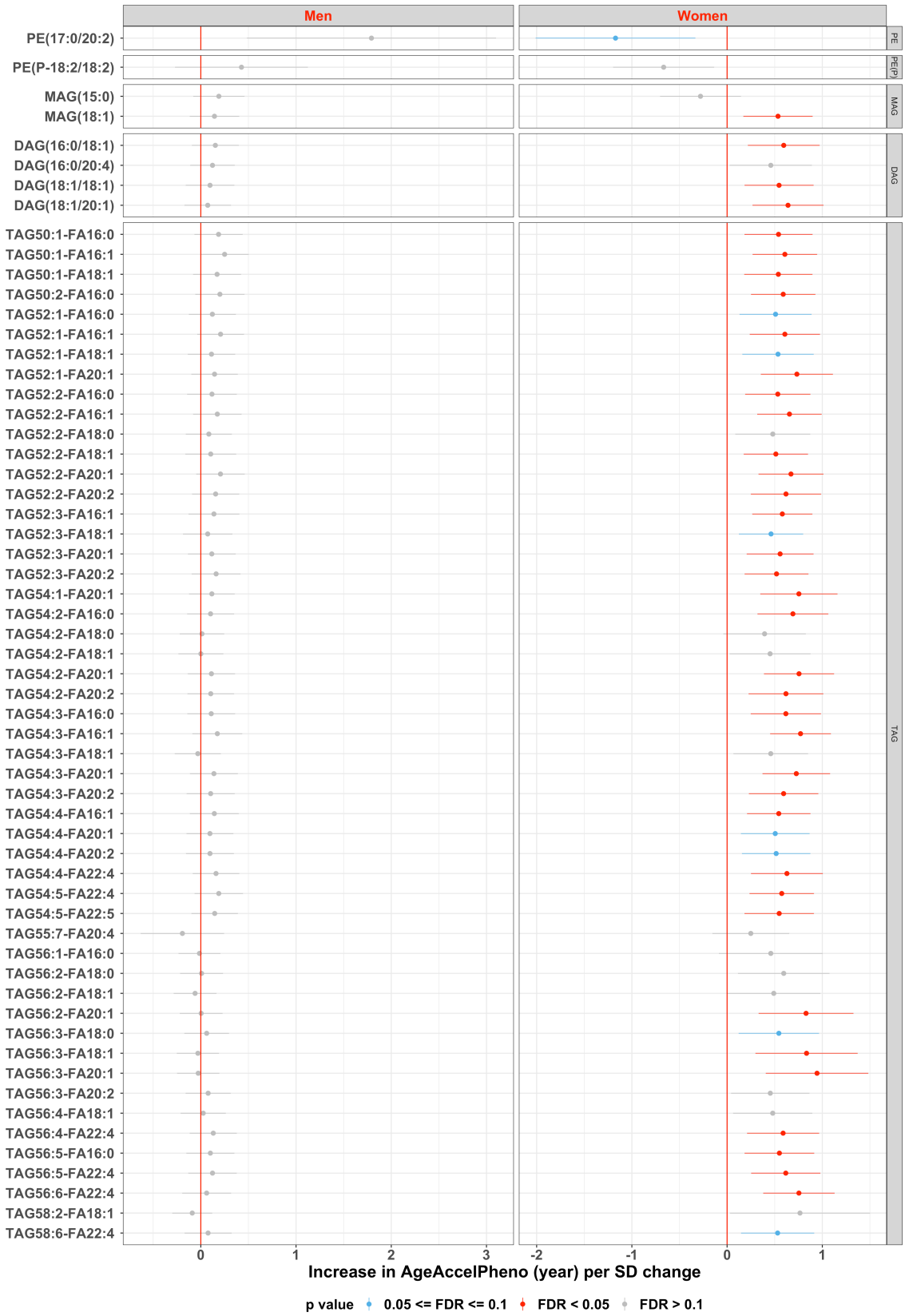

Figure 18. Sex difference between lipid species concentration and AgeAccelPheno
Abbreviations: triacylglycerol (TAG), diacylglycerol (DAG), monoacylglycerol (MAG), phosphatidylcholine (PC), phosphatidylethanolamine (PE), phosphatidylinositol (PI).

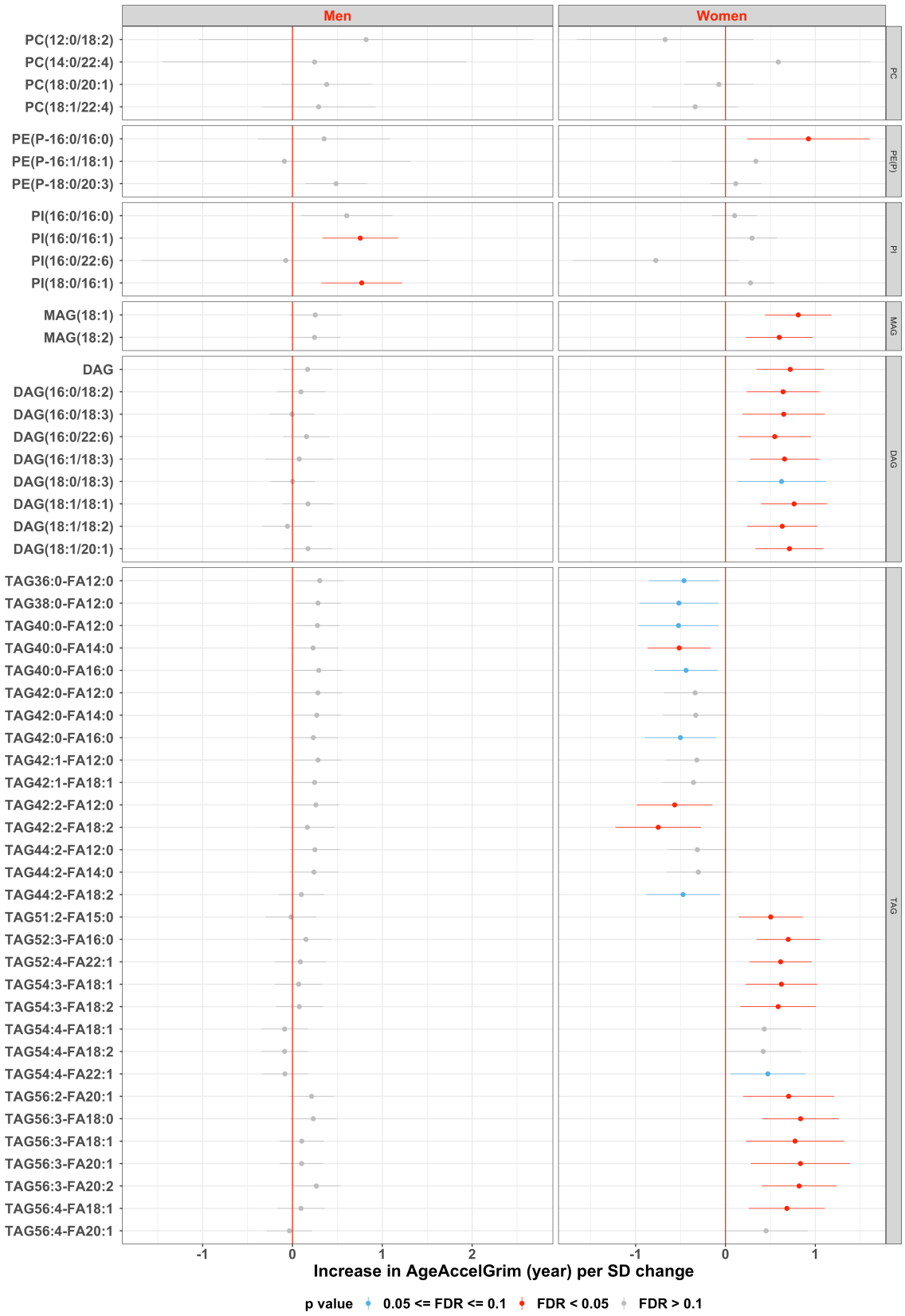

Figure 19. Sex difference between lipid species concentration and AgeAccelGrim
Abbreviations: triacylglycerol (TAG), diacylglycerol (DAG), monoacylglycerol (MAG), phosphatidylcholine (PC), phosphatidylethanolamine (PE), phosphatidylinositol (PI).

Uncovering potential pathways through which lipids affect DNAm age acceleration estimators

Epigenome-wide association analyses were performed for 525 lipids, belonging to 14 different classes, which were identified to be associated with DNAm age acceleration estimators (**Figure 10 and Figure 11**). This approach resulted in the identification of lipid-associated CpGs that were subsequently used as uniquely defined proxies for the respective lipids, enabling KEGG pathway analysis to delineate the underlying biological pathways modulated by AgeAccel-associated lipids. A total of 65 pathways were identified, including many known longevity-related pathways such as the mTOR signaling pathway, AMPK signaling pathway, MAPK signaling pathway, and growth hormone synthesis, secretion, and action pathway. Moreover, pathways involved in age-related diseases, including type 2 diabetes mellitus, insulin resistance and secretion, cortisol synthesis and secretion, and long-term depression were among those related to lipid-associated CpGs. Importantly, also molecular pathways associated with brain aging were highlighted, including cholinergic synapse, dopaminergic synapse, axon guidance, neurotrophy signaling pathway, and GABAergic synapse **(Figure 20).**

Figure 20. Biological pathways involved in the association between lipids and DNAm age acceleration estimators

Abbreviations: false discovery rate (FDR)

3.3 Results study III: Associations of Measured and Genetically Predicted Leukocyte Telomere Length with Vascular phenotypes: A Population-based Study

In the subset of 1828 participants with measured LTL data, the mean age was 54.8 years (SD = 14.1 years, range from 30 – 95 years), and 56.8 % were women. Mean LTL was 3280 kb base pairs (SD = 0.8) (**Table 5**). Measured LTL was strongly associated with chronological age, with values slightly higher in women compared to men [sex effect: 0.02 (95% CI: 0.05, 0.01), p-value = 0.04]. In 4180 participants (56.2 % women) with data on PRS of LTL, the mean age was 55.5 years (SD = 14.0 years, range 30 – 95 years). A summary of the characteristics of the study population is provided in **Table 5.**

The association between measured LTL and vascular phenotypes

Longer measured LTL was significantly associated with better endothelial function, and cardiac index (per kb increase in measured LTL: 0.07 (95% CI: 0.01, 0.14) SD increase in reactive skin hyperemia, and 0.08 (95% CI: 0.01, 0.15) SD increase in cardiac index) (**Figure 21**). These findings remained similar after adjustment for smoking, BMI, and cell counts. Longer measured LTL also tended to be associated with lower systemic vascular resistance index, although this association did not reach statistical significance [-0.06 SD change (95% CI: -0.14, 0.01)]. Measured LTL was not significantly associated with arterial stiffness or blood pressure phenotypes in the overall analyses (**Figure 21**).

There were statistically significant interactions between age and different vascular phenotypes, including total arterial compliance index (beta interaction =0.006, p = 0.006), ankle-brachial index (beta interaction = 0.005, p = 0.064), systolic blood pressure (beta interaction = -0.007, p = 0.002), and pulse pressure (beta interaction = -0.011, p =0.000), but not with other traits. Further stratified analyses by age tertiles (i.e. 30 - 48 years old, 49 – 60 years, and 61- 95 years old) showed positive associations of measured LTL with total arterial compliance index, and ankle-brachial index in the oldest age tertile. Negative associations of measured LTL with systolic blood pressure, and pulse pressure were also only observed in older (61-95 years old), but not in younger participants (**Figure 22**).

Table 5. Characteristics of the study population

	Participants with measured LTL data (N=1828)	Participants with PRS of LTL data (N=4180)
Age, year		
Mean (SD)	54.8 (14.1)	55.5 (14.0)
Median [Min, Max]	54.0 [30.0, 95.0]	55.0 [30.0, 95.0]
Sex, n (%)		
Women	1038 (56.8 %)	2349 (56.2 %)
Men	790 (43.2 %)	1831 (43.8 %)
Body mass index, kg/m^2, mean (SD)	25.8 (4.6)	25.8 (4.4)
Current smoking, n (%)	257 (14.1 %)	512 (12.2 %)
Leucocyte telomere length, kb pairs, mean (SD)	3280 (0.8)	-
Vascular phenotypes, mean (SD)		
Systolic blood pressure, mmHg	128 (16.5)	127 (16.1)
Diastolic blood pressure, mmHg	76.9 (9.6)	75.4 (9.3)
Mean arterial pressure, mmHg	93.9 (10.9)	92.6 (10.6)
Pulse pressure, mmHg	51.7 (10.7)	51.6 (10.5)
Cardiac index, L/min/m^2	3.2 (0.5)	3.2 (0.5)
Systemic vascular resistance index, dynes· sec/cm^5/m^2	2120 (475)	2120 (469)
Stroke index, mL/m^2	51.7 (8.5)	52.1 (8.7)
Reactive skin hyperemia	485 (447)	499 (492)
Total arterial compliance index, mL/mmHg/m^2	1.0 (0.3)	1.1 (0.3)
Pulse wave velocity, m/s	6.9 (3.6)	6.8 (2.9)
Ankle-Brachial index	1.1 (0.1)	1.2 (0.1)

Abbreviation: SD, standard deviation. The missingness for each variable is less than 5 %.

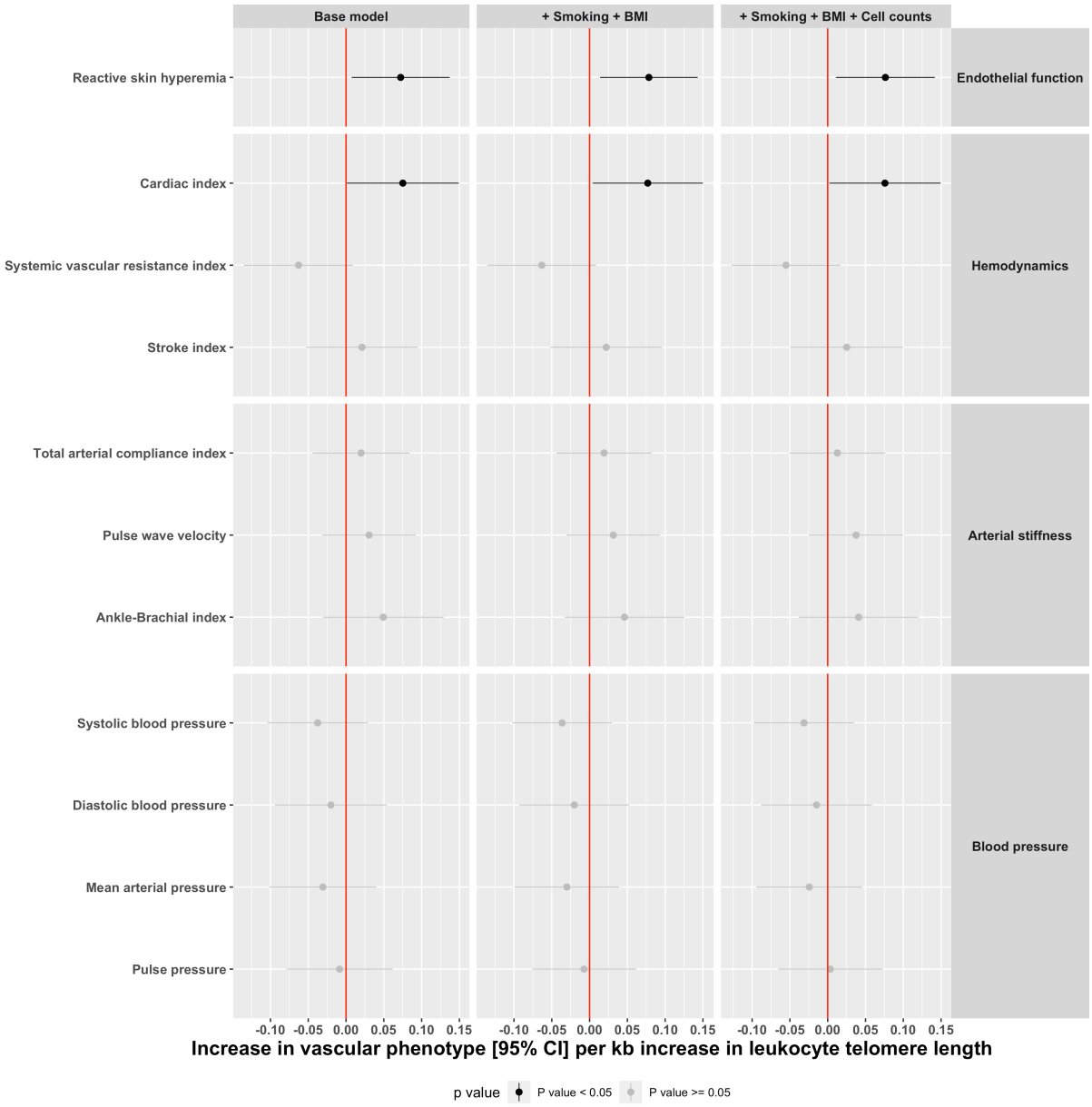

Figure 21. The association between measured leukocyte telomere length and vascular phenotypes

Base model: vascular phenotype ~ measured leukocyte telomere length (LTL) + age + sex + batch information of LTL**.**

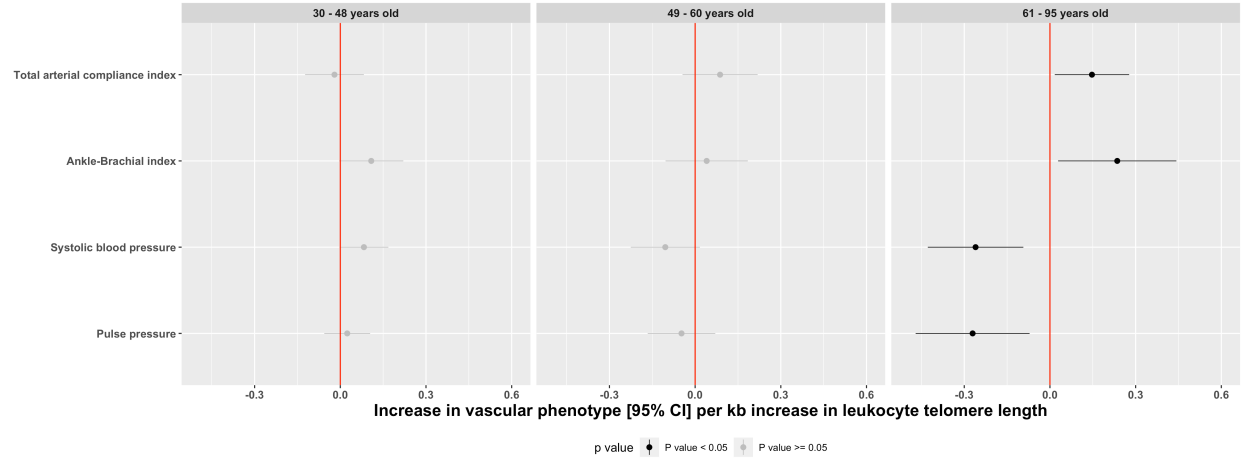

Figure 22. The association between the measured leucocyte telomere length and vascular phenotypes in different age tertiles

The associations of the previously reported variants, PRS of LTL with measured LTL

When evaluating individual SNPs that had previously been associated with LTL, we could replicate the previously reported top variants, including rs10936600 (*TERC*), rs2853677 (*TERT*), rs9419958 (*OBFC1*), rs75691080 (*STMN3*), with the same direction and even larger effect sizes (**Table 6**). Regarding other variants, although the p-values did not reach statistical significance, the direction of the associations and the magnitude of the estimates were quite similar to those previously reported. Both the PRS that was based on genome-wide significant SNPs (PRS_{GWAS}), as well as the PRS that was based on SNPs that were significant at FDR < 0.05-level (PRS_{FDR}) in the previous meta-GWAS, were associated with longer measured LTL in our cohort (PRS_{GWAS}: 0.05 SD increase (95% CI: 0.05, 0.14) and PRS_{FDR}: 0.10 SD increase (95% CI: 0.05, 0.14)). Adjustment for smoking, BMI and cell counts did not change the estimates. Taken together, these findings support the reliability of our LTL measurements and validate the derived genetic instruments.

Table 6. Genetic variants associated with telomere length in prior genome-wide association study (GWAS) and replication in the Rhineland Study

				Prior GWAS			Replication in the Rhineland study		
Chr	SNP	closest gene	EA	Estimate	SE	P	Estimate	SE	P
Genome-wide significance ($5*10^{-8}$)									
3	rs10936600	*LRRC34 (TERC)*	T	-0.0858	0.0057	6.42E-51	-0.1098	0.0354	0.0020
5	rs7705526	*TERT*	A	0.0820	0.0058	4.82E-45	0.0394	0.0375	0.2946
5	rs2853677	*TERT*	A	-0.0638	0.0055	3.12E-31	-0.0705	0.0321	0.0282
4	rs4691895	*NAF1*	C	0.0577	0.0061	1.47E-21	0.0266	0.0370	0.4727
10	rs9419958	*STN1 (OBFC1)*	C	-0.0636	0.0071	4.77E-19	-0.0814	0.0446	0.0681
20	rs75691080	*STMN3*	T	-0.0671	0.0089	5.75E-14	-0.1578	0.0559	0.0048
7	rs59294613	*POT1*	A	-0.0407	0.0055	1.12E-13	-0.0108	0.0342	0.7512
19	rs8105767	*ZNF208*	G	0.0392	0.0054	5.21E-13	0.0557	0.0342	0.1035
20	rs73624724	*ZBTB46*	C	0.0507	0.0074	6.08E-12	-0.0088	0.0477	0.8533
1	rs3219104	*PARP1*	C	0.0417	0.0064	9.31E-11	0.0128	0.0406	0.7519
20	rs932827	*ZBTB46*	T	-0.0374	0.0060	3.28E-10	-0.0557	0.0358	0.1200
6	rs2736176	*PRRC2A*	C	0.0345	0.0055	3.41E-10	0.0345	0.0360	0.3378
16	rs3785074	*TERF2*	G	0.0351	0.0056	4.50E-10	0.0259	0.0357	0.4684
16	rs7194734	*MPHOSPH6*	T	-0.0369	0.0060	6.72E-10	-0.0032	0.0388	0.9339
20	rs34978822	*RTEL1*	G	-0.1397	0.0227	7.04E-10	0.0303	0.1284	0.8137
6	rs34991172	*CARMIL1*	G	-0.0608	0.0105	6.03E-09	-0.0929	0.0739	0.2089
11	rs228595	*ATM*	A	-0.0285	0.0050	1.39E-08	0.0030	0.0317	0.9247
14	rs2302588	*DCAF4*	C	0.0476	0.0084	1.64E-08	-0.0217	0.0503	0.6664
4	rs13137667	*MOB1B*	C	0.0765	0.0137	2.37E-08	0.0383	0.0906	0.6723
3	rs55749605	*SENP7*	A	-0.0373	0.0067	2.38E-08	0.0342	0.0324	0.2902
16	rs62053580	*RFWD3*	G	-0.0389	0.0071	3.96E-08	-0.0414	0.0413	0.3157
False-discovery rate < 0.05									
2	rs754017156	*ACYP2*	D	0.0471	0.0088	7.52E-08	-	-	-
15	rs12909131	*ATP8B4*	T	-0.0308	0.0058	1.15E-07	0.0132	0.0363	0.7150
20	rs1744757	*MROH8*	T	0.0359	0.0068	1.38E-07	0.0441	0.0454	0.3314
18	rs2124616	*TYMS*	A	-0.0374	0.0072	1.72E-07	-0.0232	0.0433	0.5930
3	rs2613954	*RP11-572M11.4*	T	-0.0381	0.0078	1.10E-06	0.0074	0.0473	0.8766
1	rs12065882	*MAGI3*	G	0.0298	0.0062	1.36E-06	0.0078	0.0377	0.8367
10	rs2386642	*ASB13*	A	-0.0256	0.0053	1.44E-06	-0.0112	0.0327	0.7312
2	rs56810761	*UNC80*	T	0.0275	0.0057	1.45E-06	0.0165	0.0352	0.6392
5	rs62365174	*TENT2*	G	-0.0544	0.0113	1.50E-06	0.0486	0.0530	0.3591
12	rs112655343	*ATF7IP*	T	0.0425	0.0090	2.22E-06	0.0826	0.0514	0.1087
15	rs55710439	*ANKDD1A*	T	0.1050	0.0223	2.65E-06	0.0891	0.1378	0.5180
16	rs11640926	*CACNA1H*	G	0.0557	0.0119	2.93E-06	-0.0538	0.0461	0.2427
4	rs60160057	*DCLK2*	A	-0.0287	0.0062	3.15E-06	0.0248	0.0381	0.5158
14	rs117536281	*CDCA4*	G	0.0850	0.0183	3.31E-06	-0.0471	0.0977	0.6298

22	rs7510583	*KIAA1644*	G	0.0347	0.0075	3.38E-06	-	-	-
14	rs59192843	*BBOF1 (CCDC176)*	G	0.0655	0.0141	3.52E-06	0.0310	0.0748	0.6783
8	rs57415150	*CSMD1*	A	-0.0584	0.0126	3.68E-06	-0.1557	0.0741	0.0357
20	rs6038821	*LINC01706*	T	0.0596	0.0129	3.98E-06	-0.0044	0.0835	0.9584
17	rs144204502	*TK1*	T	-0.0896	0.0196	4.92E-06	-0.0359	0.1300	0.7824
20	rs6107615	*PROKR2*	C	-0.0228	0.0050	5.30E-06	0.0040	0.0315	0.9002
15	rs9972513	*RP11-275I4.2*	T	0.0247	0.0055	5.75E-06	-	-	-
11	rs117037102	*CEP295*	T	0.0979	0.0218	6.81E-06	-0.0469	0.1535	0.7600
21	rs7276273	*KRTAP10-4*	C	-0.1502	0.0334	6.90E-06	-0.3428	0.2033	0.0920
19	rs11665818	*IFNL2*	A	0.0278	0.0062	7.04E-06	0.0012	0.0407	0.9765
14	rs3213718	*CALM1*	T	0.0224	0.0050	7.22E-06	0.0195	0.0323	0.5458
5	rs112347796	*UBE2D2*	D	0.0691	0.0154	7.29E-06	-	-	-
19	rs143276018	*NMRK2*	C	-0.1015	0.0229	9.02E-06	0.0020	0.1411	0.9887
8	rs201375979	*COX6C*	D	0.0332	0.0075	9.11E-06	-	-	-
12	rs7311314	*SMUG1*	A	0.0240	0.0054	9.50E-06	0.0069	0.0334	0.8362
1	rs35675808	*CD247*	G	0.0736	0.0166	9.54E-06	-0.0712	0.1106	0.5201
15	rs117610974	*UNC13C*	G	-0.1540	0.0350	1.05E-05	0.0887	0.1578	0.5740

Abbreviation: Chr, chromosome; SNP, single nucleotide polymorphism; EA, effect allele; SE, standard error.
Estimate; the per-allele effect on z-scored LTL.

The association between genetically predicted LTL and vascular phenotypes

Each SD increase in PRS of LTL was associated with higher cardiac index [0.04 SD increase (95% CI: 0.01, 0.07) for both PRS_{GWS} and PRS_{FDR}]. There were also non-significant trends for the associations of genetically predicted LTL and other hemodynamic traits, including systemic vascular resistance index and stroke index (both $p < 0.10$), as well as with better endothelial function [0.03 SD increase (95% CI: -0.01, 0.06), p-value = 0.09]. There was no association between genetically predicted LTL and arterial stiffness traits (**Figure 23**). Overall, both the magnitudes and directions of the associations with vascular phenotypes were consistent between measured and genetically predicted LTL. Age, sex and smoking status did not significantly modify the association of measured and genetically predicted LTL with vascular phenotypes (all interaction P-values > 0.10).

To explore which variants drove the associations of LTL with vascular phenotypes, we further investigated the associations of the 47 individual genetic variants with vascular phenotypes that were identified to be significantly associated with genetically predicted

LTL (**Figure 24**). For reactive skin hyperemia, per-allele associations with were found for rs8105767 (*ZNF208*), rs112655343 (*ATF7IP*), rs55710439 (*ANKDD1A*), and rs144204502 (*TK1*). Per-allele associations with cardiac index were observed for rs2124616 (*TYMS*), whereas rs9419958 (*OBFC1),* rs2124616 (*TYMS*), rs56810761 (*UNC80*) and rs62365174 (*TENT2*) were associated with stroke index. Three SNPs, including rs10936600 (*TERC*), rs73624724 (*ZBTB46*), rs2302588 (*DCAF4*) was associated with pulse pressure.

The association between ΔLTL **and vascular phenotypes**

Each SD increase in **Δ**LTL was associated with 0.06 SD increase (95% CI: 0.12, 0.00) in reactive skin hyperemia, 0.07 SD increase (95% CI: 0.01, 0.13) in cardiac index, and 0.06 SD decrease (95% CI: -0.12, -0.01) in systemic vascular resistance index, after adjustment for genetically predicted LTL (**Figure 25**). The associations remained similar after further adjustment for smoking and BMI. However, **Δ**LTL was not associated with arterial stiffness traits.

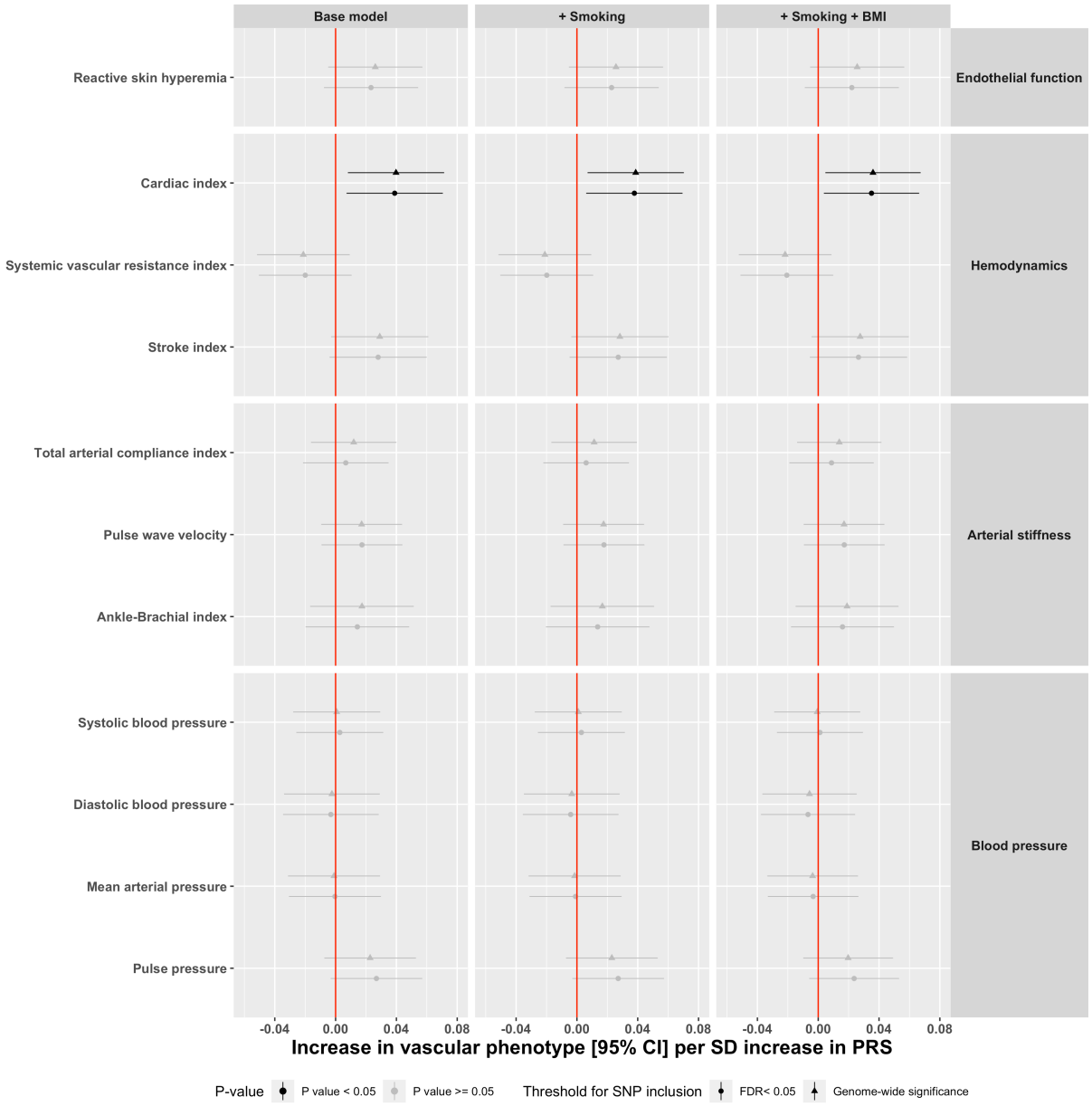

Figure 23. The association between the genetically predicted longer telomere length and vascular phenotypes

Base model: vascular phenotype~ polygenic risk score (PRS) of LTL + age + sex + population stratification (first 10 genetic principal components)

Threshold for SNP inclusion: genome-wide significance ($5*10^{-8}$) includes 20 variants; False-discovery rate < 0.05 includes 47 variants.

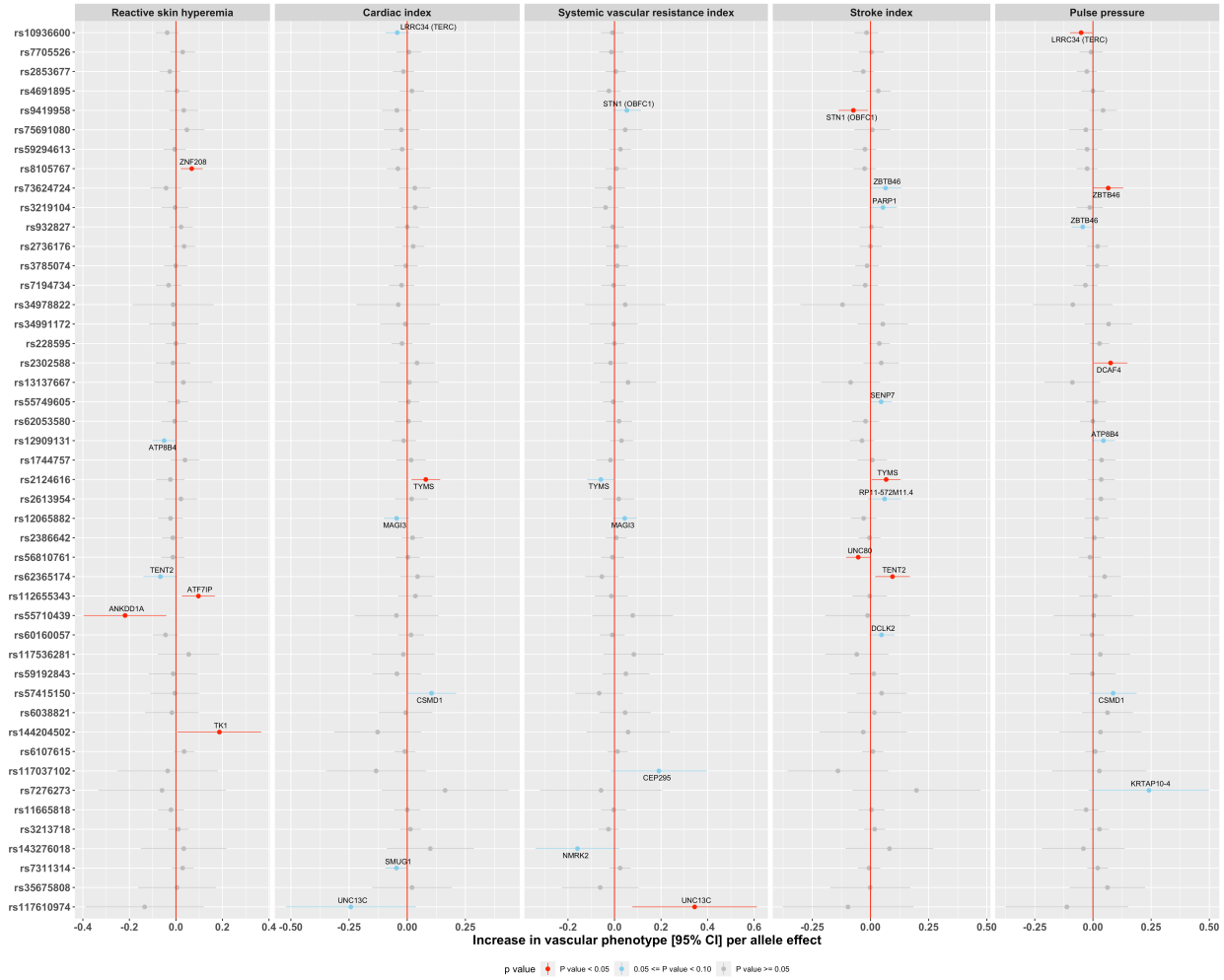

Figure 24. The association between each variant with significant vascular phenotypes

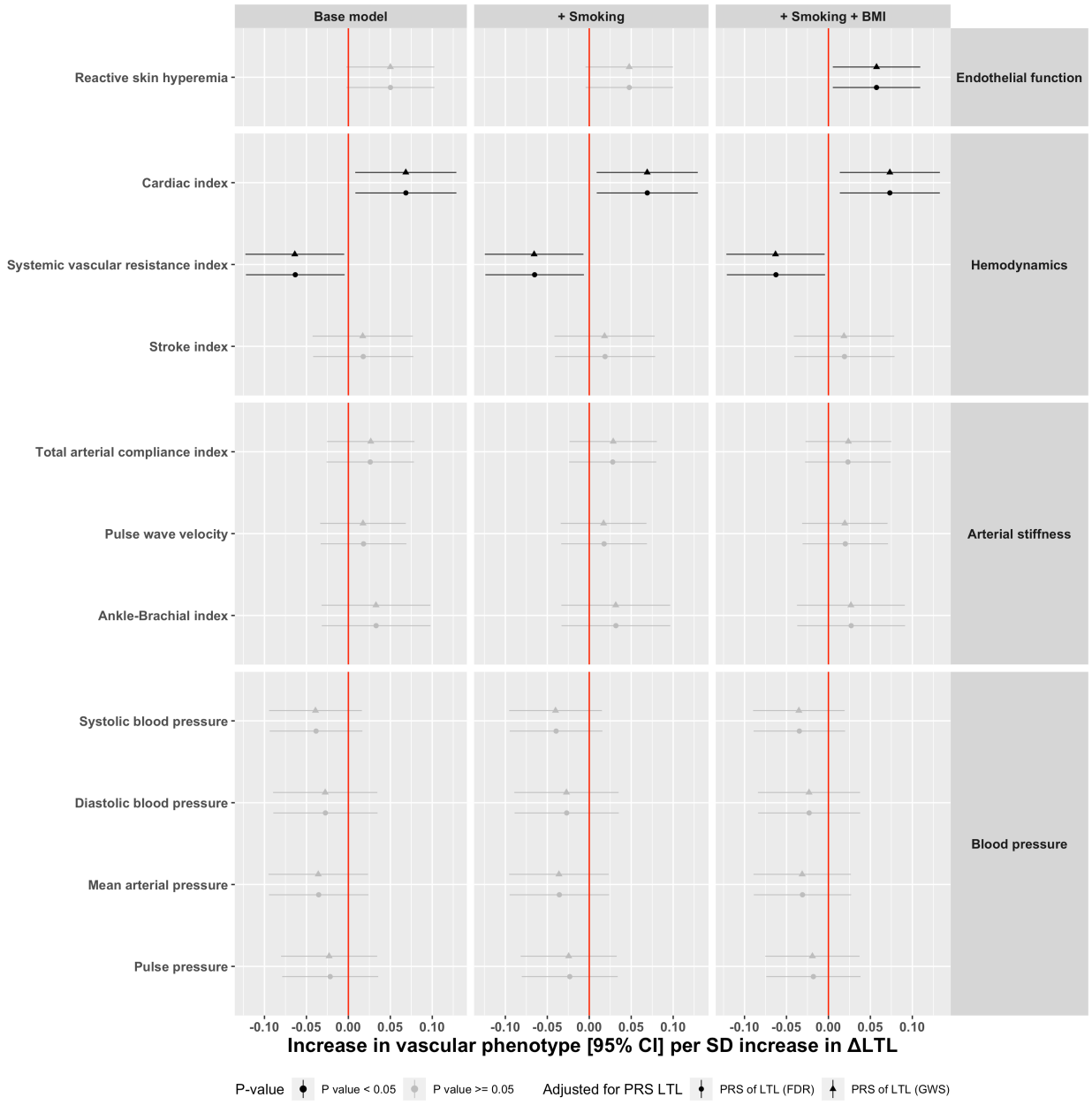

Figure 25. The association between the delta leukocyte telomere length and vascular phenotypes

Base model: vascular phenotype~ ΔLTL + polygenic risk score (PRS) of LTL + age + sex
PRS of LTL (FDR) includes 47 variants at false-discovery rate < 0.05, and PRS of LTL (GWS) includes 20 variants at genome-wide significance ($5*10^{-8}$) level.

4. Discussion

4.1 Cardiovascular and epigenetic aging

We performed one of the largest and most comprehensive studies to date on the relation between cardiovascular risk factors across multiple domains, as well as novel quantitative markers of cardiovascular aging, applying and comparing different epigenetic estimators of accelerated biological aging. Using a population-based approach, we found that across a wide age range, individuals with an unhealthy cardiovascular risk profile, as well as those who had unfavourable quantitative markers of arterial stiffness and hemodynamics, consistently displayed accelerated epigenetic aging, with lifespan acceleration estimators outperforming first-generation epigenetic age acceleration estimators in capturing multisystem dysregulation. Importantly, the effects of cardiovascular risk factors and cardiovascular aging markers on accelerated DNAm age were largely independent, suggesting that targeting of (modifiable) cardiovascular risk profiles across different physiological domains is likely to have a cumulative effect with respect to slowing of the unhealthy aging process.

These findings indicate that an unfavourable cardiovascular health profile could underlie interindividual differences in biological aging beyond chronological age, contributing to unhealthy aging-related morbidity and mortality. Biological aging has been linked to an increased risk of all-cause mortality and is strongly associated with chronological age. By assessing the association between cardiovascular aging markers with both generation epigenetic age acceleration estimators, we show that unfavourable changes in cardiovascular aging markers across multiple physiological domains are consistently associated with all epigenetic age acceleration estimators, capturing variations in the rate of biological aging beyond chronological age. Moreover, our study also provides clues on how lifespan acceleration estimators might capture more aspects of biological aging and outperform first-generation age acceleration estimators as determinants of morbidity and mortality. Aging involves complex changes across multiple physiological domains, which together determine the pace of aging (Harman 1991; Khan et al. 2017). Compared with first-generation DNAm age estimators, which use chronological age as a proxy of biological age, lifespan estimators, including DNAm PhenoAge and DNAm GrimAge,

include not only CpGs with strong time-dependent changes, but also those related to divergence in the rate of aging (Horvath and Raj 2018; Levine et al. 2018; Lu et al. 2019). Indeed, we found that more cardiovascular factors were associated with lifespan acceleration estimators, and that the effect sizes were larger for the lifespan acceleration estimators as compared to the first-generation age acceleration estimators, suggesting that lifespan acceleration estimators are more sensitive to physiological changes reflected at the epigenetic level. Collectively, these findings suggest that lifespan acceleration estimators more closely reflect the cumulative effects of the underlying aging-related molecular mechanisms on the epigenome (Gao et al. 2019; Hannum et al. 2013; Horvath 2013; Levine et al. 2018; Lu et al. 2019; Schottker et al. 2020).

Our findings confirm and substantially extend previous findings by showing that unfavourable changes in cardiovascular risk factors across multiple physiological domains are consistently associated with both first and second-generation DNAm age acceleration estimators. Moreover, the effects were largely independent and were seen across a wide age spectrum. This indicates that the effects of changes in multiple cardiovascular domains are additive at the epigenetic level, suggesting an independent modification of the rate of biological aging. The relation between many cardiovascular risk factors, including hypertension and obesity, increased cardiovascular-associated morbidity, and decreased life expectancy has been well established (Collaborators 2017; D'Agostino et al. 2008; Yusuf et al. 2004). However, the underlying molecular pathways mediating these associations are much less clear. A potential mechanism could be the influence of cardiovascular risk factors on systemic gene expression profiles through changes in DNA methylation (Mendelson et al. 2017; Richard et al. 2017). Although several studies have indeed found associations between BMI, blood pressure, metabolic syndrome, and DNAm age acceleration estimators, these were mostly small-scaled and focused on only a few cardiovascular risk factors, mainly in relation to first-generation DNAm age acceleration estimators (Huang et al. 2019; Nannini et al. 2019; Nevalainen et al. 2017; Quach et al. 2017). Conversely, our findings highlight a robust relation between most known cardiovascular risk factors and accelerated epigenetic aging, and thereby support the notion that managing common modifiable risk factors could prevent detrimental changes in DNA methylation patterns and contribute to healthy aging.

Importantly, we also found that novel quantitative markers of cardiovascular aging were robustly associated with accelerated DNAm age. Previous studies of such markers mainly focused on studying the methylation status of single genes (Jiang et al. 2014; Murray et al. 2016). They showed that hemodynamic changes may exert part of their role in the pathogenesis of vascular diseases through epigenetic remodeling (Dunn et al. 2014; Jiang et al. 2014). We found that unfavourable changes in measures of arterial stiffness and hemodynamics were associated with accelerated DNAm age. As DNAm age acceleration estimators take the methylation status of a panel of CpG changes into account, our findings support the notion that cardiovascular dysfunction may induce multiple methylation changes across the epigenome, which could have an impact on the rate of biological aging. Therefore, our findings suggest that targeting age-related changes in cardiovascular functions may beneficially influence the underlying aging process.

Our study has both strengths and limitations. First, we were able to scrutinize the effects of a wide range of cardiovascular risk factors and novel quantitative cardiovascular aging markers conjointly in one of the largest studies to date concerning the relation between cardiovascular and accelerated epigenetic aging. Second, we present results for first and second-generation DNAm age acceleration estimators, showing that although the effects are consistent across the different “epigenetic clock acceleration estimators”, the lifespan acceleration estimators more closely reflect changes in cardiovascular risk factors. Third, our estimates are based on a broad age spectrum, ranging from 30 to 95 years old, and are therefore likely to represent the association between cardiovascular and accelerated epigenetic aging across most of the adult lifespan. On the other hand, the cross-sectional nature of our study precludes formal evaluation of the directionality of the effects. So, although we consider it likely, based on findings from prior experimental studies, that cardiovascular risk factors trigger changes in DNA methylation, the converse cannot be excluded.

In conclusion, we found that multiple cardiovascular risk factors and quantitative cardiovascular aging markers across different physiological systems were consistently and independently associated with accelerated DNAm age. These classical risk factors and quantitative cardiovascular aging makers per se were highly associated with vascular

aging. Our study suggested that beyond vascular consequences, they were consistently and independently related to biological aging. These cardiovascular risk factors may hence serve as targets to modify the rate of biological aging with health impacts beyond the mere cardiovascular aspects of the aging process.

4.2 Lipidomics and epigenetic aging

We investigated 14 complex lipid classes, covering 964 molecular species and 267 one-fatty-acid-tail compositions, in relation to biological aging. We found many complex lipid species to be differently associated with different rates of biological aging. Higher levels of molecular species belonging to the neutral lipids (MAG, DAG, TAG), phospholipids (PE, PE(O), PE(P)), sphingolipids (CER, DCER) classes were associated with accelerated biological aging, whereas higher levels of distinct other molecular species (i.e. LPC, HCER and LCER) were associated with slower biological aging. CE, PC, LPE molecular species with odd-numbered (i.e. 15 and 17) fatty acid tail lengths were associated with slower biological aging, whereas even-numbered fatty acid tail lengths were associated with faster biological aging. Importantly, *in silico* pathway analysis revealed that lipids that were associated with biological aging estimators were mainly involved in known longevity and aging-related pathways, supporting their role as potential determinants of biological aging across lifespan in the general population.

We found higher levels of odd-numbered fatty acid tail lengths (15:0 and 17:0) to be associated with slower biological aging, but even-numbered fatty acid tail lengths with faster biological aging. This fits observations from previous studies. The EPIC-InterAct study (n = 27,296) found that higher levels of odd-chain saturated fatty acids (15:0; 17:0) were associated with a reduced risk of type 2 diabetes, whereas this risk was increased for people with higher levels of even-chain saturated fatty acids (Forouhi et al. 2014). The EPIC-Norfolk study (n=7354) likewise found that even-chain saturated fatty acids were positively associated with incident coronary heart disease (CHD), while odd-chain saturated fatty acids (15:0; 17:0) were inversely associated with incident CHD (Khaw et al. 2012). However, the underlying mechanisms are largely unknown. C15:0 and C17:0 have an exogenous origin, and are mainly derived from dietary dairy fats, especially from ruminant fat (Brevik et al. 2005; Smedman et al. 1999; Wolk et al. 1998). These two odd-

chain length fatty acids are produced by the rumen microbiome and then incorporated into the fat tissue of the host animal, and have been suggested as potential biomarkers of milk or dairy fat intake in humans (Brevik et al. 2005; Hodson et al. 2008; Smedman et al. 1999). Even-chain length saturated fatty acids are mainly derived from *de novo* lipogenesis, through which carbohydrates and alcohol are converted to fatty acids in the liver or adipose tissue. Biochemical experiments also demonstrated toxic effects of 16:0, 18:0, 24:0, including activation of inflammatory cytokines and lipotoxicity to pancreatic β cells (Huang et al. 2012; Maedler et al. 2001; Pararasa et al. 2016). This suggests that lipid composition of the diet might have an impact on rate of biological aging.

Very little work has explicitly assessed the value of LPC species as potential human blood-derived biomarkers of human aging. Circulating LPCs are generated by phospholipases A2 from PC. The most abundant LPC in human plasma is 16:0, followed by 18:2, 18:0, 18:1, 20:4, and other minor species (Drzazga et al. 2014). We showed that 13 out of 19 measured LPC species exhibit a robust negative association with epigenetic markers of biological aging, suggesting that many LPC species may contribute to healthy aging. Our findings expand on those from recent epidemiological studies, involving assessment of a limited number of LPC species, that also reported low concentrations of certain circulating LPCs (i.e. 18:2 and/or 17:0) to be associated with several aging-related phenotypes and disorders, including memory impairment (Mapstone et al. 2014), gait speed decline (Gonzalez-Freire et al. 2019), and incident myocardial infarction (Ward-Caviness et al. 2017). Conversely, elevated LPC (18:1) levels were reported in centenarians (Montoliu et al. 2014). A potential biological mechanism through which LPCs could contribute to biological aging and age-associated disorders is oxidative stress and inflammatory responses (Knuplez and Marsche 2020; Law et al. 2019). Accumulating evidence indicates that LPCs are involved in NADPH oxidase stimulation of the production of reactive oxygen species (ROS), thereby converting pro-cytokines to their biologically active forms (Brandes and Kreuzer 2005). Moreover, polyunsaturated LPCs (e.g. LPC 20:4, 22:6) were shown to exert anti-inflammatory effects in animal studies (Hung et al. 2012; Lucas et al. 2008). Recently, lower levels of several LPC species (LPC 16:0, 16:1, 17:0, 18:1, 18:2, 20:3) were also linked to impaired mitochondrial oxidative capacity in adults, another important hallmark of aging (Semba et al. 2019).

For other phospholipids, which are major components of cell membranes, we found that polyunsaturated PCs were generally associated with slower aging, whereas species with fewer double bonds and carbons tended to be associated with accelerated aging. These findings are in line with those from previous studies that found associations between saturated and monounsaturated PCs and cardiovascular diseases and type 2 diabetes (Tabassum et al. 2019). Moreover, unsaturated PC species (PC 36:2, 36:3, 34:1, 34:3) have been linked to longevity, which might be due to their antioxidative and cardioprotective properties (e.g. PC 34:1, 36:6) (Gonzalez-Covarrubias et al. 2013; Montoliu et al. 2014; Pradas et al. 2019). PE species, the second most abundant membrane phospholipids, have also been identified as modulators of inflammation and apoptosis (Pamplona 2008), yet little is known about the properties of specific PE species. Here we show that that higher levels of various PE species are robustly related to accelerated aging across life span, thereby supporting and substantially extending previous reports of lower PE (38:6) levels in the offspring of nonagenarians (Gonzalez-Covarrubias et al. 2013).

Higher TAG levels are linked to an increased risk of cardiovascular diseases and type 2 diabetes (Rhee et al. 2011; Stegemann et al. 2014). Small-scale lipidomic profiling in longevity studies also found lower levels of TAG species (including TAG 46:5, 47:5, 52:1, 54:7, 54:6, 56:6, 56:7, 57:2) to be associated with healthy aging (Collino et al. 2013; Gonzalez-Covarrubias et al. 2013; Montoliu et al. 2014). Our findings parallel and considerably extend these previous reports by showing that 361 out of 519 TAG species across different chain lengths and double bonds were associated with accelerated biological aging. Few studies have investigated the association between other neutral lipids (including CE, MAG, DAG) and longevity or healthy aging. Here we show that higher levels of DAG species or lower levels of CE species are related to an accelerated rate biological aging, indicating that almost all neutral lipids could potentially influence longevity.

Plasma sphingolipids have also been proposed as biomarkers of various age-related diseases, including Alzheimer’s disease, Parkinson’s disease, diabetes, obesity, and CVDs (Holland and Summers 2008; Nelson et al. 2006; Piccinini et al. 2010; Proitsi et al.

2017). We found that lower levels of SM (20:0, 20:1, 22:0, 22:1) were associated with accelerated aging, which supports previous studies showing higher levels of certain SM species in the offspring of long-lived individuals (Gonzalez-Covarrubias et al. 2013; Vaarhorst et al. 2011). Moreover, the SM species that we found to be associated with accelerated aging, have previously been associated with diabetes and hypertension (Gonzalez-Covarrubias et al. 2013; Vaarhorst et al. 2011). It is known that SM species can be hydrolyzed into ceramides by sphingomyelinase, whose activity increases with aging. Therefore, increased sphingomyelinase activity could result in declining levels of SMs and increasing levels of CERs with aging (Smith et al. 2006).

HDL and LDL levels are well-established biomarkers for various CVDs and are widely used in assessing CVD risk in the clinic (Barter et al. 2007; Toth 2004). We demonstrate that the effects of neutral lipids and phospholipids on biological aging largely depend on HDL and LDL levels, whereas those of sphingolipids are largely independent of HDL and LDL levels. This finding reflects the well-characterized role of lipoproteins in lipid metabolism: Lipoproteins are complex aggregates of lipids and proteins that render the hydrophobic lipids compatible with the body fluids and enable their transport throughout the body to tissues where they are required. Their most abundant lipid constituents are TAGs, free cholesterol, CEs and phospholipids (especially PCs and PEs). Lipoproteins are the main player in exogenous, endogenous and reverse cholesterol transport pathways, thus contributing predominantly to the neutral lipids and phospholipids metabolism (Kwiterovich 2000). In contrast, sphingolipid metabolism is more independent of lipoproteins (Borodzicz et al. 2015). Our findings provide a detailed overview of the differential effects of lipoproteins across a wide range of lipid classes and species and underscore the importance of accounting for their potentially confounding effects in lipidomics analyses.

The main strength of our study is that we were able to delineate the effects of a comprehensive quantitative panel of well-characterized plasma lipids on two novel epigenetic estimators of biological aging. Moreover, we provide in-depth analyses of the associations between the wide variation in the structure and fatty acid composition of a wide array of lipid molecules on these biological aging estimators. Third, leveraging on

extensive individual-level methylation array data, we were able to scrutinize the underlying biological pathways likely to be involved in mediating the effects of complex lipids on biological aging. In addition, our estimates are based on a broad age spectrum, ranging from 30 to 95 years, and are therefore likely to represent the lipidomic correlates of epigenetic aging across most of the adult lifespan. However, the cross-sectional nature of our study precludes formal evaluation of the directionality of the effects. Based on findings from previous studies we nevertheless consider it most likely that changes in lipid composition can alter DNA methylation (Dekkers et al. 2016; Jhun et al. 2021). Mendelian randomization analyses could possibly help inferring causality. Furthermore, longitudinal studies are needed to scrutinize the temporal dynamics of the relationship between plasma lipids and biological aging.

To sum up, we provide a comprehensive in-depth overview of the lipidomic correlates of biological aging across lifespan in a large well-characterized community-based cohort study. Our findings indicate that diverse complex lipid species are associated with different rates of biological aging, with lipid class as well as fatty acid chain length and saturation as key determinants of their influence on biological aging. These findings emphasize the importance of investigating in-depth lipidomics in aging research beyond the standard clinical lipid panel. Since lower LPC species were predominantly negatively associated with biological aging and have been linked to age-related biological mechanisms (e.g. oxidative stress and mitochondrial dysfunction), they represent promising candidate human blood-derived biomarkers of human aging. Finally, investigating the sources of different lipids which have disparate association patterns with biological aging may increase our understanding of the underlying biological mechanisms.

4.3 Leukocyte telomere length and vascular aging

Using a hypothesis-driven approach, we systematically examined the associations of measured and genetically predicted LTL with a large number of sensitive quantitative markers of cardiovascular function across four major vascular domains in the general population, including endothelial function, hemodynamics, arterial stiffness and blood pressure. We found that both measured and genetically predicted LTL, as well as **Δ**LTL, the difference between measured and genetically predicted LTL, were all consistently

associated with endothelial function and hemodynamic traits, but not with markers of arterial stiffness. Taking advantage of findings from a recent meta-GWAS, we were able to develop a robust PRS of LTL that we also validated against measured LTL values in our cohort. Importantly, the consistent associations of measured and genetically predicted LTL with vascular phenotypes indicate that longer LTL is likely to be causally related to better endothelial and cardiac function. Additionally, **Δ**LTL was associated with endothelial function, cardiac index, and systemic vascular resistance index. This suggests that telomere shortening itself, rather than genetically or non-genetically determined, contributes to cardiovascular dysfunction (Werner et al. 2019; Yeh et al. 2019). Of note, **Δ**LTL was stronger associated with endothelial function and cardiac index than either measured LTL or genetically predicted LTL. These findings have profound implications for our understanding of cardiovascular senescence and suggest that counteracting telomere shortening via non-genetic factors, including nutrition (Crous-Bou et al. 2019; Leung et al. 2018), physical activity (Tucker 2017; Werner et al. 2019), and sleep (Jackowska et al. 2012; Tempaku et al. 2018), may reduce the risk of CVDs.

We found that both longer measured and genetically predicted LTL, as well as a lower **Δ**LTL, are associated with better endothelial function. These findings support the notion that telomere-triggered cell senescence could potentially cause endothelial dysfunction, which is an early feature of atherosclerosis and vascular diseases. Although experimental studies have suggested that telomere function is a crucial determinant of endothelial function (Chang and Harley 1995; Chen et al. 2021; Maeda et al. 2019; Minamino et al. 2001; Minamino et al. 2002; Yepuri et al. 2016), only a few small-scaled clinical and epidemiological studies have investigated the association of telomere length with endothelial function (Gonzalez-Guardia et al. 2014; Nezu et al. 2015). One cross-sectional study in 102 patients with a history of cerebrovascular diseases found shortened telomeric 3'-overhang (G-tail), but not total telomere length, to be associated with endothelial function (Nezu et al. 2015). Another cross-sectional study from the LIPGENE cohort including 88 patients with metabolic syndrome also found that endothelial function, through high oxidative stress, was associated with shorter telomere length (Gonzalez-Guardia et al. 2014). Our study, with a much larger sample size and a wide age range among community-dwelling adult, not only confirms and substantially extends these

previous finding but also provides evidence for a causal connection between telomere-triggered cell senescence and endothelial dysfunction at population level.

The relationship of both measured and genetically predicted LTL with hemodynamic measures indicates that telomere-triggered cell senescence may be a biologically important factor that contributes to the age-related decline in heart function. Experimental studies highlighted the important role of cardiac telomere length in heart development, function and disease (Booth and Charchar 2017). Decreases in telomere length in cardiomyocytes induced apoptosis and heart disease (Anderson et al. 2019; Leri et al. 2003). Several lines of evidence also show that telomere-induced senescence in cardiac stem cells forces the cells to undergo apoptosis when the telomere length reaches a critical threshold, which in turn, prevents cardiomyocyte replenishment of damaged cells and consequently leads to heart disease (Aguado et al. 2017; Cesselli et al. 2011; Chen et al. 2021; Fathi et al. 2019). However, there are much fewer epidemiological studies assessing the association between LTL and hemodynamic traits. In particular, the relation between PRS of LTL and hemodynamic markers had not been examined before. Beyond the studies mentioned previously, a recent study in 566 normotensive and never-treated hypertensive subjects found that mean LTL was only associated with the augmentation index, but not with other hemodynamic variables (including aortic blood pressure and pulse wave velocity), independent of CVD risk factors; although mean LTL correlated with systemic vascular resistance in the univariate analyses (Honkonen et al. 2020). Applying a population-based approach in which we leveraged new genetic findings to create a more powerful PRS of LTL than previously possible, our findings support a causal role for telomere-triggered cell senescence in the pathogenesis of cardiovascular dysfunction across the adult life course.

There was little evidence of an association between LTL measures, arterial stiffness, and blood pressure parameters, which echoed previous studies. Prior studies have observed inconsistent associations between measured LTL/ genetically predicted LTL, arterial stiffness and blood pressure traits, with several null results reported (Bekaert et al. 2007; Brown et al. 2018; Denil et al. 2014; Nguyen et al. 2019; Rehkopf et al. 2016). The marginal associations could be residual confounding (LTL measurement and/or

environmental effects) and biological pleiotropy related to genetic determinants of LTL (Demanelis et al. 2021). Moreover, there is sparse biological evidence of telomere-triggered cell senescence with arterial stiffness and blood pressure traits.

Our study has both strengths and limitations. Strengths of our study include the relatively large sample size, inclusion of individuals across a wide age range from the general population, as well as the availability of estimates of both measured and genetically predicted LTL. This enabled internal validation of the PRS of LTL in our cohort, as well as derivation of another metric, **Δ**LTL, which allowed estimation of difference between measured LTL and genetically predicted LTL in relation to vascular phenotypes independent of genetically predicted LTL. Indeed, we were able to replicate the previously identified top hits related to LTL and were able to construct two PRSs of LTL based on SNPs with a clear relevance to telomere biology, further supporting the biological plausibility of our findings. Moreover, the availability of robust PRSs of LTL allowed us to provide evidence for a causal role of telomere length in cardiovascular senescence and dysfunction. A limitation of our study is the lack of longitudinal follow-up data, which precluded assessment of the effects of telomere shortening on incident CVDs. In addition, five SNPs previously identified to be associated with LTL were not available on our genetic arrays; however, the subset of 20 genome-wide significant variants was available.

In conclusion, both measured and genetically predicted LTL, as well as **Δ**LTL, were consistently associated with endothelial function and hemodynamic traits. Importantly, the robust association between a validated PRS of LTL and different quantitative markers of cardiovascular function support a causal role for telomere shortening in the pathogenesis of endothelial and cardiac dysfunction. These findings implicate telomere-triggered cell senescence in the mechanistic pathways underlying cardiovascular dysfunction and CVDs. Together with prior studies, our data provide evidence that lifestyle interventions may not only reduce the risk of CVDs, but also of other age-related disorders (Elks and Scott 2014; Sindi et al. 2021). These findings also suggest that besides lifestyle interventions that can slow telomere shortening, the development of treatments that target telomere shortening, might reduce the risk of CVDs, and potentially also other aging-related diseases.

4.4 Summary and outlook

Aging is a universal process of physiological and molecular changes that are strongly associated with susceptibility to disease and ultimately death (Ahadi et al. 2020). Measuring biological aging at the individual level reveals distinct aging signatures declining at faster, or slower rates (Hannum et al. 2013; Horvath 2013; Lehallier et al. 2020; Mamoshina et al. 2018; Nazish Sayed 2019; Robinson et al. 2020). Biomarkers of aging, including DNAm age acceleration estimators and LTL, can distinguish between individuals who are of the same chronological age but differ in their biological aging rates (Hannum et al. 2013; Horvath 2013; Levine et al. 2018; Lu et al. 2019; Rizvi et al. 2014).

Quantitative biomarkers of biological aging offer several benefits in that they can be utilized as: 1) proxy outcome measures in etiologic research, as they reflect individuals' physiological state and the underlying mechanisms related to aging throughout the lifespan (Horvath and Raj 2018; Jones et al. 2015; Jylhava et al. 2017); 2) predictive biomarkers of age-related phenotypes, and may even be used to predict lifespan (Chen et al. 2016; Lu et al. 2019); 3) surrogate endpoints, which enable to evaluate the efficacy and safety of interventions/treatments to slow down the biological aging process or to extend the healthspan (Belsky et al. 2020); 4) health metrics, which allow public health officials to test whether policies or programs can promote healthier and longer lives.

Assessing the determinants or correlates of biological aging is a prerequisite to apply such biomarkers as surrogate endpoint measures or predictive biomarkers. In the scope of this thesis, we found that multiple cardiovascular risk factors and quantitative cardiovascular aging markers across different physiological systems, as well as different complex lipid species, are associated with DNAm age acceleration estimators. Our data provide evidence that DNAm age acceleration estimators could be utilized not only as proxy outcome measures in etiologic research and intervention studies but also as predictive biomarkers of age-related conditions. Moreover, we found that measured, genetically predicted LTL, as well as **Δ**LTL, were consistently associated with endothelial function and hemodynamic traits. These findings suggest that telomere length could be used as a

surrogate measure in etiologic studies or in interventions to evaluate if counteracting telomere shortening could have beneficial health impacts.

These findings provide valuable evidence supporting the promising utility of these biomarkers, but also more studies are needed to address the following questions. First, it is essential to determine whether these associations reflect causal pathways or rather consequences of the aging process. Mendelian randomization analyses or other causal inference models could help to infer causality. Second, assessing how these biomarkers change across the lifespan and how these biomarkers interact with modifiable risk factors is of great importance. In this regard, longitudinal studies are essential to examine these changes and how lifestyle shapes the aging phenotypes. In addition, to have a better understanding of specific biological changes in aging and its implications, systems biology approaches could offer insights into the organ and systems-specific functions (Bell et al. 2019). Last but not the least, it has been suggested that a composite biological aging measure may be of greatest interest, which reflects the global susceptibility to disease with aging (Ferrucci et al. 2020).

In summary, this thesis provided a comprehensive in-depth overview of the cardiovascular and lipidomic correlates of biological aging across adult lifespan and the role of telomere-triggered cell senescence in cardiovascular dysfunction. These findings yield insight into the underlying process of biological aging and can lay the groundwork for future studies to explore their therapeutic relevance to promote healthy aging.

5. Abstract

The rapid aging of the global population, often accompanied by disabilities and various age-related diseases, is becoming a major public health burden (WHO 2015). Stimulating healthy aging is therefore of tremendous importance. However, substantial inter-individual variation in aging and aging-associated morbidity remain in individuals of the same chronological age, pointing towards markedly different rates of biological aging (Ben-Shlomo et al. 2014; Hamczyk et al. 2020; Medina-Lezama et al. 2018; Patel et al. 2015; Yusuf et al. 2020). The determinants of biological aging are largely unknown. Elucidation of the factors underlying interindividual differences in biological aging and delineation of their precise contributions are essential for the development of individualized approaches to promoting healthy aging.

CVDs are the leading causes of morbidity and mortality worldwide (CollaboratorsGBDCoD 2017; North and Sinclair 2012). As with other age-related diseases, inter-individual variation in cardiovascular aging and associated morbidity in individuals of the same chronological age, points towards markedly different rates of biological aging (Ben-Shlomo et al. 2014; Hamczyk et al. 2020; Medina-Lezama et al. 2018; Patel et al. 2015; Yusuf et al. 2020). Whether and to what extent different cardiovascular risk factors and cardiovascular aging markers contribute to different rates of biological aging, estimated as DNAm age acceleration, remains largely unknown. Therefore, in study I, I examined whether classical cardiovascular risk factors involving multiple domains as well as novel quantitative markers of cardiovascular aging, including arterial stiffness, endothelial function and systemic hemodynamics, have consistent and independent effects on various epigenetic age accelerations across a wide age range in the general population. Using a population-based approach with extensive deep-(endo)phenotype data on nearly 3,500 participants aged 30 years and above (30 - 95 years old), we found that multiple cardiovascular risk factors, arterial stiffness and hemodynamics were consistently and independently associated with DNAm age acceleration estimators, and could contribute to different rates of biological aging.

Lipid metabolites are essential components of biological membranes and signaling molecules, and the lipidome represents an individual's biological state (Hahn et al. 2017). Certain lipid profiles have been associated with human longevity and lifespan (Gonzalez-Covarrubias et al. 2013; Montoliu et al. 2014; Vaarhorst et al. 2011), yet systematic studies assessing which lipid species across different classes and compositions influence biological aging are lacking. The heterogeneous chemical structure of lipids poses challenges for their accurate quantification, and until now only a few lipid species have been investigated in relation to aging and age-related health outcomes. Therefore, in study II, I investigated 14 complex lipid classes, covering 964 molecular species and 267 one-fatty-acid-tail compositions, in relation to different rates of epigenetic aging – a proxy for biological aging – across the adult lifespan on the first 4181 participants of the Rhineland Study. We present the largest and most comprehensive study to date showing that across neutral lipids, phospholipids, and sphingolipids, different complex lipid species are associated with different rates of biological aging, with the effects mainly depending on lipid class and fatty acid chain length. These findings offer novel potential targets for promoting healthy aging.

Telomeres are DNA-protein complexes located at the end of chromosomes and have been proposed as another hallmark of biological aging as they shorten with age and each cell division, thereby triggering cellular senescence (Blackburn et al. 2015; O'Sullivan and Karlseder 2010). Emerging evidence has suggested that telomere-triggered cellular senescence might contribute to the pathogenesis of endothelial and hemodynamic dysfunction (Maeda et al. 2019; Minamino et al. 2001; Minamino et al. 2002). However, cross-sectional studies have yielded conflicting results regarding the associations between LTL and vascular phenotypes, and the temporality of associations remains unclear. Therefore, in study III, I assessed the association of measured, genetically predicted LTL, and **Δ**LTL with vascular phenotypes, including endothelial function, hemodynamics, arterial stiffness, blood pressure, across the adult lifespan in a population-based study. Using a hypothesis-driven approach, we observed that both measured and genetically predicted LTL, as well as **Δ**LTL, were all consistently associated with endothelial function and hemodynamic traits, but not with markers of arterial stiffness. Importantly, the robust association between a validated PRS of LTL and different

quantitative markers of cardiovascular function support a causal role for telomere shortening in the pathogenesis of endothelial and cardiac dysfunction. These findings implicate telomere-triggered cell senescence in the mechanistic pathways underlying cardiovascular dysfunction and CVDs. Additionally, **Δ**LTL was associated with endothelial function, cardiac index, and systemic vascular resistance index. This suggests that telomere shortening itself, rather than genetically or non-genetically determined, contributes to cardiovascular dysfunction (Werner et al. 2019; Yeh et al. 2019).

In summary, in this thesis I presented novel evidence about the precise contributions of cardiovascular phenotypes and complex lipids to different rates of biological aging, and the role of telomere-triggered cell senescence in cardiovascular aging. In a progressively older world population, these findings could provide the basis for the development of more potent anti-aging approaches focused on biological aspect of the aging process.

6. List of figures

7. List of tables

8. References

Aboyans V, Criqui MH, Abraham P, Allison MA, Creager MA, Diehm C, et al. 2012. Measurement and interpretation of the ankle-brachial index: A scientific statement from the american heart association. Circulation 126:2890-2909.

Aguado T, Gutierrez FJ, Aix E, Schneider RP, Giovinazzo G, Blasco MA, et al. 2017. Telomere length defines the cardiomyocyte differentiation potency of mouse induced pluripotent stem cells. Stem Cells 35:362-373.

Ahadi S, Zhou W, Schussler-Fiorenza Rose SM, Sailani MR, Contrepois K, Avina M, et al. 2020. Personal aging markers and ageotypes revealed by deep longitudinal profiling. Nat Med 26:83-90.

Anderson R, Lagnado A, Maggiorani D, Walaszczyk A, Dookun E, Chapman J, et al. 2019. Length-independent telomere damage drives post-mitotic cardiomyocyte senescence. EMBO J 38.

Aref-Eshghi E, Biswas S, Chen C, Sadikovic B, Chakrabarti S. 2020. Glucose-induced, duration-dependent genome-wide DNA methylation changes in human endothelial cells. Am J Physiol Cell Physiol 319:C268-C276.

Barter P, Gotto AM, LaRosa JC, Maroni J, Szarek M, Grundy SM, et al. 2007. Hdl cholesterol, very low levels of ldl cholesterol, and cardiovascular events. N Engl J Med 357:1301-1310.

Bekaert S, De Meyer T, Rietzschel ER, De Buyzere ML, De Bacquer D, Langlois M, et al. 2007. Telomere length and cardiovascular risk factors in a middle-aged population free of overt cardiovascular disease. Aging Cell 6:639-647.

Bell CG, Lowe R, Adams PD, Baccarelli AA, Beck S, Bell JT, et al. 2019. DNA methylation aging clocks: Challenges and recommendations. Genome Biol 20:249.

Bell JT, Tsai PC, Yang TP, Pidsley R, Nisbet J, Glass D, et al. 2012. Epigenome-wide scans identify differentially methylated regions for age and age-related phenotypes in a healthy ageing population. PLoS Genet 8:e1002629.

Belsky DW, Caspi A, Arseneault L, Baccarelli A, Corcoran DL, Gao X, et al. 2020. Quantification of the pace of biological aging in humans through a blood test, the dunedinpoam DNA methylation algorithm. Elife 9.

Ben-Shlomo Y, Spears M, Boustred C, May M, Anderson SG, Benjamin EJ, et al. 2014. Aortic pulse wave velocity improves cardiovascular event prediction: An individual

participant meta-analysis of prospective observational data from 17,635 subjects. J Am Coll Cardiol 63:636-646.

Blackburn EH, Epel ES, Lin J. 2015. Human telomere biology: A contributory and interactive factor in aging, disease risks, and protection. Science 350:1193-1198.

Booth SA, Charchar FJ. 2017. Cardiac telomere length in heart development, function, and disease. Physiol Genomics 49:368-384.

Borodzicz S, Czarzasta K, Kuch M, Cudnoch-Jedrzejewska A. 2015. Sphingolipids in cardiovascular diseases and metabolic disorders. Lipids Health Dis 14:55.

Brandes RP, Kreuzer J. 2005. Vascular nadph oxidases: Molecular mechanisms of activation. Cardiovasc Res 65:16-27.

Braun KVE, Dhana K, de Vries PS, Voortman T, van Meurs JBJ, Uitterlinden AG, et al. 2017. Epigenome-wide association study (ewas) on lipids: The rotterdam study. Clin Epigenetics 9:15.

Breitling LP, Saum KU, Perna L, Schottker B, Holleczek B, Brenner H. 2016. Frailty is associated with the epigenetic clock but not with telomere length in a german cohort. Clin Epigenetics 8:21.

Brevik A, Veierod MB, Drevon CA, Andersen LF. 2005. Evaluation of the odd fatty acids 15:0 and 17:0 in serum and adipose tissue as markers of intake of milk and dairy fat. Eur J Clin Nutr 59:1417-1422.

Broer L, Codd V, Nyholt DR, Deelen J, Mangino M, Willemsen G, et al. 2013. Meta-analysis of telomere length in 19,713 subjects reveals high heritability, stronger maternal inheritance and a paternal age effect. Eur J Hum Genet 21:1163-1168.

Brown LL, Zhang YS, Mitchell C, Ailshire J. 2018. Does telomere length indicate biological, physical, and cognitive health among older adults? Evidence from the health and retirement study. J Gerontol A Biol Sci Med Sci 73:1626-1632.

Burkewitz K, Zhang Y, Mair WB. 2014. Ampk at the nexus of energetics and aging. Cell Metab 20:10-25.

Cawthon RM. 2009. Telomere length measurement by a novel monochrome multiplex quantitative pcr method. Nucleic Acids Res 37:e21.

Cesselli D, Beltrami AP, D'Aurizio F, Marcon P, Bergamin N, Toffoletto B, et al. 2011. Effects of age and heart failure on human cardiac stem cell function. Am J Pathol 179:349-366.

Chang E, Harley CB. 1995. Telomere length and replicative aging in human vascular tissues. Proc Natl Acad Sci U S A 92:11190-11194.

Chen BH, Marioni RE, Colicino E, Peters MJ, Ward-Caviness CK, Tsai PC, et al. 2016. DNA methylation-based measures of biological age: Meta-analysis predicting time to death. Aging (Albany NY) 8:1844-1865.

Chen MS, Lee RT, Garbern JC. 2021. Senescence mechanisms and targets in the heart. Cardiovasc Res.

Choi PJ, Brunt VE, Fujii N, Minson CT. 2014. New approach to measure cutaneous microvascular function: An improved test of no-mediated vasodilation by thermal hyperemia. J Appl Physiol (1985) 117:277-283.

Collaborators GBDCoD. 2017. Global, regional, and national age-sex specific mortality for 264 causes of death, 1980-2016: A systematic analysis for the global burden of disease study 2016. Lancet 390:1151-1210.

CollaboratorsGBDCoD. 2017. Global, regional, and national age-sex specific mortality for 264 causes of death, 1980-2016: A systematic analysis for the global burden of disease study 2016. Lancet 390:1151-1210.

Collino S, Montoliu I, Martin FP, Scherer M, Mari D, Salvioli S, et al. 2013. Metabolic signatures of extreme longevity in northern italian centenarians reveal a complex remodeling of lipids, amino acids, and gut microbiota metabolism. PLoS One 8:e56564.

Crous-Bou M, Molinuevo JL, Sala-Vila A. 2019. Plant-rich dietary patterns, plant foods and nutrients, and telomere length. Adv Nutr 10:S296-S303.

D'Agostino RB, Sr., Vasan RS, Pencina MJ, Wolf PA, Cobain M, Massaro JM, et al. 2008. General cardiovascular risk profile for use in primary care: The framingham heart study. Circulation 117:743-753.

De Meyer T, Rietzschel ER, De Buyzere ML, Langlois MR, De Bacquer D, Segers P, et al. 2009. Systemic telomere length and preclinical atherosclerosis: The asklepios study. Eur Heart J 30:3074-3081.

Dekkers KF, van Iterson M, Slieker RC, Moed MH, Bonder MJ, van Galen M, et al. 2016. Blood lipids influence DNA methylation in circulating cells. Genome Biol 17:138.

Demanelis K, Jasmine F, Chen LS, Chernoff M, Tong L, Delgado D, et al. 2020. Determinants of telomere length across human tissues. Science 369.

Demanelis K, Tong L, Pierce BL. 2021. Genetically increased telomere length and aging-related traits in the u.K. Biobank. J Gerontol A Biol Sci Med Sci 76:15-22.

Denil SL, Rietzschel ER, De Buyzere ML, Van Daele CM, Segers P, De Bacquer D, et al. 2014. On cross-sectional associations of leukocyte telomere length with cardiac systolic, diastolic and vascular function: The asklepios study. PLoS One 9:e115071.

Drzazga A, Sowinska A, Koziolkiewicz M. 2014. Lysophosphatidylcholine and lysophosphatidylinosiol--novel promissing signaling molecules and their possible therapeutic activity. Acta Pol Pharm 71:887-899.

Dunn J, Qiu H, Kim S, Jjingo D, Hoffman R, Kim CW, et al. 2014. Flow-dependent epigenetic DNA methylation regulates endothelial gene expression and atherosclerosis. J Clin Invest 124:3187-3199.

Elks CE, Scott RA. 2014. The long and short of telomere length and diabetes. Diabetes 63:65-67.

Fathi E, Charoudeh HN, Sanaat Z, Farahzadi R. 2019. Telomere shortening as a hallmark of stem cell senescence. Stem Cell Investig 6:7.

Fernandez-Alvira JM, Fuster V, Dorado B, Soberon N, Flores I, Gallardo M, et al. 2016. Short telomere load, telomere length, and subclinical atherosclerosis: The pesa study. J Am Coll Cardiol 67:2467-2476.

Ferrucci L, Gonzalez-Freire M, Fabbri E, Simonsick E, Tanaka T, Moore Z, et al. 2020. Measuring biological aging in humans: A quest. Aging Cell 19:e13080.

Fitzpatrick AL, Kronmal RA, Gardner JP, Psaty BM, Jenny NS, Tracy RP, et al. 2007. Leukocyte telomere length and cardiovascular disease in the cardiovascular health study. Am J Epidemiol 165:14-21.

Fontana L, Kennedy BK, Longo VD, Seals D, Melov S. 2014. Medical research: Treat ageing. Nature 511:405-407.

Forouhi NG, Koulman A, Sharp SJ, Imamura F, Kroger J, Schulze MB, et al. 2014. Differences in the prospective association between individual plasma phospholipid saturated fatty acids and incident type 2 diabetes: The epic-interact case-cohort study. Lancet Diabetes Endocrinol 2:810-818.

Fortin JP, Triche TJ, Jr., Hansen KD. 2017. Preprocessing, normalization and integration of the illumina humanmethylationepic array with minfi. Bioinformatics 33:558-560.

Fraga MF, Esteller M. 2007. Epigenetics and aging: The targets and the marks. Trends Genet 23:413-418.

Fransquet PD, Wrigglesworth J, Woods RL, Ernst ME, Ryan J. 2019. The epigenetic clock as a predictor of disease and mortality risk: A systematic review and meta-analysis. Clin Epigenetics 11:62.

Frazier-Wood AC, Aslibekyan S, Absher DM, Hopkins PN, Sha J, Tsai MY, et al. 2014. Methylation at cpt1a locus is associated with lipoprotein subfraction profiles. J Lipid Res 55:1324-1330.

Fyhrquist F, Saijonmaa O, Strandberg T. 2013. The roles of senescence and telomere shortening in cardiovascular disease. Nat Rev Cardiol 10:274-283.

Gao X, Zhang Y, Burwinkel B, Xuan Y, Holleczek B, Brenner H, et al. 2019. The associations of DNA methylation alterations in oxidative stress-related genes with cancer incidence and mortality outcomes: A population-based cohort study. Clin Epigenetics 11:14.

Gomez-Alonso MDC, Kretschmer A, Wilson R, Pfeiffer L, Karhunen V, Seppala I, et al. 2021. DNA methylation and lipid metabolism: An ewas of 226 metabolic measures. Clin Epigenetics 13:7.

Gonzalez-Covarrubias V, Beekman M, Uh HW, Dane A, Troost J, Paliukhovich I, et al. 2013. Lipidomics of familial longevity. Aging Cell 12:426-434.

Gonzalez-Freire M, Moaddel R, Sun K, Fabbri E, Zhang P, Khadeer M, et al. 2019. Targeted metabolomics shows low plasma lysophosphatidylcholine 18:2 predicts greater decline of gait speed in older adults: The baltimore longitudinal study of aging. J Gerontol A Biol Sci Med Sci 74:62-67.

Gonzalez-Guardia L, Yubero-Serrano EM, Rangel-Zuniga O, Marin C, Camargo A, Perez-Martinez P, et al. 2014. Influence of endothelial dysfunction on telomere length in subjects with metabolic syndrome: Lipgene study. Age (Dordr) 36:9681.

Hahn O, Gronke S, Stubbs TM, Ficz G, Hendrich O, Krueger F, et al. 2017. Dietary restriction protects from age-associated DNA methylation and induces epigenetic reprogramming of lipid metabolism. Genome Biol 18:56.

Hamczyk MR, Nevado RM, Barettino A, Fuster V, Andres V. 2020. Biological versus chronological aging: Jacc focus seminar. J Am Coll Cardiol 75:919-930.

Hannum G, Guinney J, Zhao L, Zhang L, Hughes G, Sadda S, et al. 2013. Genome-wide methylation profiles reveal quantitative views of human aging rates. Mol Cell 49:359-367.

Harman D. 1991. The aging process: Major risk factor for disease and death. Proc Natl Acad Sci U S A 88:5360-5363.

Hedman AK, Mendelson MM, Marioni RE, Gustafsson S, Joehanes R, Irvin MR, et al. 2017. Epigenetic patterns in blood associated with lipid traits predict incident coronary heart disease events and are enriched for results from genome-wide association studies. Circ Cardiovasc Genet 10.

Hodson L, Skeaff CM, Fielding BA. 2008. Fatty acid composition of adipose tissue and blood in humans and its use as a biomarker of dietary intake. Prog Lipid Res 47:348-380.

Holland WL, Summers SA. 2008. Sphingolipids, insulin resistance, and metabolic disease: New insights from in vivo manipulation of sphingolipid metabolism. Endocr Rev 29:381-402.

Honkonen M, Vaaraniemi K, Saijonmaa O, Nyman A, Tikkakoski AJ, Koskela J, et al. 2020. Leukocyte telomere length is inversely associated with arterial wave reflection in 566 normotensive and never-treated hypertensive subjects. Aging (Albany NY) 12:12376-12392.

Horvath S. 2013. DNA methylation age of human tissues and cell types. Genome Biol 14:R115.

Horvath S, Erhart W, Brosch M, Ammerpohl O, von Schonfels W, Ahrens M, et al. 2014. Obesity accelerates epigenetic aging of human liver. Proc Natl Acad Sci U S A 111:15538-15543.

Horvath S, Raj K. 2018. DNA methylation-based biomarkers and the epigenetic clock theory of ageing. Nat Rev Genet 19:371-384.

Houseman EA, Accomando WP, Koestler DC, Christensen BC, Marsit CJ, Nelson HH, et al. 2012. DNA methylation arrays as surrogate measures of cell mixture distribution. BMC Bioinformatics 13:86.

Huang RC, Lillycrop KA, Beilin LJ, Godfrey KM, Anderson D, Mori TA, et al. 2019. Epigenetic age acceleration in adolescence associates with bmi, inflammation, and

risk score for middle age cardiovascular disease. J Clin Endocrinol Metab 104:3012-3024.

Huang S, Rutkowsky JM, Snodgrass RG, Ono-Moore KD, Schneider DA, Newman JW, et al. 2012. Saturated fatty acids activate tlr-mediated proinflammatory signaling pathways. J Lipid Res 53:2002-2013.

Hung ND, Sok DE, Kim MR. 2012. Prevention of 1-palmitoyl lysophosphatidylcholine-induced inflammation by polyunsaturated acyl lysophosphatidylcholine. Inflamm Res 61:473-483.

Inker LA, Schmid CH, Tighiouart H, Eckfeldt JH, Feldman HI, Greene T, et al. 2012. Estimating glomerular filtration rate from serum creatinine and cystatin c. N Engl J Med 367:20-29.

Irvin MR, Zhi D, Joehanes R, Mendelson M, Aslibekyan S, Claas SA, et al. 2014. Epigenome-wide association study of fasting blood lipids in the genetics of lipid-lowering drugs and diet network study. Circulation 130:565-572.

Jackowska M, Hamer M, Carvalho LA, Erusalimsky JD, Butcher L, Steptoe A. 2012. Short sleep duration is associated with shorter telomere length in healthy men: Findings from the whitehall ii cohort study. PLoS One 7:e47292.

Jesko H, Stepien A, Lukiw WJ, Strosznajder RP. 2019. The cross-talk between sphingolipids and insulin-like growth factor signaling: Significance for aging and neurodegeneration. Mol Neurobiol 56:3501-3521.

Jhun MA, Mendelson M, Wilson R, Gondalia R, Joehanes R, Salfati E, et al. 2021. A multi-ethnic epigenome-wide association study of leukocyte DNA methylation and blood lipids. Nat Commun 12:3987.

Jiang YZ, Jimenez JM, Ou K, McCormick ME, Zhang LD, Davies PF. 2014. Hemodynamic disturbed flow induces differential DNA methylation of endothelial kruppel-like factor 4 promoter in vitro and in vivo. Circ Res 115:32-43.

Jones MJ, Goodman SJ, Kobor MS. 2015. DNA methylation and healthy human aging. Aging Cell 14:924-932.

Jylhava J, Pedersen NL, Hagg S. 2017. Biological age predictors. EBioMedicine 21:29-36.

Khan SS, Singer BD, Vaughan DE. 2017. Molecular and physiological manifestations and measurement of aging in humans. Aging Cell 16:624-633.

Khaw KT, Friesen MD, Riboli E, Luben R, Wareham N. 2012. Plasma phospholipid fatty acid concentration and incident coronary heart disease in men and women: The epic-norfolk prospective study. PLoS Med 9:e1001255.

Knuplez E, Marsche G. 2020. An updated review of pro- and anti-inflammatory properties of plasma lysophosphatidylcholines in the vascular system. Int J Mol Sci 21.

Kwiterovich PO, Jr. 2000. The metabolic pathways of high-density lipoprotein, low-density lipoprotein, and triglycerides: A current review. Am J Cardiol 86:5L-10L.

Law SH, Chan ML, Marathe GK, Parveen F, Chen CH, Ke LY. 2019. An updated review of lysophosphatidylcholine metabolism in human diseases. Int J Mol Sci 20.

Lehallier B, Shokhirev MN, Wyss-Coray T, Johnson AA. 2020. Data mining of human plasma proteins generates a multitude of highly predictive aging clocks that reflect different aspects of aging. Aging Cell 19:e13256.

Lemaitre RN, Yu C, Hoofnagle A, Hari N, Jensen PN, Fretts AM, et al. 2018. Circulating sphingolipids, insulin, homa-ir, and homa-b: The strong heart family study. Diabetes 67:1663-1672.

Leri A, Franco S, Zacheo A, Barlucchi L, Chimenti S, Limana F, et al. 2003. Ablation of telomerase and telomere loss leads to cardiac dilatation and heart failure associated with p53 upregulation. EMBO J 22:131-139.

Leung CW, Fung TT, McEvoy CT, Lin J, Epel ES. 2018. Diet quality indices and leukocyte telomere length among healthy us adults: Data from the national health and nutrition examination survey, 1999-2002. Am J Epidemiol 187:2192-2201.

Levine ME. 2013. Modeling the rate of senescence: Can estimated biological age predict mortality more accurately than chronological age? J Gerontol A Biol Sci Med Sci 68:667-674.

Levine ME, Lu AT, Quach A, Chen BH, Assimes TL, Bandinelli S, et al. 2018. An epigenetic biomarker of aging for lifespan and healthspan. Aging (Albany NY) 10:573-591.

Li C, Stoma S, Lotta LA, Warner S, Albrecht E, Allione A, et al. 2020. Genome-wide association analysis in humans links nucleotide metabolism to leukocyte telomere length. Am J Hum Genet 106:389-404.

Lowsky DJ, Olshansky SJ, Bhattacharya J, Goldman DP. 2014. Heterogeneity in healthy aging. J Gerontol A Biol Sci Med Sci 69:640-649.

Lu AT, Quach A, Wilson JG, Reiner AP, Aviv A, Raj K, et al. 2019. DNA methylation grimage strongly predicts lifespan and healthspan. Aging (Albany NY) 11:303-327.

Lucas A, Grynberg A, Lacour B, Goirand F. 2008. Dietary n-3 polyunsaturated fatty acids and endothelium dysfunction induced by lysophosphatidylcholine in syrian hamster aorta. Metabolism 57:233-240.

Maeda M, Tsuboi T, Hayashi T. 2019. An inhibitor of activated blood coagulation factor x shows anti-endothelial senescence and anti-atherosclerotic effects. J Vasc Res 56:181-190.

Maedler K, Spinas GA, Dyntar D, Moritz W, Kaiser N, Donath MY. 2001. Distinct effects of saturated and monounsaturated fatty acids on beta-cell turnover and function. Diabetes 50:69-76.

Mamoshina P, Volosnikova M, Ozerov IV, Putin E, Skibina E, Cortese F, et al. 2018. Machine learning on human muscle transcriptomic data for biomarker discovery and tissue-specific drug target identification. Front Genet 9:242.

Mapstone M, Cheema AK, Fiandaca MS, Zhong X, Mhyre TR, MacArthur LH, et al. 2014. Plasma phospholipids identify antecedent memory impairment in older adults. Nat Med 20:415-418.

Marees AT, de Kluiver H, Stringer S, Vorspan F, Curis E, Marie-Claire C, et al. 2018. A tutorial on conducting genome-wide association studies: Quality control and statistical analysis. Int J Methods Psychiatr Res 27:e1608.

Marioni RE, Shah S, McRae AF, Chen BH, Colicino E, Harris SE, et al. 2015a. DNA methylation age of blood predicts all-cause mortality in later life. Genome Biol 16:25.

Marioni RE, Shah S, McRae AF, Ritchie SJ, Muniz-Terrera G, Harris SE, et al. 2015b. The epigenetic clock is correlated with physical and cognitive fitness in the lothian birth cohort 1936. Int J Epidemiol 44:1388-1396.

Masi S, D'Aiuto F, Martin-Ruiz C, Kahn T, Wong A, Ghosh AK, et al. 2014. Rate of telomere shortening and cardiovascular damage: A longitudinal study in the 1946 british birth cohort. Eur Heart J 35:3296-3303.

McCrory C, Fiorito G, Hernandez B, Polidoro S, O'Halloran AM, Hever A, et al. 2021. Grimage outperforms other epigenetic clocks in the prediction of age-related clinical phenotypes and all-cause mortality. J Gerontol A Biol Sci Med Sci 76:741-749.

McDonnell BJ, Yasmin, Butcher L, Cockcroft JR, Wilkinson IB, Erusalimsky JD, et al. 2017. The age-dependent association between aortic pulse wave velocity and telomere length. J Physiol 595:1627-1635.

Medina-Lezama J, Narvaez-Guerra O, Herrera-Enriquez K, Morey-Vargas OL, Bolanos-Salazar JF, Abugattas JP, et al. 2018. Hemodynamic patterns identified by impedance cardiography predict mortality in the general population: The prevencion study. J Am Heart Assoc 7:e009259.

Mendelson MM, Marioni RE, Joehanes R, Liu C, Hedman AK, Aslibekyan S, et al. 2017. Association of body mass index with DNA methylation and gene expression in blood cells and relations to cardiometabolic disease: A mendelian randomization approach. PLoS Med 14:e1002215.

Minamino T, Mitsialis SA, Kourembanas S. 2001. Hypoxia extends the life span of vascular smooth muscle cells through telomerase activation. Mol Cell Biol 21:3336-3342.

Minamino T, Miyauchi H, Yoshida T, Ishida Y, Yoshida H, Komuro I. 2002. Endothelial cell senescence in human atherosclerosis: Role of telomere in endothelial dysfunction. Circulation 105:1541-1544.

Montoliu I, Scherer M, Beguelin F, DaSilva L, Mari D, Salvioli S, et al. 2014. Serum profiling of healthy aging identifies phospho- and sphingolipid species as markers of human longevity. Aging (Albany NY) 6:9-25.

Mudry JM, Lassiter DG, Nylen C, Garcia-Calzon S, Naslund E, Krook A, et al. 2017. Insulin and glucose alter death-associated protein kinase 3 (dapk3) DNA methylation in human skeletal muscle. Diabetes 66:651-662.

Murray R, Bryant J, Titcombe P, Barton SJ, Inskip H, Harvey NC, et al. 2016. DNA methylation at birth within the promoter of anril predicts markers of cardiovascular risk at 9 years. Clin Epigenetics 8:90.

Nannini DR, Joyce BT, Zheng Y, Gao T, Liu L, Yoon G, et al. 2019. Epigenetic age acceleration and metabolic syndrome in the coronary artery risk development in young adults study. Clin Epigenetics 11:160.

Nazish Sayed TG, Robert Tibshirani, Trevor Hastie, Lu Cui, Tatiana Kuznetsova, Yael Rosenberg-Hasson, Rita Ostan, Daniela Monti, Benoit Lehallier, Shai Shen-Orr, Holden T. Maecker, Cornelia L. Dekker, Tony Wyss-Coray, Claudio Franceschi,

Vladimir Jojic, François Haddad, José G. Montoya, Joseph C. Wu, David Furman. 2019. An inflammatory clock predicts multi-morbidity, immunosenescence and cardiovascular aging in humans. bioRxiv 840363.

Nelson JC, Jiang XC, Tabas I, Tall A, Shea S. 2006. Plasma sphingomyelin and subclinical atherosclerosis: Findings from the multi-ethnic study of atherosclerosis. Am J Epidemiol 163:903-912.

Nevalainen T, Kananen L, Marttila S, Jylhava J, Mononen N, Kahonen M, et al. 2017. Obesity accelerates epigenetic aging in middle-aged but not in elderly individuals. Clin Epigenetics 9:20.

Nezu T, Hosomi N, Takahashi T, Anno K, Aoki S, Shimamoto A, et al. 2015. Telomere g-tail length is a promising biomarker related to white matter lesions and endothelial dysfunction in patients with cardiovascular risk: A cross-sectional study. EBioMedicine 2:960-967.

Nguyen MT, Vryer R, Ranganathan S, Lycett K, Grobler A, Dwyer T, et al. 2019. Telomere length and vascular phenotypes in a population-based cohort of children and midlife adults. J Am Heart Assoc 8:e012707.

Njajou OT, Cawthon RM, Damcott CM, Wu SH, Ott S, Garant MJ, et al. 2007. Telomere length is paternally inherited and is associated with parental lifespan. Proc Natl Acad Sci U S A 104:12135-12139.

North BJ, Sinclair DA. 2012. The intersection between aging and cardiovascular disease. Circ Res 110:1097-1108.

Nuotio ML, Pervjakova N, Joensuu A, Karhunen V, Hiekkalinna T, Milani L, et al. 2020. An epigenome-wide association study of metabolic syndrome and its components. Sci Rep 10:20567.

O'Sullivan RJ, Karlseder J. 2010. Telomeres: Protecting chromosomes against genome instability. Nat Rev Mol Cell Biol 11:171-181.

Pamplona R. 2008. Membrane phospholipids, lipoxidative damage and molecular integrity: A causal role in aging and longevity. Biochim Biophys Acta 1777:1249-1262.

Pararasa C, Ikwuobe J, Shigdar S, Boukouvalas A, Nabney IT, Brown JE, et al. 2016. Age-associated changes in long-chain fatty acid profile during healthy aging promote pro-inflammatory monocyte polarization via ppargamma. Aging Cell 15:128-139.

Patel SA, Winkel M, Ali MK, Narayan KM, Mehta NK. 2015. Cardiovascular mortality associated with 5 leading risk factors: National and state preventable fractions estimated from survey data. Ann Intern Med 163:245-253.

Pfeiffer L, Wahl S, Pilling LC, Reischl E, Sandling JK, Kunze S, et al. 2015. DNA methylation of lipid-related genes affects blood lipid levels. Circ Cardiovasc Genet 8:334-342.

Piccinini M, Scandroglio F, Prioni S, Buccinna B, Loberto N, Aureli M, et al. 2010. Deregulated sphingolipid metabolism and membrane organization in neurodegenerative disorders. Mol Neurobiol 41:314-340.

Pradas I, Jove M, Huynh K, Puig J, Ingles M, Borras C, et al. 2019. Exceptional human longevity is associated with a specific plasma phenotype of ether lipids. Redox Biol 21:101127.

Price AL, Patterson NJ, Plenge RM, Weinblatt ME, Shadick NA, Reich D. 2006. Principal components analysis corrects for stratification in genome-wide association studies. Nat Genet 38:904-909.

Proitsi P, Kim M, Whiley L, Simmons A, Sattlecker M, Velayudhan L, et al. 2017. Association of blood lipids with alzheimer's disease: A comprehensive lipidomics analysis. Alzheimers Dement 13:140-151.

Protsenko E, Yang R, Nier B, Reus V, Hammamieh R, Rampersaud R, et al. 2021. "Grimage," an epigenetic predictor of mortality, is accelerated in major depressive disorder. Transl Psychiatry 11:193.

Quach A, Levine ME, Tanaka T, Lu AT, Chen BH, Ferrucci L, et al. 2017. Epigenetic clock analysis of diet, exercise, education, and lifestyle factors. Aging (Albany NY) 9:419-446.

Rehkopf DH, Needham BL, Lin J, Blackburn EH, Zota AR, Wojcicki JM, et al. 2016. Leukocyte telomere length in relation to 17 biomarkers of cardiovascular disease risk: A cross-sectional study of us adults. PLoS Med 13:e1002188.

Rhee EP, Cheng S, Larson MG, Walford GA, Lewis GD, McCabe E, et al. 2011. Lipid profiling identifies a triacylglycerol signature of insulin resistance and improves diabetes prediction in humans. J Clin Invest 121:1402-1411.

Richard MA, Huan T, Ligthart S, Gondalia R, Jhun MA, Brody JA, et al. 2017. DNA methylation analysis identifies loci for blood pressure regulation. Am J Hum Genet 101:888-902.

Robinson O, Chadeau Hyam M, Karaman I, Climaco Pinto R, Ala-Korpela M, Handakas E, et al. 2020. Determinants of accelerated metabolomic and epigenetic aging in a uk cohort. Aging Cell 19:e13149.

Roetker NS, Pankow JS, Bressler J, Morrison AC, Boerwinkle E. 2018. Prospective study of epigenetic age acceleration and incidence of cardiovascular disease outcomes in the aric study (atherosclerosis risk in communities). Circ Genom Precis Med 11:e001937.

Rozing MP, Westendorp RG, Frolich M, de Craen AJ, Beekman M, Heijmans BT, et al. 2009. Human insulin/igf-1 and familial longevity at middle age. Aging (Albany NY) 1:714-722.

Schottker B, Xuan Y, Gao X, Anusruti A, Brenner H. 2020. Oxidatively damaged DNA/rna and 8-isoprostane levels are associated with the development of type 2 diabetes at older age: Results from a large cohort study. Diabetes Care 43:130-136.

Semba RD, Zhang P, Adelnia F, Sun K, Gonzalez-Freire M, Salem N, Jr., et al. 2019. Low plasma lysophosphatidylcholines are associated with impaired mitochondrial oxidative capacity in adults in the baltimore longitudinal study of aging. Aging Cell 18:e12915.

Sindi S, Solomon A, Kareholt I, Hovatta I, Antikainen R, Hanninen T, et al. 2021. Telomere length change in a multidomain lifestyle intervention to prevent cognitive decline: A randomized clinical trial. J Gerontol A Biol Sci Med Sci 76:491-498.

Smedman AE, Gustafsson IB, Berglund LG, Vessby BO. 1999. Pentadecanoic acid in serum as a marker for intake of milk fat: Relations between intake of milk fat and metabolic risk factors. Am J Clin Nutr 69:22-29.

Smith AR, Visioli F, Frei B, Hagen TM. 2006. Age-related changes in endothelial nitric oxide synthase phosphorylation and nitric oxide dependent vasodilation: Evidence for a novel mechanism involving sphingomyelinase and ceramide-activated phosphatase 2a. Aging Cell 5:391-400.

Stegemann C, Pechlaner R, Willeit P, Langley SR, Mangino M, Mayr U, et al. 2014. Lipidomics profiling and risk of cardiovascular disease in the prospective population-based bruneck study. Circulation 129:1821-1831.

Sun D, Zhang T, Su S, Hao G, Chen T, Li QZ, et al. 2019. Body mass index drives changes in DNA methylation: A longitudinal study. Circ Res 125:824-833.

Tabassum R, Ramo JT, Ripatti P, Koskela JT, Kurki M, Karjalainen J, et al. 2019. Genetic architecture of human plasma lipidome and its link to cardiovascular disease. Nat Commun 10:4329.

Tempaku P, Hirotsu C, Mazzotti D, Xavier G, Maurya P, Brietzke E, et al. 2018. Long sleep duration, insomnia, and insomnia with short objective sleep duration are independently associated with short telomere length. J Clin Sleep Med 14:2037-2045.

Toth PP. 2004. High-density lipoprotein and cardiovascular risk. Circulation 109:1809-1812.

Tucker LA. 2017. Physical activity and telomere length in u.S. Men and women: An nhanes investigation. Prev Med 100:145-151.

Vaarhorst AA, Beekman M, Suchiman EH, van Heemst D, Houwing-Duistermaat JJ, Westendorp RG, et al. 2011. Lipid metabolism in long-lived families: The leiden longevity study. Age (Dordr) 33:219-227.

van Dijk RA, Kolodgie F, Ravandi A, Leibundgut G, Hu PP, Prasad A, et al. 2012. Differential expression of oxidation-specific epitopes and apolipoprotein(a) in progressing and ruptured human coronary and carotid atherosclerotic lesions. J Lipid Res 53:2773-2790.

Verma SS, de Andrade M, Tromp G, Kuivaniemi H, Pugh E, Namjou-Khales B, et al. 2014. Imputation and quality control steps for combining multiple genome-wide datasets. Front Genet 5:370.

Wahl S, Drong A, Lehne B, Loh M, Scott WR, Kunze S, et al. 2017. Epigenome-wide association study of body mass index, and the adverse outcomes of adiposity. Nature 541:81-86.

Ward-Caviness CK, Xu T, Aspelund T, Thorand B, Montrone C, Meisinger C, et al. 2017. Improvement of myocardial infarction risk prediction via inflammation-associated metabolite biomarkers. Heart 103:1278-1285.

Werner CM, Hecksteden A, Morsch A, Zundler J, Wegmann M, Kratzsch J, et al. 2019. Differential effects of endurance, interval, and resistance training on telomerase activity and telomere length in a randomized, controlled study. Eur Heart J 40:34-46.

WHO. 2015. World report on ageing and health. Luxembourg:World Health Organization.

Wolk A, Vessby B, Ljung H, Barrefors P. 1998. Evaluation of a biological marker of dairy fat intake. Am J Clin Nutr 68:291-295.

Wu MC, Kuan PF. 2018. A guide to illumina beadchip data analysis. Methods Mol Biol 1708:303-330.

Xie T, Gorenjak V, M GS, Dade S, Marouli E, Masson C, et al. 2019. Epigenome-wide association study (ewas) of blood lipids in healthy population from stanislas family study (sfs). Int J Mol Sci 20.

Yeh JK, Lin MH, Wang CY. 2019. Telomeres as therapeutic targets in heart disease. JACC Basic Transl Sci 4:855-865.

Yepuri G, Sukhovershin R, Nazari-Shafti TZ, Petrascheck M, Ghebre YT, Cooke JP. 2016. Proton pump inhibitors accelerate endothelial senescence. Circ Res 118:e36-42.

Yin X, Willinger CM, Keefe J, Liu J, Fernandez-Ortiz A, Ibanez B, et al. 2020. Lipidomic profiling identifies signatures of metabolic risk. EBioMedicine 51:102520.

Yusuf S, Hawken S, Ounpuu S, Dans T, Avezum A, Lanas F, et al. 2004. Effect of potentially modifiable risk factors associated with myocardial infarction in 52 countries (the interheart study): Case-control study. Lancet 364:937-952.

Yusuf S, Joseph P, Rangarajan S, Islam S, Mente A, Hystad P, et al. 2020. Modifiable risk factors, cardiovascular disease, and mortality in 155 722 individuals from 21 high-income, middle-income, and low-income countries (pure): A prospective cohort study. Lancet 395:795-808.

9. Acknowledgements

The four-year PhD time at the Rhineland Study, Population Health Sciences, German Centre for Neurodegenerative Diseases (DZNE) has been a wonderful experience for me. Here I would like to thank my supervisors, colleagues, collaborators, friends and family for your great support.

First and foremost, I would like to thank my supervisor and members of the thesis committee. Thanks to **Monique M.B. Breteler**, my main supervisor, for bringing me in this international and wonderful group and guiding me in scientific research. I am always encouraged by your deep knowledge, the way you do research and the challenging but constructive feedbacks. I also appreciate that you provide me great opportunities to communicate and collaborate with other wonderful researchers. Thanks to **N. Ahmad Aziz,** thank you for always being available to discuss any question and always provide me valuable comments and solutions. It is truly my pleasure to learn from you and work with you. **Cornelia M van Duijn, Matthias Schmid, and Daniele Bano,** I would like to thank you for your time, valuable comments and suggestions, which inspire me a lot. I really enjoy sharing and discussing my progress with you. It is my honor to have all of you as my thesis committee members.

It is a great pleasure for me to work in the Rhineland Study. Thanks to all the **participants** of the Rhineland Study, all the **study assistants**, **management team**, and our **RS-IT team**, especially **Shahid**, who gave me support in processing and cleaning the data. **Gökhan, Elvire, Aslam,** thanks for your effort and nice input, I enjoy doing projects with you. Thanks to **Natacha, Sadia, Meta, Loes, Theda**, for your warmness and guiding me through when I joined. Thanks to **Lu, Annabell, Valentina, Juliana** for the awesome discussions and sharing. Thanks to **Ximena, Santiago, Davide, Konstantinos, Weiyi, Xingwang, Fabienne, Nersi, Valerie** for the nice lunch break and after work hang out. We could not have such a great working environment without all of your contributions.

I gratefully acknowledge the financial support from **China Scholarship Council**.

Finally, I would like to thank my **friends and family**. Thank you for always being here for me even when times were difficult. Without your support and encouragement, I cannot manage this. I always remember your support, optimism, humor and love, which enlightens my way. Thank you for still being here with me, and we are and will explore our life journey together.

谢谢你们!

10. Publications

- **Liu D**, McIntyre RS, Li R, Yang M, Xue Y, Cao B. 2021. Genetic association between major depressive disorder and type 2 diabetes metllitus: Shared pathways and protein networks. **Prog Neuropsychopharmacol Biol Psychiatry** 111:110339. DOI: 10.1016/j.pnpbp.2021.110339
- **Liu D**, Zhu Z, Zhou L, Yang M. 2020b. The joint effects of frailty and telomere length for predicting mortality in older adults: The national health and nutrition examination survey 1999-2002. **Aging Clin Exp Res** 32:1839-1847. DOI: 10.1007/s40520-019-01376-3
- **Liu D**, Zhao Y, Qi Y, Gao Y, Tu D, Wang Y, et al. 2020a. Benzo(a)pyrene exposure induced neuronal loss, plaque deposition, and cognitive decline in APP/PS1 mice. **J Neuroinflammation** 17: 258. DOI: 10.1186/s12974-020-01925-y
- **Liu D**, Cao B, Zhao Y, Huang H, McIntyre RS, Rosenblat JD, et al. 2018. Soluble TREM2 changes during the clinical course of Alzheimer's disease: A meta-analysis. **Neurosci Lett** 686:10-16. DOI: 10.1016/j.neulet.2018.08.038
- Zhang H*, **Liu D***, Wang Y, Huang H, Zhao Y, Zhou H. 2017. Meta-analysis of expression and function of neprilysin in Alzheimer's disease. **Neurosci Lett** 657:69-76. DOI: 10.1016/j.neulet.2017.07.060
- Zhang H, **Liu D**, Huang H, Zhao Y, Zhou H. 2018. Characteristics of insulin-degrading enzyme in Alzheimer's disease: A meta-analysis. **Curr Alzheimer Res** 15:610-617. DOI: 10.2174/1567205015666180119105446
- Wang Y, **Liu D**, Zhang H, Wang Y, Wei L, Liu Y, et al. 2017. Ultrafine carbon particles promote rotenone-induced dopamine neuronal loss through activating microglial NADPH oxidase. **Toxicol Appl Pharmacol** 322:51-59. DOI: 10.1016/j.taap.2017.03.005
- Zhou L,…, **Liu D**, et al. 2019. Diet behaviours and hypertension in us adults: The national health and nutrition examination survey 2013-2014. **J Hypertens** 37:1230-1238. DOI: 10.1097/HJH.0000000000002037
- Xu W, Wang Y, Quan H, **Liu D**, et al. 2020. Double-strained RNA induced dopaminergic neuronal loss in substantia nigra in the presence of Mac1 receptor. **Biochem Biophys Res Commun**. 533:1148-1154. DOI: 10.1016/j.bbrc.2020.09.101

In preparation/submission

- **Liu D**, et al. Cardiovascular correlates of epigenetic aging across the adult lifespan: A population-based study. In preparation.
- **Liu D**, et al. The lipidomic correlates of epigenetic aging across the adult lifespan: A population-based study. In preparation.
- **Liu D**, et al. The associations of measured and genetically determined leukocyte telomere length with vascular phenotypes: A population-based study. In preparation.
- **Liu D**, et al. Epigenome-wide association study of hippocampal volume. In preparation.

Co-author:

- Deep phenotyping and lifetime trajectories reveal limited effects of longevity regulators on the aging process. Major revision.
- Meta-analysis of epigenome-wide association studies of serum urate: new insights into urate co-regulation and the *SLC2A9* locus. Major revision.
- Epigenome-wide association studies identify DNA methylation associated with kidney function and damage. Major revision.
- Genome-wide DNA methylation and white matter hyperintensities. In preparation.